Dissertation

submitted to the

Combined Faculties for the Natural Sciences and for Mathematics

of the Ruperto-Carola University of Heidelberg, Germany

for the degree of

Doctor of Natural Sciences

presented by

Diplom-B.Sc. Özge Vargel

Born in: Ankara/Turkey

Oral-examination: March 10, 2015

Understanding The Endothelial to Hematopoietic Transition In Mouse Development

Referees: Dr. Martin Jechlinger

Prof. Dr. Stefan Wölfl

Joint Ph.D. programme of the European Molecular Biology Laboratory and Ruperto-Carola University of Heidelberg

Supervisor:

Dr. Christophe Lancrin, EMBL Monterotondo

Thesis Exam Committee:

Dr. Martin Jechlinger, EMBL Monterotondo

Dr. Stefan Wölfl, Heidelberg University

Dr. Michael Milsom, DKFZ Heidelberg

Dr. Darren Gilmour, EMBL Heidelberg

Acknowledgement

In my point of view, science is always a cumulative process and the best scientific work comes from the best team. During my PhD I had the uttermost team in the lab and the perfect people around, which at the end led me to reach the finish line. Words can be hollow to express my gratitude to them, but I believe they know already.

First of all, I want to thank Dr. Christophe Lancrin for giving me the opportunity to work in his lab, trusting me in every stage of the work and not hesitating to invest his time and resources on my project. His scientific mentoring not only taught me a lot but also laid a solid foundation of my academic career. It will be always my honor to be the first PhD student of his lab. Secondly I thank my thesis advisory committee, Dr. Martin Jechlinger, Dr. Kerry Lee Tucker, Dr. Darren Gilmour for their scientific advise on my project.

I would like to thank our collaborators, Dr. Sarah Teichmann and Dr. Jeroen Krijgsveld, who supported my project technically and widened its scientific perspective. This work would not be possible without the support from EMBL facilities. I am grateful for the sincere cooperation with Vladimir Benes' team at gene core facility in EMBL Heidelberg. I thank particularly Paul Collier and Bianka Baying, who helped me on the optimization of the single cell qRT-PCR technique patiently for 2 years. I would like to thank Maria Kamber and Violetta Paribeni for taking care of our mice. I would like to thank Philip Hublitz invaluable advices on cloning. Last but not least, I am indebted to Daniel Bilbao for his guidance on flow cytometry analysis and also for his great mental support and wise conversation, which I will remember for the rest of my life.

Starting a new life in Italy, without knowing a single word in Italian, was not easy for me, but I had great friends who made me feel at home. I am thankful to all former (Madhu Elango, Ezgi Bulca, Gülce Perçin, Ana Cristina Santos) and current (Kerstin Ganter, Irina Pinheiro, Isabelle Bergiers, Maya Shvartsman) CL lab members for their

scientific advices and also for making our lab a peaceful working environment. A special thank to Yang Zhang, whom I had the chance to work with and who was relentlessly caring and helpful. It is my pleasure to know James Ding as a person, to have him as a great lab mate and share joyful memories, who later introduced me to another great person Weronika Gutowska. I am thankful to all EMBL Monterotondo community (Claudia, Stefano C., Nereo, Daniela, Bjarki, Rossana, Stefano G., Jens, Martina, Kalina, Tomoko, Shane, Tina) for those are who made my day with a chat near the coffee machine. A special thank is necessary for Marcos Morgan and Janko Gospocic, as the evil axes club members for the sake of delightful dinners. Lastly, I thank Christian Much, Kerstin Ganter and Andreas Hierholzer for translating my abstract to German.

My endless gratitude is to my friends (Aylin Göke, Dilan Çelebi, Fatma Ayhan, Arda Mızrak, Cem Şengel, Cansu Okur, Hande Astarcı) with whom we maintained the warm relations despite the fact that we are spread around the world.

Finally my greatest gratitude goes to my biggest supporters, my mother Serpil Vargel, my father İbrahim Vargel and my boyfriend Mehmet Fatih Bölükbaşı. They were there with me in every obstacle to keep me going and in every success to celebrate with me. There is no word to express completely my gratitude towards them, but I show my appreciation by dedicating this thesis to them.

Abstract

The endothelial to hematopoietic transition (EHT) is a key developmental event leading to the formation of blood stem and progenitor cells during embryogenesis. A small subset of cells called hemogenic endothelial cells (HE) undergoes the EHT by becoming pre-hematopoietic stem and progenitor cells (Pre-HSPC). Eventually after losing all their endothelial characteristics they become HSPC. Despite extensive studies on this process, there are several questions remaining: What are the differences between hemogenic and non hemogenic endothelial cells? How different is the EHT process in the aorta-gonad-mesonephros (AGM) generating mostly blood stem cells (self-renewing and generating all cell types) and the yolk sac (YS) producing mostly blood progenitors (non self-renewing and generating only a few cell types)? To address these questions, I used single cell transcriptomics because of the scarcity of the HE and the Pre-HSPC within the endothelial population in the AGM and YS. I examined the cells isolated at E9.0, E10.5 and E11.0 mouse embryos. I showed that the major endothelial population of AGM and YS is different from each other, which might be linked with their distinct hematopoietic program. I showed that the pre-HSPC in AGM and YS are transcriptionally alike suggesting that the different hematopoietic program between AGM and YS could be due to the microenvironment. Additionally, I identified a new population detected only in YS at E10.5 co-expressing endothelial and erythroid genes.

The molecular mechanism of the EHT is still not understood. Since the TGFβ signaling triggers a similar event during heart development called endothelial to mesenchymal transition (EndMT), we hypothesized that TGFβ activity may play a similar role in EHT. When I activated the TGFβ signaling by adding TGFβ2 during in vitro EHT differentiation, I observed surprisingly a complete block of the hematopoiesis. When I inhibited it by adding the Tgfbr1 inhibitor, it enhanced blood development. Additionally, the mRNA profile of the treated cells confirmed that inhibition of Alk5 is promoting the EHT, while the TGFβ activation results in cells with a phenotype closer to

cardiac and mesenchymal cells. Consequently, despite the fact that both EndMT and EHT lead to a loss of endothelial cell identity and the generation of mobile cells, our study suggests that the signaling events initiating both processes are different.

Zusammenfassung

Die endotheliale-hämatopoetische Transition (EHT) ist ein Schlüsselereignis in der Embryonalentwicklung, das zur Bildung von Blutstamm-und Vorläuferzellen führt. Eine kleine Gruppe von Zellen, hämogene Endothelzellen (HE), durchläuft die EHT, in der sie sich zu prä-hämatopoetischen Stamm-und Vorläuferzellen (prä-HSVZ) entwickeln. Nachdem sie alle Endotheleigenschaften verloren haben, gehen aus diesen Zellen schließlich die HSVZ hervor. Trotz intensiven Arbeiten auf diesem Gebiet sind noch viele Fragen offen. Was sind die Unterschiede zwischen den hämogenen und nicht hämogenen Endothelzellen? Wie unterscheidet sich die EHT in der Aorta-Gonade-Mesonephros Region (AGM-Region), die hauptsächlich Blutstammzellen generiert, von der im Dottersack, die überwiegend Blutvorläuferzellen hervorbringt? Um diese Fragen zu beantworten wurden die Transkriptome einzelner Endothelzellen aus der AGM-Region sowie des Dottersacks untersucht. Diese Zellen wurden vorher aus 9-11 Tage alten Mausembryonen isoliert. Mit dieser Arbeit konnte gezeigt werden, dass sich die Endothelpopulationen der AGM-Region und des Dottersacks unterscheiden, was mit dem unterschiedlichen hämatopoetischen Programm in Verbindung gebracht werden könnte. Dagegen sind prä-HSVZ aus der AGM-Region und vom Dottersack transkriptionell ähnlich, was darauf hinweist, dass die unterschiedlichen Programme der Zellen zwischen der AGM-Region und des Dottersacks auf einen Effekt der Mikroumgebung zurückzuführen sein könnte. Darüber hinaus konnte eine neue Zellpopulation identifiziert werden, die nur im Dottersack von 10,5 Tage alten Embryonen zu finden ist und endotheliale sowie erythroide Gene co-exprimiert.

Der molekulare Mechanismus der EHT ist noch nicht geklärt. Da der TGFβ Signalweg einen ähnlichen Vorgang während der Herzentwicklung, die sogenannte endotheliale-mesenchymale Transition (EndMT) steuert, haben wir eine vergleichbare Rolle von TGFβ in der EHT vermutet. Jedoch führte die Aktivierung des TGFβ Signalweges in einem in vitro EHT Modell überraschenderweise zu einer kompletten Hemmung der

Hämatopoese. Die Inhibition dagegen begünstigte die Blutbildung. Das Transkriptom der behandelten Zellen bestätigte zusätzlich, dass die Inhibition von Alk5 die EHT fördert, wohingegen die Aktivierung TGFβ Signalweges in Zellen resultiert, deren Phänotyp denen von Herz- und mesenchymalen Zellen ähnelt. Obwohl EndMT und EHT zu einem Verlust der Endothelzellidentität und der Bildung von mobilen Zellen führen, zeigt unsere Studie somit, dass die zu Grunde liegenden Signalprozesse unterschiedlich voneinander sind.

Table of Contents

Figures Index

Tables Index

List of Abbreviations

Abbreviation	
7AAD	7-Aminoactinomycin D
AGM	Aorta gonad mesonephros
Alexa647	Alexa Fluor 647
APC	Allophycocyanin
bFGF	Basic Fibroblast Growth Factor
BL-CFC	Blast colony forming cell
BSA	Bovine Serum Albumin
CFU-C	Colony forming unit, culture
CFU-S	Colony forming unit, spleen
Cre	Cre-recombinase
DA	Dorsal aorta
DMEM	Dulbecco's modified Eagle's medium
DMEM-KO	Dulbecco's modified Eagle's medium, knockout
DMSO	Dimethyl sulfoxide
eGFP	Enhanced green fluorescent protein
EHT	Endothelial to hematopoietic transition
EMT	Epithelial to Mesenchymal Transition
EndMT	Endothelial to Mesenchymal Transition
EPO	Erythropoietin
EryP	Erythrocyte Progenitor
FACS	Fluorescence-activated cell sorting
FBS	Fetal Bovine Serum
FC	Flow cytometry
GFP	Green fluorescent protein
GM-CSF	Granulocyte Macrophage – Colony Stimulating Factor
GO	Gene Ontology
HE	Hemogenic endothelium
HP	Hematopoietic progenitor
Hpf	Hour post-fertilization
HSC	Hematopoietic stem cell
HSPC	Hematopoietic stem/progenitor cell
HUVEC	Human umbilical vein endothelial cells
IAHC	Intra-aortic hematopoietic cluster
IL11	Interleukin 11
IL3	Interleukin 3
IL6	Interleukin 6
IMDM	Iscove's modified Dulbecco's medium
iPSC	Induced pluripotent stem cell
LIF	Leukemia inhibitory factor
M-CSF	Macrophage – Colony Stimulating Factor
MACS	Magnetic activated cell separation
MEF	Mouse embryonic fibroblast
mESC	Mouse embryonic stem cell
mRNA	Messenger ribonucleic acid
mRNA seq	mRNA sequencing
MTG	Mono-thio-glycerol

MTG	Monothioglycerol
P-Sp	Para-aortic Splanchnopleura
PCR	Polymerase Chain Reaction
PE	Phycoerythrin
Pre-amp	Preliminary amplification
Pre-HSPC	Pre-hematopoietic stem/progenitor cell
qRT-PCR	Quantitavive real time polymerase chain reaction
RT	Reverse transcription
RT-STA	Reverse Transcription-Specific Target Amplification
SCF	Stem Cell Factor
SMC	Smooth muscle cell
TGFβ	Transforming Growth Factor beta
TRE	Tetracycline response element
UA	Umbilical artery
VA	Vitelline artery
VEGF	Vascular Endothelial Growth Factor

Chapter1: Introduction

1. Why studying blood cell development is important

A single cell needs to have continuous uptake of nutrients and export of metabolites. For organisms like Hydra, with simple two cell layers, nutrient transportation does not require a specialized circulatory system. However, for bilateria animals with three germ layers (tripoblastic) and complex tissue structure, osmosis would not be enough to support each and every cell's needs. Development of blood system in vertebrates fulfilled the need of each cell regardless of the organism size and complexity.

The development of vertebrates begins with the fertilization of egg with sperm, forming the first totipotent cell, the zygote. The zygote goes through consecutive mitotic divisions, which is followed by the organization of cells to form tissues. As a cluster of cells at the blastocyst stage, each cell can uptake their nutrients from the environment, so would not need a blood system. Later during embryogenesis, where the cell number increase dramatically in a short time and the inside of embryo is hypoxic, how does the each cell of a developing organism take the nutrients and oxygen inside? Before development of any other organ systems, to fulfill the nutrient and oxygen need of every cell, the development of blood system is required.

Regarding the vital role of blood system in sustaining vertebrate organism since the beginning of its development, any kind of defect or absence of blood cell leads to mostly deadly diseases in human. Answering how blood cells are generated is not only important for general developmental biology knowledge but also bears keys to use in treatments of hematopoietic disorders. Current technology is facilitating the production of various cell types, such as adipocytes, chondrocytes, myocytes in in vitro conditions, ultimately aiming at using them for therapeutic transplantation into humans. Knowledge about mouse embryonic hematopoiesis would have enormous contributions to the improvement of in vitro production of blood cells. Particularly in vitro

hematopoietic stem cell (HSC) production by using someone's own cell would open a big window by eliminating search for a matching donor.

2. Ontogeny of blood system: Where does the first blood cell come from?

2.1. First observations and hemangioblast hypothesis

Where are the first blood cells generated? The answer to that question came in 1920s, from the first observation made in chick embryos. Florence Sabin hypothesized the presence of a mesoderm origin, common precursor for blood and vascular endothelial lineages (Sabin, 1921). She named that precursor cell 'angioblast'. In 1932, P. Murray cultured ex vivo the sections of primitive streak of chick embryos and supported Sabin's hypothesis, by renaming the common progenitor of blood vessels and primitive blood cells as 'hemangioblasts' for the first time (Murray, 1932).

Inactivation of one gene in mouse development is a powerful technique to understand the function of that gene. Regarding the questions about the cellular origins of hematopoietic system, several gene knockout mice with both defective vascular and hematopoietic system phenotype took attention. If a disruption of one gene results in malformation of two distinct cell types, it may mean that these two cell types are used to share a common precursor cell. There are several examples of such gene knockout studies. As an example inactivation *Flk-1*, as a gene used to be considered endothelial specific, it surprisingly leads to failure in hematopoiesis as well as vasculogenesis and embryonic lethality at E8.5-9.5 (Shalaby et al., 1995). Similarly, *Scl/Tal1* mutation leads to embryonic lethality at E9.5-10.5 due to disruption of both endothelial and hematopoietic lineages (Robb et al., 1995; Shivdasani, Mayer, & Orkin, 1995). Another study showed that the lack of Tal1 in the endothelium leads to the ectopic activation of the cardiac program in endothelial cells (Van Handel et al., 2012).

2.2. Advances in mouse embryonic stem cell techniques

Although there were several observations supporting the existence of hemangioblasts, direct experiment on those cells were technically challenging. Firstly, there was no marker to locate a hemangioblast cell within mesoderm layer during embryonic development. Secondly, even if it would be possible to identify hemangioblasts among all the other mesodermal cells, studying their in vivo differentiation steps would be difficult due to the limited imaging techniques available for mouse embryogenesis at that time. Nevertheless these challenges were overtaken by the embryonic stem cell differentiation system.

2.2.1. mES cell differentiation system as in vitro model of hematopoiesis

2.2.1.1. Use of mouse ES cells as a technique to study development

At the blastocyst stage of mouse embryo the inner cell mass cells is shown to generate teratocarcinoma, a type of tumor composed of cells from mesoderm, endoderm and ectoderm origin cells(Stevens, 1970). The potential of this cell to differentiate into three germ layers is called pluripotency, which took immediate attention for in vitro differentiation studies to produce tissues and organs in culture conditions. The big obstacle was to expand those pluripotent cells derived from blastocyst, while preserving their pluripotency and prevent their differentiation towards any lineage. In 1981, two groups almost simultaneously published two papers, describing how to culture blastocyst derived mouse embryonic stem cells (mESCs) (Evans & Kaufman, 1981; Martin, 1981). Afterwards the first successful attempt to create chimeric mouse by using these mESCs demonstrated the capacity of these cells to contribute to the germ line (Bradley, Evans, Kaufman, & Robertson, 1984).

2.2.1.2. Establishment of hematopoiesis differentiation protocol development

In vitro mESC culture and differentiation towards several cell fates become an epoch-making technique for developmental biology and yet provided an ideal method to study hematopoietic lineage tracing. In general three types of in vitro differentiation protocols towards mesoderm were developed: differentiation in embryoid bodies (EBs), differentiation on stromal cell line, or differentiation on a plate coated with ECM proteins (G. M. Keller, 1995; Smith, 2001). Especially with embryoid body culture appearance of hemoglobinized red blood cells (erythrocytes) at day 5 of EB culture was evident (Doetschman, Eistetter, Katz, Schmidt, & Kemler, 1985). Several groups also study hematopoietic differentiation in culture condition (Burkert, von Rüden, & Wagner, 1991; G. Keller, Kennedy, Papayannopoulou, & Wiles, 1993; Nakano, Kodama, & Honjo, 1994; Schmitt, Bruyns, & Snodgrass, 1991; Wiles & Keller, 1991). The embryoid body culture and other in vitro differentiation techniques were further refined to enhance hematopoietic lineage choice (Faloon et al., 2000; G. Keller et al., 1993).

2.3. Identifying hemangioblast in vitro and in vivo

2.3.1. Hemangioblast like cells found in in vitro differentiation

Several decades after Florence Sabin's observations, with the advancement of mESC in vitro differentiation system, the presence of hemangioblast cells was investigated. At day4 of EB differentiation, primitive erythroid cells are generated (G. Keller et al., 1993). When the precursor of these primitive erythroid cells are isolated from EBs at day3, it is found to be giving rise to definitive erythroid, myeloid and multi-lineage progenitors. This gives the first results to support a common precursor (blast colony forming cells BL-CFC) idea for both primitive and definitive hematopoiesis (Kennedy et al., 1997). Further study with the same BL-CFCs isolated from EBs, suggested that they might be

the hemangioblast cells, previously hypothesized (Choi, Kennedy, Kazarov, Papadimitriou, & Keller, 1998). Development of Brachyury-GFP ES cells enabled researchers to follow Brachyury+ cells through its differentiation, and suggests Flk-1+, Brachyury+ cells can give rise to endothelial, hematopoietic cells, therefore Bra+, Flk-1+ can be the marker of BL-CFC (Fehling et al., 2003).

2.3.2. Hemangioblast like cells found in vivo yolk sac

The in vivo counterpart of BL-CFC is soon identified in gastrulating mouse embryo as the mesodermal Flk-1+, Brachyury+ cells, which can differentiate to vascular endothelial and/or hematopoietic cells in vitro conditions. Hemangioblasts are located mostly at the posterior primitive streak of E7.5 mouse embryos, which suggests a migration towards yolk sac and form the first blood cells surrounded by vascular endothelial cells, so called blood islands at stage E8 (Huber, Kouskoff, Fehling, Palis, & Keller, 2004).

2.4. Yolk Sac as the first hemogenic site

2.4.1. First observations of yolk sac hematopoiesis

Alexander Maximow first observed the primitive blood cells characterized by their red color within chick embryos in 1909 and later by Florence Sabin in 1921 (Sabin, 1921). They named that particular structure of the clusters of blood cells encapsulated by the vascular endothelial, as blood islands of yolk sac, although we currently know that it is more like a ring of vessel structure surrounding blood cells.

2.4.2. Stages of hematopoietic progenitors rising from YS

Similar to chick, the first hematopoietic cells in mouse embryo are arising from yolk sac mesoderm at the neural plate stage of mouse embryo of E7.5 (Haar & Ackerman, 1971). These first hematopoietic cells were primitive erythrocytes with nucleus and expression of embryonic hemoglobin. However these primitive erythrocyte progenitors (EryP) are transient, only within E7 and E9, cannot be detectable after E9.

After the primitive erythrocytes, a precursor of definitive erythrocyte progenitors (BFU-E) arises in the yolk sac. The definitive erythroid progenitors are found as early as E8.25 of mouse embryos, before circulation. Unlike primitive erythroid progenitors, definitive erythroid progenitors give rise to enucleated, βmajor globin expressing erythrocytes.

The wave of definitive erythroid progenitors is followed by the emergence of myeloid/erythroid progenitors starting from E9.5 of mouse embryo. Although the contractions of the heart started at E8.5 (McGrath, Koniski, Malik, & Palis, 2003) and some of these progenitors are detected in the blood stream and embryo proper, the majority of the progenitors are in the yolk sac at E9.5. Those progenitors later give rise to definitive erythrocytes, macrophages, mast cells, and granulocytes.

Despite early argument about incapability of yolk sac derived hematopoietic progenitor to differentiate into lymphoid cells, recent studies proves that argument wrong. When the hematopoietic progenitors from yolk sac are pulse labeled at E7.5, before the intra-embryonic hematopoiesis start and traced afterwards, the lymphoid progenitors derived from yolk sac is detected in the fetal liver and adult mouse (Samokhvalov, Samokhvalova, & Nishikawa, 2007).

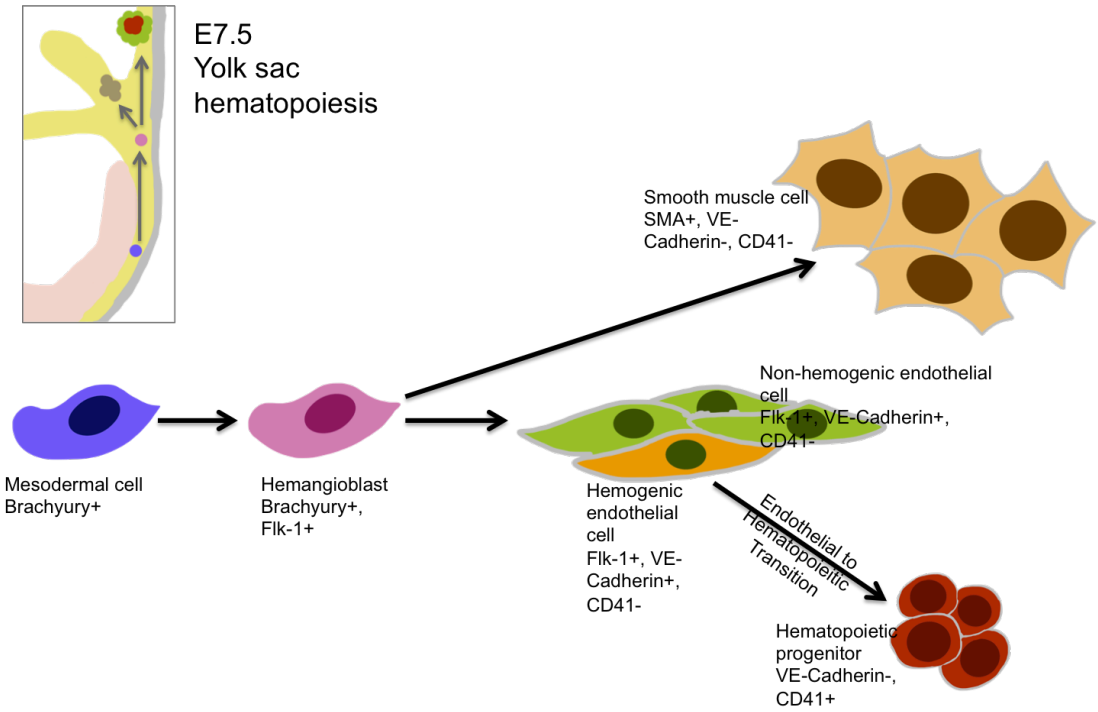

Figure 1.0.1 The YS hematopoiesis starting at E7.5. The top left image depicts the series of cell differentiation events with regards to cell locations and their direction of migration during differentiation. The cells shown below is to give the detailed cell identity and markers, found based on the mESC and mouse YS studies. The differentiation scheme is drawn based on the model (Lancrin et al., 2010)

2.5. Aorta Gonad Mesonephros as the main intra-embryonic hemogenic site

2.5.1. First experiments for intra-embryonic origin of hematopoiesis

While yolk sac is known to be the site of hematopoietic origin, that perspective is changed for the first time when F. Dieterlen-lievre grafted embryo of quail into chick's yolk sac and observed all adult hematopoietic cells were of quail origin (Dieterlen-Lievre, 1975). That experiment clearly shows the intra-embryonic origin of the adult avian hematopoiesis. Further support to understand yolk sac and intra-embryonic hematopoiesis came from the same group (Beaupain, Martin, & Dieterlen-Lièvre, 1979; Lassila, Martin, Toivanen, & Dieterlen-Lièvre, 1982). Studies of frog embryos also supported the two types of hematopoiesis depending on the site (Turpen, Knudson, & Hoefen, 1981).

The intra-embryonic origin of hematopoiesis of zebrafish is identified at 14hpf in posterior lateral mesoderm and the mouse equivalent of this would be the paraaortic splanchnopleura (PsP) at E8.5 embryo. PsP is differentiating later in the development towards a region named as aorta-gonad mesonephros (AGM) due to its differentiation to form the dorsal aorta and the urogenital system.

2.5.2. Hematopoietic Stem Cell emergence from AGM

Hematopoietic stem cell (HSC), by definition, is a cell, which can generate itself and at the same time differentiate into all erythroid, myeloid and lymphoid blood cells to produce the complete blood system throughout the life of a mouse. To test pluripotency capacity of an HSC, a classical but robust experiment is to inject the cells into an irradiated adult mouse and test the presence of donor origin cells in the mature differentiated blood cells, at least four months after transplantation. This type of experiment is called functional repopulation and become a keystone criterion for defining a HSC.

The studies with clonogenic hematopoietic progenitors found in the pre-circulation yolk sac were not successful to show long term (more than 4 months) functional repopulation after the transplantation into adult mouse. Therefore, progenitors originated from pre-circulation (before E8.25) yolk sac accepted as transient and does not remain until the adult hematopoiesis. On the other hand, the cells fitting the HSC criteria was found first in the AGM region at E10 (A. L. Medvinsky, Samoylina, Müller, & Dzierzak, 1993). Several studies claimed that definitive hematopoietic stem cells are originating only from AGM region of E10-E12 of mouse embryos (I. Godin, Dieterlen-Lièvre, & Cumano, 1995; I. E. Godin, Garcia-Porrero, Coutinho, Dieterlen-Lièvre, & Marcos, 1993; A. L. Medvinsky et al., 1993) (Müller, Medvinsky, Strouboulis, Grosveld, & Dzierzak, 1994). Although the yolk sac contribution to the AGM hematopoiesis is still a

big debate, several mouse, zebrafish, and chick studies confirm the formation of HSCs in the AGM.

The evidences from mouse studies were suggesting AGM origin HSCs. The use of transparent zebrafish embryos would be the ideal model to trace the HSCs from the time point they are generated. Several groups looked at AGM equivalent tissues in zebrafish and traced the cells expressing hematopoietic markers. Blood precursors expressing *CD41* and *gata1* were first detected in the region between the dorsal aorta and the axial vein, called sub-aortic mesenchyme. The definitive HSC characteristic of this *CD41*+, *gata*1+ cells is shown by their migration to caudal hematopoietic tissue and then to thymus and kidney (Murayama et al., 2006). Similar study confirms the HSC emergence at AGM of zebrafish (Bertrand, Kim, Teng, & Traver, 2008). Later, *CD41-gfp* zebrafish line was used to trace the HSC and clearly showed the $CD41^{low}$ cells emergence at the DP joint of AGM and later entrance into circulation through axial vein (Kissa et al., 2008). Unlike in mammals, in zebrafish the first HSPCs were not detected in the dorsal aorta but at the mesenchymal region underneath. Further information coming from several groups enlightened further the situation showing that actually dorsal aorta endothelial cells were giving rise to HSCs, but those HSCs reaches the axial vein after extravasation through the sub-aortic mesenchyme (Bertrand et al., 2010; Kissa & Herbomel, 2010; E Y N Lam, Hall, Crosier, Crosier, & Flores, 2010).

2.5.3. Intra-aortic clusters arisen from AGM

During the examination of tissue sections of AGM region, hematopoietic progenitor cells are marked as cluster of cells located in the lumen of the aorta. These cells are called intra-aortic clusters. Several studies point out the heterogeneity of those cluster of cells, in terms of number of cells in a cluster, expression of hematopoietic and endothelial markers, and their capacity to generate different hematopoietic cell types. The high resolution imaging techniques showed that an attached hematopoietic cell

cluster has consistent distribution of cells in terms of its marker protein expression. The round cells closer to endothelial layer can be labeled with Flk-1, CD31, C-kit and sometimes CD41 but no CD45. On the contrary, the cells closer to the aortic space can be labeled with CD45 but not with Flk-1 (Yokomizo & Dzierzak, 2010). Regarding the pluripotency capacity of hematopoietic cells present in intra-aortic clusters, Alexander Medvinsky's group put forward the idea of step-wise maturation of HSCs. The hematopoietic cells with close contact with endothelial layer of dorsal aorta can be identified as VE-Cadherin+, CD41lo, CD45- and CD43+ population, which is named as type I pre-HSCs. The maturation of type I pre-HSCs forms type II pre-HSCs with VE-Cadherin+, CD45+, CD43+ marker identity (A. Medvinsky, Rybtsov, & Taoudi, 2011). A recent study from Catherine Robin's group confirmed that intra-aortic clusters are harboring pre-HSCs, which will mature later into fully functional HSCs (Boisset et al., 2014).

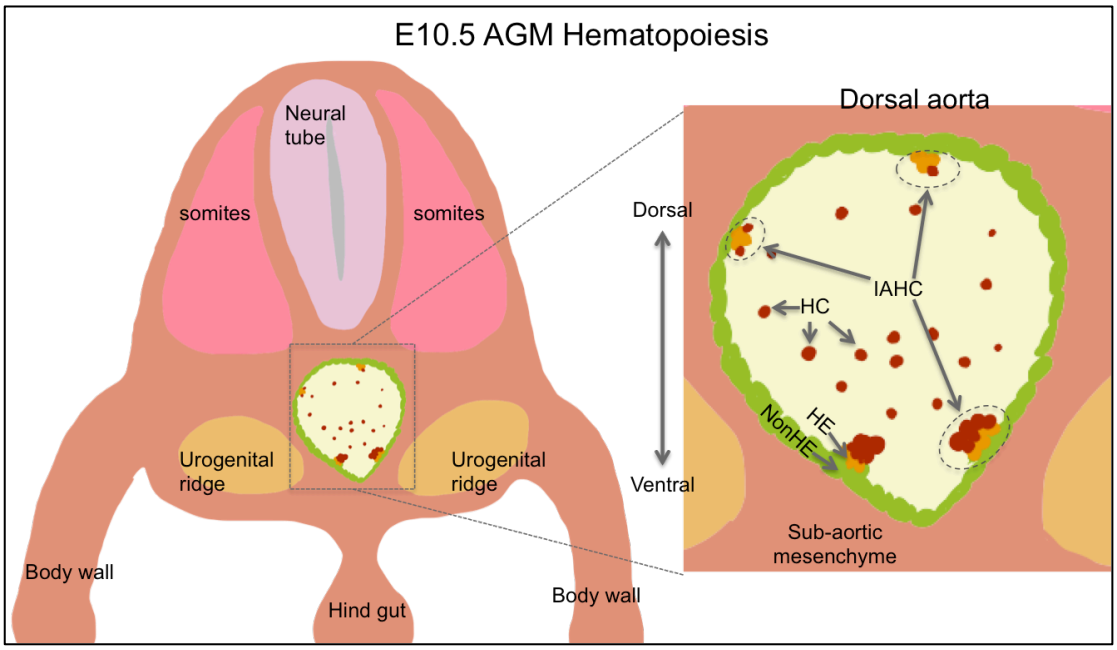

Figure 1.0.2 ***The AGM hematopoiesis at E10.5 of embryo proper. The scheme is drawn based on the information provided by Boisset et al., 2010, 2014. Non-hemogenic endothelium is shown in green, hemogenic endothelium is shown in orange, hematopoietic cells are shown in red, intra-aortic hematopoietic clusters are composed of heterogeneous cell types including the HC and HE cells. IAHCs***

appear in every side of the aortic wall but HSC forming capacity is detected only in the IAHCs emerge from the ventral wall of the dorsal aorta (Taoudi & Medvinsky, 2007).

2.6. Other hemogenic sites

2.6.1. Placenta

In avian embryos, the allantois is an appendage of mesodermal and endodermal origin. First in 1998, its potential role in hematopoiesis was investigated by using quail-chick chimeras. Both endothelial and hematopoietic precursor cells are shown to emerge from grafted quail and contributed into adult chicken bone marrow cells (A. Caprioli, Jaffredo, Gautier, Dubourg, & Dieterlen-Lièvre, 1998). Later by the same group, the origins of the hematopoietic cells emerging from allantois were investigated in chick embryos. Beginning from HH17 stage chick the allantois shows the expression of *VEGFR2 (FLK1, KDR*), followed by expression of *GATA2, SCL* and *GATA1*, a gene expression change suggested to resemble the differentiation of hemangioblast towards hematopoietic cells. Then the observation of CD45+, hemoglobinized cells in structures similar to yolk sac blood islands further strengthens the argument of allantois as a site of hematopoietic differentiation from hemangioblast (Caprioli et al., 2001).

In mouse embryo, the allantois and chorion fuse and forms placenta at E8.0-8.5 stages. Placenta is an extraembryonic tissue composed of trophoblast and two types of mesoderm: allantoic and chorionic mesoderm (Adamson et al., 2002; Downs & Gardner, 1995; Rossant & Cross, 2001). Hemangioblast theory, which argues a mesoderm originating hematopoietic cells, took also attention for chorio-allantoic mesoderm of murine placenta. The first clue for hematopoietic capacity of placenta came from the finding of fetal precursor B cells in the placenta (Melchers, 1979). A few decades later, a comprehensive analysis of hematopoietic potential of the placenta was done by using an in vitro colony assay. Beginning with E9.5, placenta harbors CFU-C and BFU-E as much as caudal half of embryo. Later at E15 and E17, placenta has the highest CFU-C counts

compared with yolk sac, caudal half of embryo and fetal liver. In addition, RT-PCR analysis of placenta at late E9 stage shows Runx1 expression, consistent with the timing of progenitor detection (Alvarez-Silva, Belo-Diabangouaya, Salaün, & Dieterlen-Lièvre, 2003). Yet, this study does not provide enough information to conclude about placenta's contribution to adult hematopoiesis.

In 2005 two groups took one step further from Alvarez-Silva's work and proved the presence of HSCs beginning from E10.5 mouse embryo (Gekas, Dieterlen-Lièvre, Orkin, & Mikkola, 2005; Ottersbach & Dzierzak, 2005). The placenta derived HSCs are shown to express CD34, C-kit and can repopulate myeloid and lymphoid blood cells in primary and secondary adult mouse for longer then 4 months. This clearly shows the presence of definitive HSC with confirmed pluripotency and self-renewal capacity. Although both studies underlie the fact that the HSCs found in placenta outnumbers the AGM, YS and FL, they have different reasoning for it. The group of Stuart Orkin emphasize the presence of more undifferentiated HSCs and less hematopoietic progenitors in the placenta; therefore placenta may serve as a niche for HSC expansion without differentiation (Gekas et al., 2005). On the other hand, Elaine Dzierzak's group draws attention to the presence of endothelial cells expressing hematopoietic markers at the placenta labyrinth site and concludes that HSCs may originate from the hemogenic endothelial cells, similar to AGM and YS hematopoiesis (Ottersbach & Dzierzak, 2005). Mouse placenta surprisingly harbors HSCs but is it because placenta is a site for HSC expansion or placenta is a site for de novo hematopoiesis?

Another study came from Hanna Mikkola's group to investigate de novo hematopoiesis capacity of mouse placenta (Rhodes et al., 2008). They found hematopoietic cells stained with CD41 early hematopoietic marker on placenta of Ncx1 $^{-/-}$ mouse line (Koushik et al., 2001), which lacks heartbeat; therefore it has no blood circulation. Using that mouse line eliminates the idea of detecting hematopoietic cells

generated in other regions. Isolated placenta of Ncx1$^{-/-}$ mouse is shown to generate myeloid, B and T lymphoid cell in vitro culture. However, the lack of adult functional repopulation assay of those cells, in my point of view prevents us to call those placenta originated hematopoietic cells HSCs. Altogether this study provides the first evidence for de novo hematopoiesis capacity of mouse placenta, yet doesn't argue against its function for hematopoietic niche.

2.6.2. Vitelline and Umbilical Arteries

In mouse embryos at E8.0 continuation of dorsal aorta forms omphalomesenteric artery, which then connects with allantoic bud. That connection is called umbilical vessel, while allantoic bud fuses with chorion and forms placenta at E8.5. After E9.5 it makes another connection with the dorsal aorta and forms the vitelline artery. At E10.5 the connection between vitelline and umbilical arteries is lost. The vitelline artery has the connection with yolk sac vasculature and dorsal aorta, while the umbilical artery is connected to chorio-allantoic mesenchyme and placenta (Garcia-Porrero, Godin, & Dieterlen-Lièvre, 1995).

Initial examinations of mouse embryo spotted first detection of hematopoietic cells at E9.5 of vitelline artery and E10 of umbilical artery (Garcia-Porrero et al., 1995). Another mouse study with finely dissected vitelline and umbilical arteries was used to test for its functional repopulation capacity. Similar to dorsal aorta, before E10, no HSC with successful functional repopulation in irradiated host mouse is detected. Starting from E10.5, the dorsal aorta, umbilical artery and vitelline artery are proven to bear HSCs (M. F. de Bruijn, Speck, Peeters, & Dzierzak, 2000). 3 dimensional imaging done by using hematopoietic and endothelial markers, also confirmed the presence of hematopoietic clusters in the major arteries (dorsal aorta, umbilical and vitelline arteries) at E10.5 and E11.0 mouse embryos (Yokomizo & Dzierzak, 2010). In parallel with the timing of identified hematopoietic cells, Runx1, the major transcriptional

regulator of definitive hematopoiesis, is shown to be expressed in the umbilical and vitelline arteries (T. North et al., 1999).

Since the heartbeat starts at E8.25, all produced hematopoietic cells are circulating around yolk sac, embryo proper, vitelline artery, umbilical artery and placenta. Because of that, the origin of hematopoietic cells found in a certain tissue at a certain time of embryo development is uncertain. It doesn't give enough information about the de novo hematopoietic capacity of umbilical and vitelline arteries. When the heart does not beat in Ncx1 mutant mouse, CD41 expressing hematopoietic cells are observed to appear in the umbilical artery (Rhodes et al., 2008), yet the functional hematopoietic analysis of those cells are inadequate. Latest studies showed that umbilical and vitelline arteries bear hematopoietic cells that can generate HSCs upon IL3 introduction (Gordon-Keylock, Sobiesiak, Rybtsov, Moore, & Medvinsky, 2013). Therefore it is highly probable that vitelline and umbilical artery originated cells may contribute to adult hematopoiesis.

2.7. Sites for colonization and expansion of hematopoietic progenitors

2.7.1. Fetal Liver

By the time circulation starts at E8.5 of mouse embryo, all the progenitors with yolk sac origin start to be found in the blood stream, embryo proper and fetal liver. Starting from E9.5, fetal liver becomes a site of colonization for the progenitors generated from other sites. Starting from E12.5 of mouse embryo, among other hematopoietic sites, fetal liver has the highest number of colony forming progenitors and adult repopulating HSCs. The hematopoietic progenitors in fetal liver are dividing and committing to mature hematopoietic cells. In that term, fetal liver is more of a site for hematopoietic cell differentiation rather than the site of initiating hematopoietic program. Mobilized progenitor cells start to colonize in the fetal liver and differentiate to become fully committed hematopoietic cells, and then are released back to the circulation. Although

the liver functions as hematopoietic site until 2 weeks after birth, the main site of residing hematopoietic progenitors is taken over gradually by bone marrow.

Definitive HSCs emerged from AGM of zebrafish embryos detected at the caudal hematopoietic tissue (CHT). The newly formed HSCs go through circulation and to CHT region while still expressing hematopoietic markers *c-myb* and *ikaros* (Murayama et al., 2006). Afterwards it is shown to migrate to thymus and kidney to colonize and contribute to the adult hematopoiesis (Kissa et al., 2008). Regarding the role of CHT as a stop site before seeding the adult hematopoietic organs, CHT may serve as expansion and differentiation site like an equivalent of fetal liver in mammals.

2.7.2. Bone Marrow

Bone marrow is the site of final destination of all hematopoietic stem and progenitor cells, which will stay along the adulthood. Circulating hematopoietic stem/progenitor cells (HSPCs) start to colonize in the bone marrow at E15 stage of mouse embryo(Dzierzak & Speck, 2008; A. Medvinsky et al., 2011) .Bone marrow consists of highly vascularized niche with stromal cells and osteoblast to support definitive HSC's self-renewal and differentiation towards all blood cell types. Different cytokines, which are secreted from nearby cells in the bone marrow niche trigger various programs in the HSPCs. The cell is either promoted to differentiate and form mature blood cells to be released into the circulation or kept quiescent to stay as HSC reservoir for the rest of organism's life. Thanks to that highly specialized niche, HSCs are producing itself and all types of blood cells continuously.

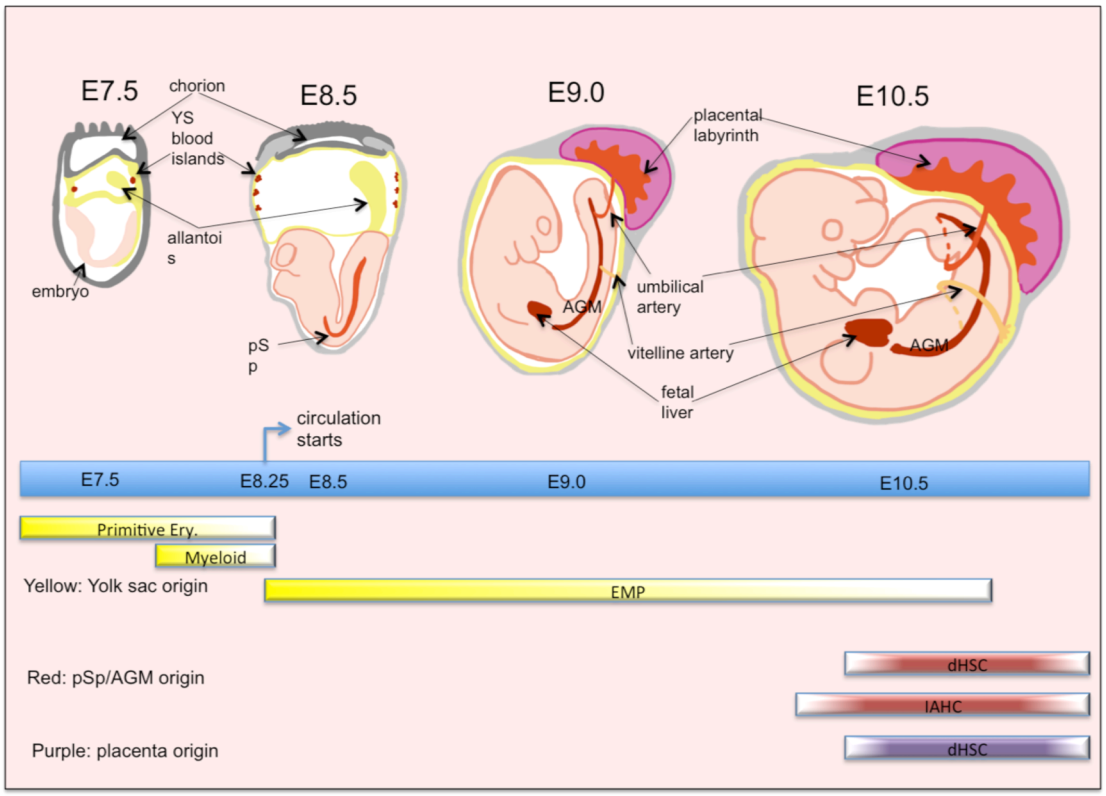

Figure 1.0.3 ***Embryonic hematopoiesis time line with their tissue origin.***

3. *Mechanism of blood cell emergence: How is it generated?*

3.1. Hemogenic endothelial cells as ancestor of hematopoietic cells

In chick and mouse embryos intra-aortic cluster cells are always in close proximity with ventral part of the endothelial lining of dorsal aorta. Hematopoietic progenitor cells also observed to be juxtaposed with endothelial cells of the yolk sac vasculature. Wide range of organisms from avian to murine embryos, finding hematopoietic progenitor cells near the endothelial lining of vessels regardless of the site of origin indicates an evolutionarily conserved relation of endothelial and hematopoietic cells. The hypothesis of endothelial originating hematopoietic cells was proposed.

Supporting evidence comes from commonly expressed genes in both endothelial cells and hematopoietic cells. As an example CD34 expression is detected at the vascular lining and in the hematopoietic cells of E9.0 mouse yolk sac (Young, Baumhueter, & Lasky, 1995). Similarly, in 5 weeks old human embryos, CD34 is expressed in both

endothelial lining of dorsal aorta and the intra-aortic hematopoietic clusters (Tavian et al., 1996). Another gene SCL/Tal1 is a transcription factor expressed in two types of cells, which is shown by studies done by chicken (Drake, Brandt, Trusk, & Little, 1997), mouse embryos (Kallianpur, Jordan, & Brandt, 1994) and human umbilical cord cells (Hwang, Siegelman, Davis, Oppenheimer-Marks, & Baer, 1993). The common gene expression studies indicate a developmental link between hematopoietic cells and the endothelial cells in the surrounding vessel. By these studies, the hypothesis of an endothelial precursor for hematopoietic cells is favored.

Emphasizing the nature of the cell phenotype change, the formation of hematopoietic cells from endothelial precursor is called endothelial to hematopoietic transition (EHT) and those precursor cells are called hemogenic endothelium. The EHT is highly regulated both temporally and spatially, that only rare hemogenic endothelial cells and for a short time window can go through the transition. EHT is now accepted as the birth of first blood precursors and reported in several vertebrate species (i.e. zebrafish, chick, quail, mouse, human). Such a strict regulation of EHT indicates a conserved mechanism, which is tightly controlled by series of intrinsic and extrinsic cellular mechanisms.

3.2. Endothelial to hematopoietic transition

Time-lapse imaging and live cell tracking technology shed more light on the complete process of EHT. At the beginning hemogenic endothelial cells seem not different then other endothelial cells of the vascular lining with flat, highly attached morphology. When the EHT program is initiated in hemogenic endothelial cells, they loose their attachment gradually and gain more round morphology. Afterwards they detach and bud off to the lumen. The morphology change happens in parallel with gene expression and marker protein synthesis change. The hemogenic endothelial cells are gradually losing their endothelial markers and gain hematopoietic markers. The

complete process is a transition of one cell, rather then one asymmetrically dividing cell leading to two different daughter cells.

Our current knowledge about the EHT is based on several studies done by using chicken, quail, zebrafish, mouse and lastly the mES cell models. Since emergence of first hematopoietic progenitors from endothelial cells is observed among that variety of animals, we can conclude that EHT is a well-conserved mechanism responsible of hematopoiesis in vertebrates.

3.2.1. Studies of EHT during development

3.2.1.1. In vivo avian studies

The first observations of endothelial originating hematopoietic cells are done on the developing chick embryos. (Sabin, 1921). Later with the usage of antibodies, endothelial marker proteins are used to trace hematopoietic origin. One of the endothelial marker KDR (a.k.a. *VEGF-R2/FLK-1* and Quek-1 in chicken) is used to sort endothelial cells from gastrulating chick embryo and found to give rise to hematopoietic and endothelial progenitors (Eichmann et al., 1997). Later Dieterlen-Lievre's group used both endothelial marker KDR and hematopoietic marker CD45 to identify the relation of endothelial cells and hematopoietic intro-aortic clusters in chick embryo. Dual staining marked endothelial cells as KDR+, CD45- and intra-aortic clusters as KDR-,CD45+. Acetylated-low density lipoprotein (Ac-LDL) can be up taken by endothelial cells, which makes it very useful to trace endothelial lineage (Voyta, Via, Butterfield, & Zetter, 1984). When they traced the endothelial cells with Ac LDL-DiI, they observed some hematopoietic cells stained with AcLDL, proving the link of endothelial to hematopoietic transition in dorsal aorta of chicken embryo (Jaffredo, Gautier, Eichmann, & Dieterlen-Lièvre, 1998).

3.2.1.2. In vivo zebrafish studies

In parallel with avian and mouse studies, close relation of endothelial and hematopoietic lineage in zebrafish was investigated. The first evidence of developmental link between endothelial cells and hematopoietic cells came from mutant zebrafish lines. Mutation in the *cloche* gene is an example of such defective phenotype effecting expression of both vascular markers (Stainier, Weinstein, Detrich, Zon, & Fishman, 1995) and definitive and primitive hematopoietic markers (Thompson et al., 1998).

Several studies detected definitive HSCs not within intra-aortic clusters but at the sub-aortic mesenchyme in AGM (Bertrand et al., 2008; Kissa et al., 2008; Murayama et al., 2006). A big advantage of zebrafish over mouse is that zebrafish embryos are transparent which facilitates in vivo live cell imaging and cell tracing with reporter lines. Considering that advantage of zebrafish model in hematopoiesis, three groups managed to trace HSCs back to their endothelial progenitor.

Philippe Herbomel and Karima Kissa have showed the endothelial origin HSCs by using zebrafish lines *kdr:EGFP* transgenic line for in vivo time-lapse imaging from stage 28hpf till 100hpf. Their work became prominent by clearly showing at the single cell level the morphological changes that hemogenic endothelial cell is going through while becoming HSC. All endothelial cells are expressing Kdr but only a few have hematopoietic capacity. During EHT, the rare hemogenic endothelial cell bends towards the intra-aortic space and form a round shape while the neighboring lateral endothelial cells are filling the space on the endothelial lining. After staying slightly attached to the endothelial layer, the round cell goes through the sub-aortic mesenchyme and joins the circulation through the cardinal vein. They also showed that in Runx1 morphant *kdr:EGFP* embryos, EHT is initiated more rarely than normal ones and the rare emerging cells die afterwards. They conclude that Runx1 is crucial for a successful EHT and formation of HSCs (Kissa & Herbomel, 2010).

David Traver's group used double transgenic line with *kdrl:mCherry* to trace endothelial cells and *c-myb:eGFP* line to trace hematopoietic cells. Fluorescent imaging clearly spots endothelial cells at the ventral wall of the dorsal aorta with Kdrl+ expression has initially flat endothelial morphology, which then some of them express C-myb and transform to a spherical shape. That Kdrl+, C-myb+ cells migrate towards ventral side and goes into the circulation via caudal vein. They also showed EHT transitions steps by combining markers they used to image and sort with qRT-PCR analysis of important endothelial and hematopoietic markers. They define the hemogenic endothelial cells with isolated Kdrl+, C-myb- gate, expressing genes of endothelial markers *cdh5* and *kdrl* high, some hematopoietic regulators *lmo2*, *runx1* high and hematopoietic marker *CD41*, *CD45* low. It might indicate that hemogenic endothelial cells have already initiated EHT by expressing *lmo2* and *runx1* but not bearing the hematopoietic features yet. Lineage tracing of those endothelial origin HSCs confirm their long-term repopulation and multi-lineage commitment capacities (Bertrand et al., 2010).

A few months later, Maria Vega Flores's group showed time-lapse imaging of EHT by using *runx1P2:EGFP* transgenic zebrafish line, which is shown before to be marking definitive HSCs specifically (Enid Yi Ni Lam et al., 2009). Together with Runx1, to mark endothelial cells they crossed with *kdrl:nls-mCherry* transgenic line and imaged from 22 to 35 hpf. The first co-expressing Runx1 and Kdrl cells are seen at 25hpf at the endothelial lining of the ventral wall of the dorsal aorta. Approximately 9 hours after the co-expression starts, the round shape replaces the flat morphology of endothelial cell. All Runx1 positive round cells are expressing Kdrl, so the endothelial origin of HSCs is confirmed. The Runx1+ Kdrl+ cells are shown to enter the circulation via axial vein and seed thymus and kidney at 5df, therefore HSC nature of the double positive cells are validated. Lastly they did morpholino study on the double transgenic line and showed that deficiency of Runx1 activity, no blood flow or aberrant dorsal aorta can reduce the

number of double positive HSCs. Therefore they conclude that Runx1, blood flow and vascular integrity are regulators of EHT (E Y N Lam et al., 2010).

3.2.1.3. Mouse studies

The close relation between hematopoietic cells and the vasculature in the mouse embryo sections are observed in several studies (Garcia-Porrero et al., 1995; I. Godin et al., 1995). In the mouse yolk sac at E8.25 and E9.5 embryos, isolated Tie2+,Flk-1+ endothelial cells are shown to give rise to CD41 expressing hematopoietic cells as well as endothelial cells upon cultured in vitro (W. Li, Ferkowicz, Johnson, Shelley, & Yoder, 2005) .

Only after the development of genetic cell tracing methods in mouse and knowledge of better cell type specific markers, the clonal link of developing hematopoietic cells from endothelial cells was established. Elaine Dzierzak's lab showed the direct evidence of endothelial derived hematopoietic cell formation by using VE-Cadherin reporter mouse line. Temporally labeled endothelial cells in the time window of E9.5 to E12.5, forms long-term HSCs and contribute to adult hematopoiesis (Zovein et al., 2008). Runx1 is accepted as the major regulator of EHT so that Runx1 KO leads to complete depletion definitive hematopoiesis and embryonic lethality (Okuda, van Deursen, Hiebert, Grosveld, & Downing, 1996; Q Wang et al., 1996). Interestingly, the same phenotype occurs with no definitive hematopoiesis when Runx1 is depleted only in VE-Cadherin+ endothelial cells (Chen, Yokomizo, Zeigler, Dzierzak, & Speck, 2009). Thus, it emphasizes the endothelial origin of Runx1 dependent definitive HSCs. Lastly, the concrete evidence for EHT in mouse came from ex vivo live cell imaging of endothelial cells of dorsal aorta while transiting into hematopoietic cells. Sagitally dissected AGM sections are stained with endothelial marker CD31, and hematopoietic marker Ly6A, and kept alive during time-lapse imaging. Although it includes ex vivo culture of dorsal aorta sections without intact environment, a few hours were enough to capture very

rare EHT events. Similar to chicken and zebrafish studies, this work shows that EHT in mouse is characterized with morphology change from flat to round cells, coupled with marker change from endothelial to hematopoietic (Ly6A, c-kit, CD41) (Boisset et al., 2010).

3.2.1.4. In vitro differentiation studies

In vivo studies on EHT are helpful to see the localization and timing of EHT inside the living embryo, however in vivo techniques are limited especially with mouse, to analyze the transition of each cell and characterization of the stages. Fortunately in vitro mES cell differentiation model passes over the technical obstacles of in vivo cell tracing and system manipulations. By using in vitro differentiation of mES cell techniques, two articles were published in 2009, both present invaluable information about the identification of transiting cells and the stages of EHT.

Georges Lacaud's group showed the hemangioblast cells can give rise to hemogenic endothelial cells and those cells are forming hematopoietic progenitors by going through EHT. Differentiated mES cells were harvested and hemangioblast equivalent Flk-1 expressing cells were put into blast colony assay for time-lapse imaging. After approximately 1.5 days, tightly attached, flat cells appeared and some of them were forming semi-adherent, round cells. FACS analysis of that stage suggest that $Tie2^{hi}$, $C\text{-}kit^{+}$, $CD41^{-}$ cells may further differentiate into CD41 expressing round, non-adherent hematopoietic cells. Those round hematopoietic progenitor cells eventually detached from the adherent cells and can give rise to committed blood cells. They also found that Scl deficient cell lines cannot produce $Tie2^{hi}$, $c\text{-}kit^{+}$ cells, therefore no hematopoietic cells are generated. When they tested Runx1 deficient cells line, they found the formation of $Tie2^{hi}$, $C\text{-}kit^{+}$ cells but no $CD41^{+}$ cell emergence, which can be rescued by re-introduction of Runx1. All together, in vitro differentiation experiment showed a stepwise generation of hematopoiesis. The first step is the differentiation of hemangioblast to hemogenic

endothelium, under the control of Scl then the second step is the differentiation of hemogenic endothelium to definitive hematopoietic progenitors, which is under the control of Runx1 activity. Their study provides the first link between the theory of mesodermal hemangioblast cells as the common precursor for endothelial, hematopoietic and smooth muscle lineages with the recent findings of endothelial originating hematopoietic cells (Lancrin et al., 2009a).

In the same issue of Nature, there was another article from Shin-Ichi Nishikawa's and Tim Schroeder's groups showing in vitro single cell imaging together with marker expressions of the cells going through EHT. Isolated Flk-1 positive hemangioblast-like cells were grown on stromal cells and the formation of hemogenic endothelium, then hematopoietic progenitors was traced at the single cell level. Similar to findings from Lancrin et al. (2009) from single hemangioblast cell, formation of adherent, flat cells with endothelial specific labeled tight junctions (VE-Cadherin::Venus-claudin5) was observed and Ac-LDL uptake was used to mark their endothelial phenotype. Some of those endothelial cells become semi-adherent and round while gaining first CD41, early hematopoietic marker, expression then CD45, late hematopoietic commitment marker, expression. At last, $CD41^{+}CD45^{+}$ round hematopoietic cells loose tight junctions, adherence to the other cells and start floating in the culture. The quantified data for all single cell tracing experiments showed that only 1.5% of mesodermal colonies can generate hematopoietic cells and the timing for all EHT events are roughly synchronized. The same precise transition of adherent, endothelial cells to CD41 expressing non-adherent hematopoietic cells was observed also from the isolated $Flk\text{-}1^{+}$, $VE\text{-}Cadherin^{-}$, $CD41^{-}$ mesodermal cells from E7.5 mouse embryos. In summary, this study confirms the presence of hemangioblast like cells and their capacity to give rise to rare hemogenic endothelial cells, while emphasizing a rare hemogenic endothelium population and time wise tight control of EHT (Eilken, Nishikawa, & Schroeder, 2009a).

3.2.2. Markers to study EHT

EHT can be defined by the change from endothelial to hematopoietic morphology in parallel with change of marker protein expressions. Endothelial cells are forming tight adhesion within each other and have elongated phenotype. VE-Cadherin (Cdh-5), Flk-1, Tie-2, CD31 are a few markers of vascular endothelial cells. While these endothelial cells in the vascular lining going through the EHT, they lose their attachments with the neighboring cells and express less endothelial markers. The transiting cell has a round shape with slight attachment to the endothelial layer and start to express some early hematopoietic markers like CD41 and C-kit. Later those cells detach completely from the endothelial lining of the vessel and express less or no endothelial markers, in parallel with late hematopoietic marker expression like CD45. As a result of the EHT, the hematopoietic progenitor cells with round shape and hematopoietic marker expression appear in the vessel space.

3.2.3. The important transcriptional regulators of EHT

The compilation of abovementioned studies on chicken, zebrafish and mouse puts forward a clear notion of EHT as highly regulated and conserved event, which is vital for development of blood system. Exploring the regulatory mechanisms of EHT will open a gate to understand the basics of EHT and more importantly to use that knowledge to generate blood cells for therapeutical applications. Until now, researchers revealed a few transcription factors, which has regulatory functions on EHT.

Runt-related transcription factor 1, AML1/Runx1 is one of the crucial genes for EHT. The mutant Runx1 mice die at E11-13, due to severe hemorrhage in the brain and the trunk (Okuda et al., 1996; Q Wang et al., 1996). In the Runx1 mutant embryos primitive erythropoiesis in the yolk sac is not affected but the lack of lymphoid and myeloid progenitors and HSCs indicate the vital role of Runx1 in definitive hematopoiesis. (Yokomizo et al., 2008). Cbfb, a binding partner of Runx1, also has similar defective

hematopoietic phenotype when mutated (Qing Wang et al., 1996). Further studies with mES cells reveal that Runx1 deficient EBs generate normal primitive erythroid colonies but less BL-CFC colonies coupled with less committed myeloid and lymphoid progenitors. This indicates that primitive erythropoiesis is independent of Runx1 activity, on the other hand, Runx1 seems regulating hematopoietic commitment of hemangioblasts and also further at EHT (Lacaud et al., 2002).

Although the knockout Runx1 mice have clearly hematopoietic and cardiovascular deficient phenotype, Runx1 gene is not only expressed during hematopoietic commitment. It is also expressed in brain and hair follicle cells. This means differential functions. Regarding the importance of its expression to define hematopoietic commitment, the understanding of its gene expression regulation is the key to trace the hematopoietic program. Studies about its promoter and enhancer show that only distal promoter of Runx1 can be related with definitive hematopoietic development. (Bee et al., 2009; Enid Yi Ni Lam et al., 2009; Nottingham et al., 2007). To use that specific function of distal Runx1 promoter, a mouse reporter line is made with GFP on +23 promoter/enhancer position of Runx1(Bee et al., 2010). Aiming at isolation of hemogenic endothelium, another reporter mouse ES cell line is generated by integration of human CD4 gene into the distal promoter (Sroczynska, Lancrin, Kouskoff, & Lacaud, 2009b).

Since Runx1 is vital for EHT, downstream targets of Runx1 took the interest of Christophe Lancrin for the potential to understand the mechanism of EHT. When they studied the transcriptome of Runx1 mutant mES cell line by microarray analysis, they found that Gfi1 and Gfi1b genes are up-regulated by Runx1. Furthermore, ectopic Gfi1 expression rescues the deficient EHT phenotype in Runx1-/- mESCs. Gfi1 and Gfi1b are transcriptional repressors which are also found mutated in blood cancer cases(Grimes, Chan, Zweidler-McKay, Tong, & Tsichlis, 1996). Further assessment of Gfi1 over-

expression suggested that the expression of Gfi1 and Gfi1b at the early stages of EHT is responsible for the endothelial phenotype loss (Lancrin et al., 2012).

3.2.4. The important signaling pathways of EHT

Hematopoietic clusters are found all around the main arteries of E10.5 and E11.0 embryos, but within dorsal aorta the hematopoietic clusters are reported to be dominantly at the ventral wall (Yokomizo & Dzierzak, 2010). It has been argued that hematopoietic stem cells are originating only from the ventral wall endothelium (Taoudi & Medvinsky, 2007). Previous studies on chicken may explain the dorsal-ventral axis dependence of EHT with different growth factors secreted from dorsal and ventral part of the aorta. Hematopoiesis suppressor EGF is present in the dorsal while hematopoiesis enhancer BMP is present in the ventral part of the chicken AGM. Therefore, gradient of EGF versus BMP signals are formed at the dorsal-ventral axis(Pardanaud & Dieterlen-Lièvre, 1999). Additionally, the ventrally expressed BMP4 is shown to enhance HSC growth in AGM (Durand et al., 2007).

Not only the signaling molecules but surprisingly also the blood flow and biomechanical forces are shown to be crucial for EHT. When Ncx1 gene is inactive, it results in embryonic lethal phenotype with no heartbeat although a fully formed vasculature and normal endothelial cells (Koushik et al., 2001).

Ncx-1 mutant mouse is shown to have normal yolk sac hematopoiesis but embryo proper doesn't have hematopoietic progenitors(Lux et al., 2008). This may mean either the role of migration of yolk sac derived hematopoietic cell to initiate intra-embryonic hematopoiesis or the role of normal biomechanical forces in circulation with functional heart to initiate EHT. Additional studies shed light on the later option.

Sheer stress generated with blood flow can be sensed by the endothelial cells of the vessels through mechanoreceptors and triggers a signaling pathway. Two groups

showed that sheer stress triggers nitric oxide signaling even in vitro cultured cells and absence of this biomechanical force leads to decreased HSC emergence(Adamo et al., 2009; T. E. North et al., 2009) .

Chapter2: Materials and Methods

1. Mouse embryonic stem cell culture and in vitro differentiation

1.1. General conditions of in vitro cell culture

All in vitro cell culture experiments done under the laminar hood (Heraeus Hera Safe HS12, ThermoScientific), authorized to be used by only Lancrin lab members and for only cell lines derived from mouse. Before each use, the laminar hood was turned on for at least 15 minutes. Only sterile pipette tips and plastic pipettes are used. Every item put inside the hood is cleaned first with surface disinfectant 1:100 Chemgene HLD4L solution (MediMark Scientific Ref#: 15126686). The regular cleaning is done with 1:100 Chemgene solution in every use of equipment, and weekly change of water in the waterbath, cleaning inside of the laminar hoods, cleaning of the aspirating pumps. The cell incubators are with steady state at 37°C and 5% carbon dioxide (Heraeus HeraCell and Thermo Scientific Series II Water Jacket).

1.2. mES cell maintenance culture

1.2.1. Medium preparation

To decrease the risk of contamination, some measures are taken in advance. All the mediums are prepared under the laminar hood. Most of the reagents are aliquoted and each person uses a separate aliquot or a complete bottle. If the medium is going to be used for cells to be plated, they are sterile filtered with 0.22μm porous syringe driven filters (Millipore Millex, Ref#: SLGP033RS) or vacuum driven filters (Millipore SteriCup, Ref#: SCGPU01RE). Prepared mediums are stored at 4°C fridge to be used within maximum1 month.

1.2.2. Gelatinization of culture plates and dishes

Culture treated dishes and plates are used to culture adherent cells, with exception of embryoid body culture in suspension. To increase adhesion and survival of the seeded cells, coating the dishes and plates with 0.1% gelatin is needed. First sterile filtered 1xPBS (Oxoid tablets, Cat: BR00146) solution is prepared in distilled water (GIBCO, Cat: 15230-147) for cell culture use only. Sterile filtered 0.1% gelatin (BDH, Cat: 440454B) solution in 1xPBS is prepared. Before seeding the cells, gelatin solution is put into dishes to cover the bottom and kept at room temperature at least 20 minutes under the laminar hood.

1.2.3. Mouse embryonic fibroblast (MEF) coating as feeder cells

Embryonic fibroblast cells are isolated from 13 days post coitus stage embryos from mouse line with Neomycin resistance transgene. Primary cell line is generated from the freshly isolated embryonic fibroblasts and then frozen in 40% Fetal Bovine Serum (FBS) (PAA Clone, Cat: A15-102) at -80°C freezer, transferred to liquid nitrogen tank. To make a stock of MEFs, the primary cell containing vial is thawed in one 15cm dish. Cells are passaged for two times in 15 cm dishes and grown for 5 days. After 5 days, the MEFs are in 15 x 15cm dishes with 70-90% confluence. The old medium is removed and the cells are incubated in a medium containing Mitomycin C at 10μg/ml final concentration (Sigma, Ref#: M4287-2mg dissolved in 1xPBS and mixed with MEF medium) solution for 3 hours in the incubator. After 2 washings with 1xPBS, all MEFs are harvested and counted. The mitomycin treated, neomycin resistant MEFs are frozen as approximately $2x10^6$ cell per vial in a freezing medium containing DMEM (GIBCO, Ref: 41965-039) with 40% FBS (PAA Clone, Cat: A15-102) and 10% DMSO (Sigma, Ref: D2438). All cells are suspended in freezing medium and frozen at -80°C first then transferred into liquid nitrogen tank for long-term storage.

At least one day before starting the ES cell culture, the culture plate has to be coated with Mitomycin treated Neomycin resistant MEF. One vial of stock MEF consisting of $2x10^6$ cells, is thawed in 10 gelatinized wells of 6-well-plate. The medium to be used for MEF thawing is the same medium of ES cell growing, because afterwards ES cells will be introduced on top of this MEFs.

1.2.4. Mouse embryonic stem (mES) cell expansion culture

The mES cell lines I used in my experiments are feeder dependent, so coating of the culture dishes with MEFs beforehand is necessary, as it is described in the previous section. Minimum after 12 hours of coating with MEFs, one vial of mES cell line (0.6-1.2x10^6 cells/vial) is thawed on 1 well of MEF coated 6-well-plate in the medium containing DMEM-KO (GIBCO, Ref: 10829-018) with 15% FBS (PAA Clone, Cat: A15-102), 0.024μg/ml LIF (produced in EMBL HD protein expression facility, stock concentration 1mg/ml), 0.12mM β-Mercapto-ethanol (GIBCO, Ref: 31350-010), 1% Penicillin/Streptomycin (GIBCO, Ref: 15140-122), 1% L-Glutamine (GIBCO, Ref: 25030-024), 1% non-essential amino acids (GIBCO, Ref: 11140-035).

The same medium is used for splitting the mES cells. The next day after thawing mES cells, the cells are harvested. First of all, the medium is aspirated and 1ml of warm TrypLE-Express (GIBCO, Ref:12605-010) is kept on cells for 3 minutes. The reaction is stopped by adding 1ml of medium and the detached cells are collected in a tube. Then the cells are counted by using hemocytometer. For splitting into MEF coated wells of 6-well-plate, cell density of 0.3*10^6 cell/well is needed. The volume is calculated and mixed with necessary amount of fresh medium. The old medium inside the MEF coated wells is aspirated. The homogenized cell mix is added on top of wells. The cells are passaged on MEFS exactly 2 times after thawing.

For making a stock of mES cells, at the second passage after the thawing, the harvested cells can be frozen. There should be at least 0.6*10^6 cells/vial. The freezing

medium is the DMEM-KO with 1% Penicillin/Streptomycin (GIBCO, Ref: 15140-122), 1% L-Glutamine (GIBCO, Ref: 25030-024), 1% non-essential amino acids (GIBCO, Ref: 11140-035), 40%FBS (PAA Clone, Cat: A15-102) and 10%DMSO(Sigma, Ref: D2438). Freezing is done first at -80°C and then the vials are transferred into liquid nitrogen tank.

After 2 passages on MEFs, feeder cells should be eliminated before starting the differentiation of mES cells. For that, 2 more passages are needed on gelatin coated wells. The splitting process is exactly the same from cells on MEF, except that the TrypLE reaction takes place only for 2 minutes to detach less MEFs. Although some MEFs can still be carried over to the new wells, since MEFs cannot proliferate, there will be less MEFs after 2 passages. Before starting the differentiation of mES cells, in the last passage on gelatin, the medium base DMEM-KO is replaced by IMDM for better adaptation into the differentiation medium later. The IMDM based stock medium; IMDM (Lonza, Ref: BE12-726F), 1% Penicillin/Streptomycin (GIBCO, Ref: 15140-122), 1% L-Glutamine (GIBCO, Ref: 25030-024), is preraed and named as IMDM* in the rest of the protocol.

1.2.5. Embryoid body (EB) culture

EB mix is prepared with IMDM (Lonza, Ref: BE12-726F), 1% Penicillin/Streptomycin (GIBCO, Ref: 15140-122), 1% L-Glutamine (GIBCO, Ref: 25030-024), 0.6% Transferrin (Roche, Ref: 10652), 0.03% MTG (Sigma, Ref: M6145-25ml), 50mg/ul Ascorbic Acid (Sigma, Ref: A-4544) and sterile filtered through 0.22μm vacuum driven filtration unit (Millipore SteriCup, Cat: SCGPU 01RE). mES cells on gelatin with IMDM-ES medium are harvested after 2 minutes of treatment of TrypLE and total cell number is counted. The cell density should be 0.25*10^6 cell/10 cm dish in 10mL EB mix. The necessary amount of cells are mixed with calculated volume of warm EB medium and then distributed into 10cm dishes (Sterilin) very slowly through the walls

of the dishes. The dishes are non-culture treated, for non-adherent cultures. The cells are kept in the incubator for 3 days and monitored daily monitoring. Usually the EBs are forming from the day 1 and some of them attached to the bottom, which is inhibiting their proper differentiation. At the second day, to eliminate those sticky EBs, the medium with floating EBs is slowly transferred into a fresh dish. At day 3 of EB culture, the diameter of the EBs can reach to 200μm.

1.2.6. Isolation of blast colony forming cells from EBs

Inside the EBs, there are several types of cells differentiating, including the blast colony forming cells (BL-CFCs), which can give rise to hematopoietic cells, endothelial cells and smooth muscle cells. BL-CFCs inside the EBs are present in the Flk-1+ population between day 3 and day 3.5 and can be isolated with this cell surface marker. The maximum amount of Flk-1+ cells can be isolated at day3.25. In order to isolate the BL-CFCs at day3.25 EB culture, I used magnetic-activated cell separation (MACS) technique to elute cell population enriched for Flk-1 expressing cells. All EBs are pooled down together in the same tube, centrifuged to pellet them and remove the media. Then 2ml TrypLE/tube is applied for 2 minutes in the 37°C waterbath while shaking the tubes. The reaction is stopped by adding 5ml of IMDM+20%FBS. The single cell suspension is filtered through 0.22μm pores. The dead cells are removed in cell suspension with a separate phase of lymphocyte separation medium 1077 (GE Healthcare, Ref: J11-004) by centrifuging at 800g for 20 minutes without acceleration and brake. After centrifuging the middle phase includes alive cells. They are resuspended and counted with a hemocytometer. The first staining of cells is in MACS buffer (1xPBS, 0.5% FBS, 0.5mM EDTA sterile filtered) with cell density of 1*10^8 cell/ml and 1/33 diluted Flk-1-APC antibody (eBioscience, Ref: 17-5821-81) for 5 minutes at 4°C fridge, light-protected. Afterwards the cells are washed with 10ml MACS buffer and spun down with 1200rpm for 5minutes. The second staining is done with cell density of 1*10^8 cell/ml in MACS buffer and 1/5 diluted anti-APC magnetic beads

(Miltenyi Biotech, Ref: 130-090-855) for 15 minutes at 4°C fridge, light-protected. Again the cells are washed and resuspended in 500ul of MACS buffer. For magnetic sorting, the cell suspension is put through LS columns (Miltenyi Biotec, Ref: 130-042-401) attached to medium size magnet. After 3 washings with MACS buffer, the column is separated from the magnet and the plunger made the Flk-1+ cell population is eluted in the tube. With that method, approximately 90% purity can be reached in the Flk-1+ fraction.

1.2.7. Blast culture

The Flk-1+ cells are resuspended and counted in IMDM*+20% FBS (PAA Clone, Cat: A15-102) medium. The cell density should be 0.10*10^6 cells/cm2, which makes 0.55*10^6 cells per 10cm dish or 0.10*10^6 cells per 1 well of 6 well plate. The needed wells or dishes are gelatinized beforehand. The Blast medium is prepared as IMDM*+ 15%FBS (PAA Clone, Cat: A15-102), 0.03% MTG (Sigma, Ref: M6145-25ml), 0.025mg/ml Ascorbic acid (Sigma, Ref: A-4544), 1% L-Glutamine (GIBCO, Ref: 25030-024), 0.6% Transferrin (Roche, Ref:10652-202-001), 0.005μg/ml VEGF (RandD, Ref: 293-VE-010), 0.01μg/ml IL-6 (RandD, Ref: 406-ML), D4T supernatant and sterile filtered. D4T supernatant is prepared as the medium (30mg Endothelial Cell growth supplement (Lot 81879) added into 500 ml of IMDM 10% FBS) of D4T endothelial cells collected after culture for 4-10 days. The cells are mixed with necessary amount of blat mix and put on the gelatinized wells and dishes.

1.2.8. Hemogenic endothelium culture

In order to facilitate endothelial to hematopoietic transition, we used another culture medium consisting of IMDM* (IMDM with 1% L-Glutamine and 1% L-Ascorbic Acid), 10% FBS (PAA Clone, Cat: A15-102) + 1% L-Glutamine (GIBCO, Ref: 25030-024), 0.6% Transferrin (Roche, Ref:10652-202-001), 0.03% MTG (Sigma, Ref: M6145-25ml), 0.05mg/ml Ascorbic acid (Sigma, Ref: A-4544), 0.024μg/ml LIF (produced in EMBL HD protein expression facility, stock concentration 1mg/ml), 0.05μg/ml SCF (Peprotech, Cat:

250-03), 0.025μg/ml IL-3 (RandD, Cat: 403-ML), 0.005μg/ml IL-11 (RandD, Cat: 418-ML), 0.01μg/ml IL-6 (RandD, Cat: 406-ML), 0.01 μg/ml OncostatinM (RandD, Cat: 495-MO), 0.001μg/ml bFGF (recombinant human bFGF, RandD, Ref:233-FB). The sterile filtered medium prepared and the cells are plated in the density of 0.20*10^6 cells/cm2. It can be kept in the incubator for maximum 3 days without changing the medium.

1.2.9. Hematopoietic progenitor culture

Later to test the potential of cells to give rise to myeloid and erythroid cells, we used hematopoietic progenitor culture, which contains growth factors to facilitate hematopoietic commitment. It is a semi-liquid medium with 55% methylcellulose (VWR, Ref: 9004-67-5 500g dissolved in 1L IMDM solution). The medium is first prepared with liquid ingredients, which are IMDM* (Lonza, Ref: BE12-726F), 15% PDS serum replacement (Antech), 1% L-Glutamine (GIBCO, Ref: 25030-024), 0.05mg/ml Ascorbic acid (Sigma, Ref: A-4544), 0.6% Transferrin (Roche, Ref:10652-202-001), 0.03% MTG (Sigma, Ref: M6145-25ml), 10% PFMH-II (GIBCO, Ref:12040-077), 0.05μg/ml murine SCF (Peprotech, Cat: 250-03), 0,025μg/ml IL-3 (RandD, Cat: 403-ML), Epo (RandD, Cat: 959-ME), GM-CSF (RandD, Cat: 425-ML), M-CSF (RandD, Cat: 416-ML), Oncostatin M (RandD, Cat: 495-MO), 0.01μg/ml IL-6 (RandD, Cat: 406-ML), 0.005μg/ml IL-11 (RandD, Cat: 418-ML), 0.024ug/ml LIF (produced in EMBL HD protein expression facility, stock concentration 1mg/ml), 0.001mg/ml bFGF (recombinant human bFGF, RandD, Ref:233-FB). The sterile filtered medium is prepared and then the 0.09*10^6cells are mixed in 1.7ml of the filtered medium, and they are mixed with 1.8ml of warm methyl-cellulose. To make a homogenous mix, the tube is vortexed for a minute. By using syringe, the viscous liquid is distributed into 3 dishes (50mm, Sterilin, item code 122). Then 3 dishes are incubated for 8 days. The number of colonies with their phenotype is counted at day5 and at day8 of the culture. The classification of colonies is done according to literature. The average of the counts from 3 dishes is taken for each condition.

2. Defining cell type and population identity

2.1. Flow cytometry and Fluorescent-activated cell sorting

All stainings are done with single cell suspensions with known cell count. Staining is performed in 1xPBS+5%FBS (PAA Clone, Cat: A15-102) if the cells are used only for flow cytometry analysis. Otherwise, when the cells are going to be seeded afterwards, the staining is done in IMDM*+10%FBS and sorted cells are collected in IMDM*+20%FBS. Fluorophore conjugated antibodies are used for single staining otherwise a primary antibody with secondary and/or tertiary antibodies are used, as it is explained in the table. The equipment and technical support is provided by the EMBL Monterotondo flow cytometry facility. Flow cytometry analysis is performed on FACS Canto and FACS Aria (both from BD Biosciences), cell sorting is performed only with the FACS Aria. All of the raw data is analyzed by using the FlowJo software (Tree Star). The graphs shown in the figures are after gating of live cell population without doublets. For dead cell staining, either 100X 7AAD (Sigma, Cat:A9400-1MG, dissolved in 1xPBS+Mg+Ca, final concentration 1mg/ml) or 100X Sytox Blue (Invitrogen, Cat: S34857, dissolved in DMSO, final concentration is 0.1mM) is used, depending on the combination with other flurophores.

Anti-	Alternative name	Clone	Conjugated	Catalog n. (eBiosciences)	Dilution
CD309	Flk-1	Avas12a1	APC	17-5821-81	1/33
hCD4	T4, L3T4	S3.5	PE	MHCD04044 (invitrogen life tech.)	1/300
CD41	Integrin alpha2b	eBioMWReg30	Bio	13-0411-81	1/200
CD41	Integrin alpha2b	eBioMWReg30	PE	12-0411-82	1/400
CD144	VE-Cadherin, Cdh-5	eBioBV13	Fluor® 660 (replacement of Alexa647)	50-1441-82	1/200
Streptavidin	SA, SAV		PE-Cy7	25-4317-82	1/300

Table 2.1 ***Antibodies used for flow cytometry analysis and sorting***

2.2. Bright field and time-lapse imaging

Cell morphology and growth is regularly monitored by using Leica bright field microscopy. The phase-contrast, time lapse images were taken with the IncuCyte HD (Essen Biosciences) inside the incubator, every 15 minutes, 9 spots in a well. The time-lapse video is generated as 10 frames per second by using Fiji software. For quantification of the number of round cells in each frame, the image stacks from each spot is analyzed by CellProfiler software with a customized pipeline written by Christian Tischer from EMBL Heidelberg Advanced Light Microscopy Facility. For each time point, the average and standard deviation of counts from each 9 spots is calculated to make graph on Microsoft Office Excel software.

2.3. Total RNA extraction from frozen cell pellets

The in vitro cultured cells are collected in a tube and centrifuged for 5 minutes at 2000rpm. Then the supernatant is aspirated, leaving only the cell pellet at the bottom of the tube, which is snap-frozen on dry-ice. The cell pellet is kept at -80°C for maximum 1 month storage. For RNA extraction the supplier's (Qiagen) protocol is followed. The cells are lysed into RLT buffer with 1% β-Mercapto ethanol and homogenized by centrifuging on QIAshredder columns. If the number of cells are within the range of 3*10^6cells to 0.5*10^6 cells, RNA extraction is done by using Qiagen RNeasy Plus Mini kit. If the cell number is lower than 0.5*10^6cells, the Qiagen RNeasy Micro kit is used for RNA extraction. After the elution of total RNA with RNase free water, the concentration is measured with Nanodrop and the samples are stored at -80°C freezer for long term storage.

2.4. Reverse transcription

For synthesizing cDNA, total RNA samples are thawed on ice. Depending on the measured concentration, necessary amount of RNA sample is put into the tubes. Reverse transcription reaction is done according to the RevertAid H Minus First Strand cDNA

Synthesis kit (Thermo Scientific, K#1631). Random hexamer primers are used from the kit. Denaturation step is applied at 65°C for 5 minutes. Then after addition of dNTP mix, RNase inhibitor, reaction buffer and reverse transcriptase enzyme, the tube is incubated at 25°C for 5 minutes and at 42°C for 60 minutes. For 0.2ng template RNA, I diluted the final volume up to 100µl. That concentration I kept for further qPCR reaction.

2.5. Quantitative real time polymerase chain reaction

Primer design is done by using primer3 based online tool from Roche universal probe center (http://lifescience.roche.com/shop/en/be/overviews/brand/universal-probe-library). We selected specifically intron spanning primers, which will recognize all transcript variants of a gene. We excluded primers with high probability of hybridization with itself or with its pair. Lastly the primers were checked for recognition of wanted transcripts but not other genes, by using nucleotide BLAST website (http://www.ncbi.nlm.nih.gov/blast/Blast.cgi?PROGRAM=blastn&PAGE_TYPE=BlastSearch&LINK_LOC=blasthome). The designed primers were synthesized by Sigma Aldrich and resuspended at 100mM in distilled water. The stock primers are kept at -20°C freezer. (See Table 2.2 for the complete list of primers)

For qRT-PCR reaction, LightCycler 480 SYBR Green I Master kit (Roche, 04707516001) is used with Roche LightCycler 480 RT-PCR instrument. For each reaction, 2ul of PCR-grade water (provided in the kit), 0.5ul of 10uM of forward and reverse primer mix, 5ul of 2x master mix (provided in the kit) and finally 2.5ul of cDNA template is added into one well in a 96 well plate. The reaction program has initial denaturation at 95°C for 5 minutes, then 45 amplification cycles of 95°C, 60°C, 72°C for 10seconds in each temperature. At the end of amplification cycles, melting curve step is added as 95°C for 5 seconds, 65°C for 1 minute and continuously increasing up to 97°C. At last as a cooling step, the temperature is dropped to 40°C for 30 seconds. For the ct value quantification and amplification curves, "Absolute Quantification/2nd Derivative

Max" analysis is done through the Light Cycler software. For quantification of melting peaks and melting curves, "TM Calling" analysis is done through the software. The primers forming amplicons with different length (with different melting peaks), strong amplicons in no template control samples (strong primer dimers), secondary melting peaks (uneven denaturation) were eliminated. For those, the primer design and test steps are repeated.

Gene Name	Forward primer sequence	Reverse primer sequence
H2afz	Acagcgcagccatcctggagta	ttcccgatcagcgatttgtgga
Hprt1	gcttgctggtgaaaaggacctctcgaag	ccctgaagtactcattatagtcaagggcat
Ppia	cgcgtctccttcgagctgtttg	tgtaaagtcaccaccctggcacat
Adcy4	ggccaggatttcgagtagc	tggccatagtgaataccagga
Cacna2d1	caatggacaaatgtgtatttgga	gacgttgaagactggtagagttcc
Cdh5	Tcatcaaacccacgaagtcc	ggtctgtggcctcaatgtaga
Col4a2	Gcgcacaaccaggaccta	tacaggaaaggcatggtgct
Col4a5	Ccctggagagagaggtagtcc	Catacccatttcgcctttga
Dpysl3	Agaaggccacgttctgagc	Tgatggcacggaacacag
Enpp1	Cggacgctatgattccttaga	agcacaatgaagaagtgagtcg
Eps8	Cactgggagatagttgggtga	ggacgtaaggtgggatgaac
Esam	Tgctcagtaccagtgggaga	ctttaaagatccacgaacagca
Fam122b	Cgagtcctgttctcaatccaa	accaagaacactgggcctaa
Flrt2	Ggagacaaggctgccaga	caggcaggcaaatcttcttt
Fmo1	Tggcctccatcaagtgct	Gactggctctcccttcttca
Gpr126	Aatgcaccttcaaattttagcat	Ctgtccgttcccgaagt
Lad1	Ctagggactgcctccctttc	ttggcaaaataacccagctt
Lgr5	Cttcactcggtgcagtgct	cagccagctaccaaataggtg
Meis2_set1	Ccagtcaaatcgagcaggtt	gggctgaccctctggactat
Meis2_set2	Catcatcattccctgtcagc	caggtgaagctacgctgttg
Meis2_set3	Tgacctcgtgattgatgagag	Aggatgaagggttgtggtc
Met	Caccaccaagtcagatgtgtg	Aggggctcctctcgtcat
Myb	Tgtcaacagagaacgagctga	Gctgcaagtgtggttctgtg
Npr1	Tggagacacagtcaacacagc	cgaagacaagtggatcctgag
Pcdh12	Cctgttggaccctaatacaggt	gtgaggggcaatgacaatct
Pdzd2_set1	Gccgacaccctaatccaaa	Gtgctgcgtgctatcacttc
Pdzd2_set2	Ggaagctgtggctattctgc	Ctcttctgacccgagcatct
Plcd1	Tacagtcccgtggagatgtg	ggggtttggaagttcagagc
Ppp1r16b	Ccatggatgagatgccaata	ccaacagcaggaccttgaat
Samd4_set1	Ttagacaagtgtcttgttcatgagg	gagggaaagaccgaaagagc
Samd4_set2	Caagcgcgtaagccagac	ttgccattggttaatgattcc
	Gtacccaagcccgctttc	gcaggtggatatcattgcag
Sash1	Agaaatgaaaaagcccagca	ttcatcttggactggggaat

Serca3	Agcagttcatccgctacctc	gaattgctgtgaggaagatgc
Sla	Gaggccgttatccagcagt	aggagatgggtagtcagtcagc
Upp1	Accgctacgccatgtataaag	Atgccgatggaaggaatg
Gdpd5	Cttctcagagatcagtgatgg	ttagcataggtgtcgtaactg
Gria4	Gacgaaactaatggatcgct	gcagaagtgtactttggagg
Palld	Tgctgatggatacccagtg	Tcctggtgcatgcttactc
Dcaf12l1_set1	Caatgcgctctacactcac	cagttccactctgagaagga
Dcaf12l1_set2	Cactcactgctacaactgg	Cagttccaccttagctcca
Ptprm	Gaattggtagttaaagagccac	ctgtatccacagataggttgc
She	Ggacacgcaggagaagaatgg	gggtcagcgtagtcctctaaaa
Myom1	Cacctattcttgtgatgtgacag	Agcagacgtttcatttcctc
Notch1	Tcaatgttcgaggaccagatg	tcactgttgcctgtctcaag
Lat	Gtccctgttgtctcctctg	atcttcacacgactccacag
Fbn1	Cagatccatccaacactgc	Taccctttctggcacagac
Ptprb	Atggctctacagtaccatctc	cacgagaccaggaaattagga
Kdr	Tctttgcgctaggtatcca	agagtaaagcctatctcgctg
Tek	Cttagtgacattctccctcc	tgtccaagaaaccatagctg
Cldn5	Ttcccggtcaagtactctg	Tcttcttgtcgtaatcgcc
Eng	Gttgcaacttagctctgcg	Aaggcctttaccagacagg
Akt1	Agctcttcttccacctgtc	Gaggttctccagcttcagg
Akt2	Cgacccaacacctttgtca	Gatagcccgcatccactct
Akt3	tggaccactgttatagagagaacattt	Tggatagcttccgtccactc
Cdh2	Gccatcatcgctatccttct	ccgtttcatccataccacaaa
Tgfb1	Accaaggagacggaatacag	Cgttgatttccacgtggag
Tgfb2	Ggcttcaccacaaagacag	aattattagacggcacgaagg
Snai1	Gaagatgcacatccgaagc	Gaatggcttctcaccagtg
Snai2	Gacacattagaactcacactgg	Aaagccctattgcagtgag
Csfr1	Cagcaatgatgttggcaca	ggtcaagtttaagtaggcactctcc
Mpo	Tacatgtggccctagacct	Gcaggtgtcaacacatctg
Lmo2	Gacggaaattgtgcaggag	Gatgcacagagaccatcct
Lef1	Ccgtcagatgtcaactccaa	gggtagaaggtggggatttc
Sfrp4	Acctgagcaaaaactacagctatg	ctaccacagttgtgacctcattg
Wnt7b	Tcatgaaccttcacaacaatga	Tggtccagcaagttttggt
Axin2	Ctgctggtcaggcaggag	Tgccagtttctttggctctt
Porcn	Tgcttcttaccatctgcttcg	Tgcttgcatgcttcaggtaa
Nxn	Ttgccaagtacaaagccaaa	ggtgtaatctctcagggagtcagt
Tle3	Agaaagacagcctcagcag	Ttgctgggtcctcattagag
Htra3	Ctgcagaagggtgcctgt	Gaacttgtaccgcggactg
Bmp2	Cttccatcacgaagaagcc	Tgagaaactcgtcactggg
Ltbp1	Ctcaagccaaagccatcaa	ctgggaagataagggtgcaa
Ltbp1_1	Cagaggtgcaccaaacagg	Gctggacagcgcaggtat
Ltbp1_2	Gggcccacattgtgagaa	cattccaccaggacagatttc
Ltbp1_3	Cccacattgtgagaaatgtcc	Gttcccacgaggaggtca
Tgfb3	Cgagtggctgttgaggaga	gctgaaaggtgtgacatgga
Gpr97	Aacttcgctgagcactgatg	Ctcttccgtggtctcctcat

Gpr141	Gaacaaggagggtggatgtg	tcgagagtcagtcattaccacct
Gpr39	Ctccagctgaggaagtcag	caccacaatcagtctcagga
Gnao1	Ggagtgcttcaaccgatctc	gatccaggctgtccaggtag
Gpr77	Gaatgagaggcagagaacag	gtggtgtggttcatcattctg
Gpsm3	Gcaccatccttagtcaccagt	ctccaccctgaactctcagc
Acvrl1	Acacccaccatccctaacc	tggggtaccagcactctctc
Acvr1	Attgaagggctcatcaccac	Aagaccggagccacttcc
Bmpr1a	Tggctgtctgtatagttgctatgat	tgcttgagatactcttacaataatgct
Acvr1b	Agagggtggggaccaaac	Tgcttcatgttgattgtctcg
Tgfbr1	Aaattgctcgacgctgttct	ggtacaagatcataataaggcaactg
Bmpr1b	Tcgatggagcagtgatgagt	Cgcccagcactctgtcata
Acvr1c	Tgggaaatagctcgaaggtg	gtaaggcaactggtactcctcaa

Table 2.2. ***List of primers used for conventional qRT-PCR***

2.6. mRNA microarray

The total RNA extracted as it is explained above was sent to EMBL Heidelberg Gene Core facility. Jelena Pistolic performed the quality control analysis of RNA samples by BioAnalyzer, concentration measurement by Qubit. Then she runs samples by using Affymetrix GeneChip Mouse Gene 2.0 ST Array. She made the initial analysis of the raw data with Gene Script software then by using the customized code in R. Each pair of samples were compared to calculate the log2 fold change values and corresponding p values. Those values are used to draw fold change graphs and to assess the gene ontology (GO) terms. For GO analysis the web based Gene Ontology enRIchment anaLysis and visuaLizAtion tool (Gorilla http://cbl-gorilla.cs.technion.ac.il/) is used; only the GO biological process terms are shown.

3. Sample isolation from mouse embryos and population identity

For in vivo analysis C57B6/N wild type mouse line is used. Violetta Paribeni and Maria Kamber from the EMBL Monterotondo Mouse Facility took care about the mice maintenance and breeding. All mice related procedures are in accordance with European and Italian ethics regulations. For time control mating, 2-6 months old one male and two female mice are put together in a cage at around 3pm. The next morning the males and females are put in separate cages. If there is any vaginal plug seen in the

females, it is accepted as E0.5 time point of embryo development. The pregnant mouse is then sacrificed to isolate the embryos from the womb. During the embryo dissection, embryos are kept in 1xDPBS (GIBCO, Ref:14190-136)+10% FBS (PAA Clone, Cat: A15-102) on ice. First the tissues belonging to the mother, such as womb and fat, are removed. Then the placenta and covering vasculature is removed. Lastly the yolk sac is torn gently and separated from embryo proper by tearing off the umbilical and vitelline vessels. At that stage, the somite pairs of the mouse are counted to determine the developmental stage of the embryo. Further dissection is done to remove head, tail, limb buds, ventral organs and somites to ultimately isolate the aorta-gonad mesonephros (AGM) region (if it is earlier then E9.5 the region is named para-aortic splanchnopleura). Yolk sac and AGM samples from the same embryonic development stage within corresponding somite pair stages are pulled down in the same tube.

In order to use the isolated AGM and yolk sac samples for FC analysis and FACS sorting, single cell suspension is made by collagenase treatment for 30 min. at 37°C in 1 ml of 1xDPBS+10%FBS solution. To stop the reaction, 9ml cold 1xDPBS+10%FBS is added. If the cells are going to be used only for FC analysis, the same 1xDPBS+10%FBS solution is used for the rest of the procedures. If the cells are going to be sorted and plated in culture IMDM+10%FBS solution is used for later steps. The single cell suspension of AGM and yolk sac is counted by using a hemocytometer. Cells are resuspended at a density of 5*10^6 cells/ml and stained with appropriate antibodies: 1/200 VE-Cadherin- eFluor® 660, 1/400 CD41-PE, 1/200 CD41-Biotin are used for staining for 15 minutes at room temperature, light-protected, on shaker. Then the tubes are washed and centrifuged. If any primary antibody with biotin is used as the primary staining, 1/300 Streptavidin-Pecy7 is used as a secondary staining. Lastly the cells are suspended and filtered through FACS strainer tubes. For dead cell staining, 7AAD or Sytox Blue is added to the cell suspension. The samples are always put on ice. The

samples are run through FACS Aria for single cell sorting provided by the EMBL Monterotondo FACS facility.

4. Single cell gene expression analysis

4.1. Primer design

In total I needed to have primers for 96 genes to use in 96*96 chip assays. A nested primer strategy was followed; basically to have 2 pairs of primers for reverse transcription and pre-amplification reactions and 2 pairs of primers for qPCR reaction. The first 48 primers were designed by DeltaGene company while the second set of 48 primers were designed by me, by using the same parameters of DeltaGene. Primer3 web based tool (http://primer3.ut.ee/) was used to design intron spanning outer and inner primers for each gene. Specifically primers were chosen to recognize two exons common for all transcript variants. The melting temperature (TM), G-C content (GC%), primer size, amplicon size parameters are deciphered based on the statistics of first 48 primer design by DeltaGene. (See Table 2.3 and 2.4 for the parameters) Primers with high probability of self-complementary or secondary structure formation were eliminated. (See Table 2.5 for the complete list of primers for single cell qRT-PCR)

	Min.	Opt.	Max.
TM (°C)	60.5	65.5	70.2
G-C%	40	50	61.2
Primer Size (bp)	18	20	25
Amplicon length (bp)	95		130

Table 2.3 ***Outer primer parameters for RT and pre-amp.***

	Min.	Opt.	Max.
TM (°C)	58.6	65.5	78.9
G-C%	36.7	52.4	68.8
Primer Size (bp)	16	20	30
Amplicon length (bp)	40		Size of the cDNA

Table 2.4 ***Inner primer parameters for qPCR***

Gene name	Outer forward	Outer reverse	Inner forward	Inner reverse
Acvr1	cgaGTGCTAATGATGATGGCTTTCCC	cgtTTCACAGTGGTCCTCGTTCC	cgaTTCCCCGAGTGTGGAAGATGA	cgaTTCCCCGAGTGTGGAAGATGA
Acvrl1	cgaATTGCCCATCGTGACCTCAA	cgtGGTTGTTGCCGATATCCAGGTA	cgaAGTCGCAATGTGCTGGTCAA	cgaAGTCGCAATGTGCTGGTCAA
Adcy4	cgaTGGTGGCATCTTGTTCCCTA	cgtTCAGCTTGGGTTCCTTCAGTA	cgaCATTCCCACGCCTGGCTGTC	cgaCATTCCCACGCCTGGCTGTC
Atp2a3	cgaCCATTGTGGCTGCAGTAGAA	cgtCCCAGAATTGCTGTGAGGAA	cgaGAGGGCAGGGCCATCTACA	cgaGAGGGCAGGGCCATCTACA
Bmpr1a	acgTTCACCGAAAGCCCAGCTA	tcgCGGATGCTGCCATCAAAGAA	acgCGCAGGACAATAGAATGTTG	acgCGCAGGACAATAGAATGTTG
Cacna2d1	acgCCAATGGTTTTAGCTGGTGACA	cgtGATTGGCCAGTGACGTTGAA	acgAGCAAGTTCAATGGACAAATGTG	acgAGCAAGTTCAATGGACAAATGTG
Cdh5	cgaCACCATCGCCAAAAGAGAGAC	cgtCTTAGCATTCTGGCGGTTCAC	cgaGGATTTGGAATCAAATGCACATCG	cgaGGATTTGGAATCAAATGCACATCG
Col4a2	cgaCCCTGGAAGCCCTGGATTTA	cgtTGTCTTCCCTTAAGTCCCAACA	cgaTGGCAGGGATGCCTGGT	cgaTGGCAGGGATGCCTGGT
Col4a5	cgaGGACTCTCTGTGGATTGGCTA	cgtATGAAGGGAGCGGAACGAA	cgaTTCATGATGCATACAAGTGCAGGA	cgaTTCATGATGCATACAAGTGCAGGA
Dcaf12l1	cgaAGGCCTCCATGGCAACTAC	cgtGGTGGGGAGACCCAGAAAA	cgaGCAGGCCTCTGGAGCTA	cgaGCAGGCCTCTGGAGCTA
Dpysl3	cgaCCATTGGGAAGGACAACTTCAC	cgtCGGCCACAAACTGGTTTTCA	cgaCCATCCCTGAAGGCACCAAT	cgaCCATCCCTGAAGGCACCAAT
Enpp1	cgaCCATGAAAGGAACGGCATCA	cgtAATTTCCTGGCTTCGGATGAC	cgaTCAGCGGTCCCGTGTTT	cgaTCAGCGGTCCCGTGTTT
Eps8	cgaAGGCTGCCATGCCTTTCAA	tcgTGCTGTTCCTCGCCACAAA	acgCTCCTAATCACCAAGTAGATAGGAATTATG	acgCTCCTAATCACCAAGTAGATAGGAATTATG
Esam	cgaAGTCTATGTCTGCAAGGCTCAA	cgtCCCAACAAAAGTGCCCACAA	cgaCAGAGTGGGCTTTGCCAAGT	cgaCAGAGTGGGCTTTGCCAAGT
Fam122b	cgaAGTTTCTCCAGCTCCTTCCC	cgtAAATGTCTTGGATTGAGAACAGGAC	cgaCAACCAGAGGATTTGGAAAGCAATG	cgaCAACCAGAGGATTTGGAAAGCAATG
Fbn1	acgTGGCGGGGAATGTACAAACA	cgtCAGAGCTGTGTAGCAGTAACCA	cgaCTGTCAGCAGCTACTTCTGCAAAT	cgaCTGTCAGCAGCTACTTCTGCAAAT
Flrt2	cgaTGCCGCTCTAGCTTCTTCC	cgtAGTGGAGAGCAGCCTAGGAA	cgaCCGGACCCGGTTGGATT	cgaCCGGACCCGGTTGGATT
Fmo1	cgaAACCACGTGAATTACGGTGTA	tcgCCTTGATGCTGGGCTTGATA	cgaGCTCCAGAAGACAGGACTCA	cgaGCTCCAGAAGACAGGACTCA
Gdpd5	cgaACTTCCGACA	cgtTGCCGATGAT	cgaTTTCTCGGG	cgaTTTCTCGG

	ACTCCCATACC	GAGGCTGAA	TGCCTTCTCCA	GTGCCTTCTCCA
Gfi1	cgaGAGATGTGCGGCAAGACC	cgtAGCGTGGATGACCTCTTGAA	cgaGTGAGCCTGGAGCAACACAA	cgaGTGAGCCTGGAGCAACACAA
Gfi1b	cgaTGGACACTTACCACTGTGTCA	cgtAGGTTTTGCCACAGACATCAC	cgaAGTGCAACAAGGTGTTCTCC	cgaAGTGCAACAAGGTGTTCTCC
Gpr126	cgaCTGTGCAGCCACTTCACTCA	cgtGGCAGATATTCCGCACCCAATA	cgaTGGAGTTCTGATGGATCTTCC	cgaTGGAGTTCTGATGGATCTTCC
Gria4	cgaCGCCCATGGTGACGAAACTA	cgtGCCATTACCAAGACACCATCGTA	acgATGGATCGCTGGAAGAAACTAGA	acgATGGATCGCTGGAAGAAACTAGA
Lad1	cgaCCTCTTTGAGAAGGAGCTGTCA	cgtCCTGGGTCTTGCTGATCCA	cgaGGCCAGAACCGCACAGAAC	cgaGGCCAGAACCGCACAGAAC
Lat	cgaTGCTGCCTGACAGTAGTCC	cgtTCACTCTCAGGAACATTCACGTA	cgaCTGCCGTCCCTGTTGTCT	cgaCTGCCGTCCCTGTTGTCT
Lgr5	cgaGCAACAACATCAGGTCAATACC	cgtCAGGCAAATGCTGAAAAGCA	cgaGGAGCGAGCGTTCGTAGG	cgaGGAGCGAGCGTTCGTAGG
Meis2	cgaCCCGTACCCTTCAGAAGAACAGAA	cgtTGGTCAATCATGGGCTGCACTA	cgaGAAACAGTTAGCGCAAGACAC	cgaGAAACAGTTAGCGCAAGACAC
Met	cgaGATCATTGGTGCGGTCTCAA	tcgACTCTTGCGTCATAGCGAAC	cgaGTAGTTTTGTTATTATCCGGGCTCTT	cgaGTAGTTTTGTTATTATCCGGGCTCTT
Myb	cgaGTGGCAGAAAGTGCTGAACC	cgtTGCTTGGCAATAACAGACCAAC	cgaCATCAAAGGTCCCTGGACCAAA	cgaCATCAAAGGTCCCTGGACCAAA
Myom1	cgaTTCCGTGTACGTGCTGTCAA	cgtTCCGTCATCATCCACACTCAC	acgCCAGGCAGGCGTTGGAAAG	acgCCAGGCAGGCGTTGGAAAG
Notch1	cgaCCAACCCTGTCAACGGCAAA	cgtATTTGCCTGCGTGCTCACAA	cgaTGCCCCTCGGGGTACA	cgaTGCCCCTCGGGGTACA
Npr1	cgaCAGATTTGTGGGAGCTTGTACC	cgtCGAAACATCCAGTCCAGGGTA	cgaGACCCTCCCAACATCTGTATC	cgaGACCCTCCCAACATCTGTATC
Palld	cgaGCTTCGCTTCAAGGAGGAC	cgtTCTGGCTCCTGGATGTTGAA	cgaCTTCTGAACAATGGCCAACC	cgaCTTCTGAACAATGGCCAACC
Pcdh12	cgaTGGCTGCTTTTGCGGAAC	tcgTGGTTTGGTTTGGGCTGGAA	cgaGGAACCCGGTGGAGGA	cgaGGAACCCGGTGGAGGA
Pdzd2	cgaCAACTTGGAAAGCCCCAAAC	cgtGTCCCCATTTCGTACCATCA	cgaAGGGCAACAGTAAAATGAAACTCAAG	cgaAGGGCAACAGTAAAATGAAACTCAAG
Plcd1	cgaTGGCTTCTCCAGTCCTAGCA	cgtCCCACGTTATGGCGGACAA	cgaTCTGGGCAGGCATTCTATGAGATGG	cgaTCTGGGCAGGCATTCTATGAGATGG
Ppia	cgaCCGACTGTGGACAGCTCTAA	cgtAGTGAGAGCAGAGATTACAGGAC	cgaTTTCTTTTGACTTGCGGGCATT	cgaTTTCTTTTGACTTGCGGGCATT
Ppp1r16b	cgaGCGTGTGGA	cgtGATGTCCTGG	cgaATGGCTGGG	cgaATGGCTGG

	TGTGAAGGAC	CACTGAGACTA	AGCCTCT	GAGCCTCT
Ptprb	acgCCAAGAGCG GCAATTATGCA	cgtTGCACCCAGG ACACCTTTAA	cgaCCACTCCTT CACCGAGGAA	cgaCCACTCCTT CACCGAGGAA
Ptprm	cgaCAGACCTCCT CCAACACATCA	tcgTCTCGTCTTT CTTAGCAGAGTC C	cgaTCAGATGAA GTGCGCTGAG	cgaTCAGATGA AGTGCGCTGAG
Runx1	cgaACTACTCGGC AGAACTGAGAA	cgtACGGTGATGG TCAGAGTGAA	cgaATGCTACCG CGGCCATG	cgaATGCTACC GCGGCCATG
Samd4	cgaACAGCTCCGT CCAGAAGAC	cgtACTCCAGCCT ATTGTTGATGTC A	acgTCGCTGCCC GTGCATA	acgTCGCTGCCC GTGCATA
Sash1	cgaTTGATCTCAC TGAGGAGCCCTA	tcgCCATGTTGGT GGCAACATCC	cgaCTGATAAGC ATGGCCGTTGT	cgaCTGATAAG CATGGCCGTTG T
She	cgaACATGGAAC CGTACGATGCA	tcgTCACAGTCTC CCCTGGTTCA	acgTAACAGAAA TCAGACGCCGT GGTT	acgTAACAGAA ATCAGACGCCG TGGTT
Sla	cgaCGAATCTTCC GTCTTCCCAAC	tcgGGTGAGCACA CAGCATAGAC	cgaACTGGTACT ACATCTCACCA AGG	cgaACTGGTAC TACATCTCACC AAGG
Snai1	cgaTCTGCACGAC CTGTGGAAA	cgtGAGCGGTCAG CAAAAGCA	cgaCTCTAGGCC CTGGCTGCTT	cgaCTCTAGGCC CTGGCTGCTT
Snai2	cgaGCACATTCG AACCCACACA	cgtTGCAGTGAGG GCAAGAGAAA	cgaTTGCCTTGT GTCTGCAAGA	cgaTTGCCTTGT GTCTGCAAGA
Upp1	cgaGAAGGAAGA CGTGCTCTACCA	cgtATGAAGGTGT TCATCCGGGAA	cgaTTCAACCTC AGCACTAGCAC AC	cgaTTCAACCTC AGCACTAGCAC AC
Acta2	AGGCACCACTGA ACCCTAAG	CACAGCCTGAAT AGCCACAT	CCAACCGGGAG AAAATGAC	ATGGCGGGGAC ATTGAAG
Acvr1b	ATGCTGCGCCAT GAAAACATC	TCGTGATAGTCA GAGACAAGCCAC A	TTGGCTTTATT GCTGCTGACA	TGGGTCCAGGT GCCATTATC
Acvr2a	GCTGGCAAGTCT GCAGGTGA	TCAGAAATGCGT CCCTTTGGA	ACCCATGGGCA GGTTGGTA	TTTATAGCACC CTCCAACACCT CTG
Acvr2b	GAAGGGCTGCTG GCTAGATGA	AGTTGCCTTCGC AGCAGCA	TCAATTGCTAC GACAGGCAGGA	AAGTACACCTG GGGGTTCTCCT C
Bmp4	CAGCCGAGCCAA CACTGTGA	TGGGATGCTGCT GAGGTTGA	AGTTTCCATCA CGAAGAACATC TGG	GAGGAAACGA AAAGCAGAGC
Bmpr2	CAGACGGCCGCA TGGAGTAT	ATGAGCCAGACG GCAAGAGC	TGCTTGTGATG GAGTATTATCC CAATG	TACCCAATCAC TTGTGTGGAGA CTCA
Cdh2	ATCAACAATGAG ACTGGGGACATC A	CTTCCATGTCTG TGGCTTGAA	CACTGTGGCAG CTGGTCTGG	ATTAACGTATA CTGTTGCACTT TCTCTCG
Cldn5	TGGCAGGTGACT GCCTTCCT	TGCATGTGCCCG GTACTCTG	ACCACAACATC GTGACGGCGCA GA	ACCACGCACGA CATCCACAG
Ctnnb1	AACTCCTGCACC CACCATCCCA	GTTCCCGCAAAG GCGCATGA	TGGCCTCTGAT AAAGGCAACTG	TGCTGGGCAAA GGGCAAG

Eng	GCCTGACTTTCT GGGACTCCAGC	TGCTGACCACAT GGGCTGTCAC	GCCAGGCTGAA GACACTGACG	TCATGCCGCAG CTGGAGTAG
Epo	GGTTGTGCAGAA GGTCCCAGA	GGGACAGGCCTT GCCAAACT	CTGAGTGAAAA TATTACAGTCC CAGA	TATGGCCTGTT CTTCCACCTCC A
Epor	TGAAGTGGACGT GTCGGCAG	ACAGCGAAGGTG TAGCGCGT	CAACCGGGCAG GAGGGACA	CCGCCCCGCAG GTTGCTCAGAA
Erg	TCCCGAAGCTAC GCAAAGAA	TTTGGACTGAGG GGTGAGGTG	TACAACTAGGC CAGATTTACCT TATGA	TGTGGCCGGTC CAGGCTGAT
Fli1	TGCTGTTGTCGC ACCTCAGTT	TTCCTTGACATT CAGTCGTGAGGA	CTCAGGGAAAG TTCACTGCTGG CCTA	TGGTCTGTATG GGAGGTTGTG
Gata1	CCTGTGCAATGC CTGTGGCT	TGCCTGCCCGTT TGCTGACAA	GTATCACAAGA TGAATGGTCAG AACC	CATTCGCTTCT TGGGCCGGATG
Gata2	AAGCAAGGCTCG CTCCTG	CACAGGCATTGC ACAGGTAGT	CAGAAGGCCGG GAGTGTGTC	GCCCGTGCCAT CTCGT
Hbb-b1	GCCGATGAAGTT GGTGGTGA	CCCATGATAGCA GAGGCAGAGG	GCCCTGGGCAG GCTGCTGGTTG TCT	TAGGTCTCCAA AGCTATCAAAG TACCG
Hbb-bh1	GAGCTGCACTGT GACAAGCTTCA	GGGGTGAATTCC TTGGCAAAA	TGGATCCTGAG AACTTCAAGC	GAGTAGAAAG GACAATCACCA ACA
Itga2b	TTCCAACCAGCG CTTCACCT	TGCTCGGATCCC CATCAAAC	CGACAACAGCA ACCCAGTGTTT	GCCCACGGCTA CCGAATATC
Itgam	AGCAGGGGTCAT TCGCTACG	CAGCTGGCTTAG ATGCGATGG	ATTGGGGTGGG AAATGCCTTC	GTCGAGCTCTC TGCGGGACT
Itgb3	TCCTCCAGCTCA TTGTTGATGC	AGGCAGGTGGCA TTGAAGGA	ACGGGAAAATC CGCTCTAAA	AGTGACAGTTC TTCCGGCAGGT
Kdr	TGTGGGGCTTGA TTTCACCTG	TCGCCACAGTCC CAGGAAAG	CACTCTCCACC TTCAAAGTCTC ATCA	TTTCACATCCC GGTTTACAATC TTC
Kit	CTGGCTCTGGAC CTGGATGA	CCTGGCTGCCAA ATCTCTGTG	TGCTGAGCTTC TCCTACCAGGT G	ATACAATTCTT GGAGGCGAGGA A
Lmo2	TCGGCCATCGAA AGGAAGAG	GCGGTCCCCTAT GTTCTGCT	CTGGACCCGTC TGAGGAACC	GCAGCCACCAC ATGTCAGCA
Lyl1	GCTGAAGCGCAG ACCAAGCCAT	GCTCACGGCTGT TGGTGAACACT	GTGAGCTGGAC TTGGCTGACG	CCGAGCCACCT TCTGGGGTTG
Mpo	TGGCCCTAGACC TGCTGAAGAG	TTGACACGGACA ACAGATTCAGC	AAGCTGCAGCC CCTGTGG	GAGCAGGTGTC AACACATCTGT AA
Pecam1	TGCGGTGGTTGT CATTGGAG	CTGGACATCTCC ACGGGTTT	GTCATCGCCAC CTTAATAGTTG CAG	TGTTTGGCCTT GGCTTTCCTC
Ptprc	GGCTTCAAGGAA CCCAGGAAATA	TGACAATAACTG TGGCCTTTTGCT C	ATTGCTGCACA AGGGCCCCGGG ATG	CAGATCATCCT CCAGAAGTCAT CAA
Ramp2	TCCCACTGAGGA CAGCCTTG	TCCTTGACAGAG TCCATGCAA	TCAAAAGGGAA GATGGAAGACT ACGA	TCTTGTACTCA TACCAGCAAGG TAGGACA
Serpine1	AAAACCCGGCGG	CTTGTTCCACGG	GATGCTATGGG	CCTTGGAGAGC

	CAGATCCA	CCCCATGA	ATTCAAAGTCAA	TGGCGGAGGGCATGA
Sfpi1	GTGGGCAGCGATGGAGAAAG	TGCAGCTCTGTGAAGTGGTTCTC	ATAGCGATCACTACTGGGATTTCTCC	GGGAAGTTCTCAAACTCGTTGTTG
Smad1	TCTCAGCCCATGGACACGAA	CACCAGTGTTTTGGTTCCTCGT	ATGATGGCGCCTCCACTGC	GCAACTGCCTGAACATCTCCTC
Smad2	TGCTCTCCAACGTTAACCGAAA	TCAGCAAACACTTCCCCACCT	GCCACTGTAGAAATGACAAGAAGACA	TGTAATACAAGCGCACTCCCCTTC
Smad3	CCAATGTCAACCGGAATGCAG	TGAGGCACTCCGCAAAGACC	CGTGGAACTTACAAGGCGACA	CCCCTCCGATGTAGTAGAGC
Smad4	TTGCCTCACCACCAAAACG	TGGAATGCAAGCTCATTGTGA	CCATCTTCAGCACCACCCGCCTA	TGGCCAGTAATGTCCAGGATG
Smad5	AACCATGGATTCGAGGCTGTG	TGACGTCCTGTCGGTGGTACTC	TGAGCTCACCAAGATGTGTACC	GCTCCCCAGCCCTTGACAAA
Smad6	TTCTCGGCTGTCTCCTCCTGAC	TTCACCCGGAGCAGTGATGA	GTACAAGCCACTGGATCTGTCCGATT	GGAGTTGGTGGCCTCGGTTT
Smad7	GGAAGATCAACCCCGAGCTG	TGAGAAAATCCATTGGGTATCTGGA	TGTGCTGCAACCCCCATCAC	AAGGAGGAGGGGGAGACTCTA
Smad9	GCACGATTCGGATGAGCTTTG	TGCAGCGGTCCATGAAGATG	GAAGGGCTGGGGAGCAGAGT	TCTCGATCCAGCAGGGGGTGCT
Sox7	AGAACCCGGACCTGCACAAC	CCGCTCTGCCTCATCCACAT	CGGAGCTCAGCAAGATGC	GGTCTCTTCTGGGACAGTGTCAGC
Tal1	ACCGGATGCCTTCCCCATGTT	GCGCCGCACTACTTTGGTGT	CCAACAACAACCGGGTGAAGA	AGGACCATCAGAAATCTCCATCTCA
Tek	TCCAAAGGAGAATGGCTCAGG	TCCGGATTGTTTTTGGCCTTC	TTCCAGAACGTGAGAGAAGAACCA	TGTTAAGGGCCAGAGTTCCTGA
Tgfb1	ACCCCCACTGATACGCCTGA	GCAGTGAGCGCTGAATCGAA	TGGCTGTCTTTTGACGTCACTG	GCCCTGTATTCCGTCTCCTTGG
Tgfb2	GGCATGCCCATATCTATGGAGTTC	CAGATCCTGGGACACACAGCA	GACACTCAACACACCAAAGTCCTCA	GGGAAGCGGAAGCTTCGGGATTTA
Tgfb3	CATGTCACACCTTTCAGCCCAAT	CTCCACGGCCATGGTCATCT	GAGACATACTGGAAAATGTTCATGAGGTG	CATTGTCCACTCCTTTGAATTTGA
Tgfbr1	GCAGACTTGGGACTTGCTGTGA	CATCTAGAACTTCAGGGGCCATGT	CATGATTCTGCCACAGATACAA	CCTTTTAGTGCCTACTCTGTGGTTTGG
Tgfbr2	TGGCCGCTGCATATCGTCCT	GCATCTTTCTGGGCTTCCATTTCCA	TGGACGCGCATCGCCAGCA	ATCCGACTTGGGAACGTG
Thpo	CCGACGTCGACCCTTTGTCT	TGCCCCTAGAATGTCCTGTGC	TCCCTGTTCTGCTGCCTGCT	TGCTCTGTTCCGTCTGGGTTTT

Table 2.5 ***Primer list used for the single cell qRT-PCR analysis. The green shaded cells indicate the primers designed by the DeltaGene, and the blue shaded cells indicate the primers designed by me.***

4.2. Primer test

The designed primers are tested in silico to make sure it recognizes only the target transcripts within the right sequences, which are aimed. The primers are ordered for synthesis through Sigma Aldrich. The primer stock is prepared to be 100mM for storage. The 96 outer primers are pooled to have 500nM as final concentration for all assays, which makes 10x STA primer stock. The forward and reverse inner primers are kept in 100mM stock concentration, which will be 5μM in each inlet, and 500nM in each reaction chamber. Afterwards the synthesized outer primer pool of 96 genes was tested with sample mouse cDNA first in STA reaction then for each 96 inner primers in conventional qPCR reaction. Later the primers are tested with our own cells sorted as 500 cell/well followed by RT and pre-amplification with outer primers and conventional qPCR with inner primers. At last, the real single cell experiment is tested with our cells sorted as 1cell/well, RT and pre-amplification reactions for 20 cycles; diluted cDNA in varying ratios (1/5, 1/10, 1/20) and loaded for BioMark microfluidics chip run of qPCR. Primer dimer formation, transcriptome size within samples and the compatibility of results with the biological expectation was evaluated. The 20 pre-amplification cycles and 1/5 dilution of cDNA was determined to have a good ct values between 6-20 for all 96 genes within our cells.

4.3. Single cell sort

For the RT-STA reactions, the reagents are from the CellsDirect One-Step qRT-PCR kit (Invitrogen cat. No. 11753). The complete protocol for sorting, following RT-STA reactions and chip run in BioMark is followed as it is written in Fluidigm Advanced Development Protocol, section 41. Each well of the 96 well plate (Bio-Rad Hard-Shell PCR plates cat. No. HSP9611) is filled with 5 μl of 2x reaction mix, which serves as a lysis solution. The plate with reaction mix is kept on ice before sorting. When the sorting gates are determined in FACS Aria, the plate with reaction mix is put on the cold platform for 96 well plates. The sorting precision is set for single cells and sorting on 96

well plate is calibrated before sorting. Depending on the population frequency, complete sorting may take time between a few seconds to 5 minutes. When the sorting is finished, the plate is snap-frozen on a pre-cooled metal block in a closed box full of dry-ice, then the plate is stored at -80°C freezer for not longer then 2 weeks.

4.4. Reverse transcription and pre-amplification reactions

A master mix for each well is prepared on ice. For one well 2.8μl of DNA suspension mix, 1μl of outer primer mix (STA pool), 0.2μl of SuperScript III enzyme is needed. When the master mix ready on ice, 4μl of it is added on top of the frozen reaction mix with cell. After a short spin down, the plate is put into the thermal cycler and the RT-STA program is immediately initiated. RT reaction takes place in first 15 minutes at 50°C, followed by inactivation of RT at 95°C for 2 minutes. Then 20 cycles of pre-amplification (STA) reaction at 95°C for 15 seconds and 60°C for 4 minutes are performed. When the program is finished, the temperature is set at 4°C. The plates are shortly spun down and stored at -20°C before sending them to EMBL Heidelberg Gene Core facility. The shipment is done on dry ice.

4.5. BioMark microfluidics chip run for qPCR reaction

Bianca Baying and Paul Collier in EMBL Heidelberg Gene Core Facility performed this part. The cDNA within each well of the shipped 96 well plate is diluted as 1/5 and sample mix is prepared with loading reagent (Fluidigm) and EvaGreen SuperMix (Bio-Rad). In parallel 96 individual assay mixes are prepared as 5μM primer inner primer mix, with DNA suspension buffer and assay loading reagent. After the priming of 96.96 dynamic array IFC, the sample mix and assay mixes are put together in the corresponding inlets and loaded into the chip. Finally the chip is run in BioMark by using the BioMark Data Collection Software and the GE 96x96 PCR+Melt v2.pcl program. After the run, the chip is discarded.

4.6. Analysis of the data

Raw data can be opened and analyzed by the Fluidigm Real Time PCR Analysis software. For each primer dynamics, Ct values and melting curves can be visualized. For detailed bioinformatics analysis, the raw data is imported in analysis view, AutoGlobal Ct threshold method, quality threshold 0.65 and linear derivative baseline correction method. The imported Ct values are analyzed by using Fluidigm SingularToolSet3.0 package scripts and R software. The outliers are removed which has all (or the majority of) genes not working according to global gene expression with the limit of detection 24 Ct. By using the build functions of Singular ToolSet3.0, I have generated hierarchical clustering heatmap for samples and genes, principal component analysis, violin or box plot for sample cluster's gene expression.

5. In vitro treatment with TGFB inhibitor and activator

To observe the results of inhibiting the TGFβ pathway, SB-431542 (Tocris, Cat. No. 1614, re-suspended in DMSO) small molecule inhibitor is added into the culture ng/medium in 10nM concentration. In contrast, to see the results of activation of TGFβ pathway, recombinant mouse TGFβ-2 (R&D systems, Cat. No. 7346-B2, re-suspended in 4mM HCl +0.1% BSA in 1xPBS) is added into the culture medium in 5ng/ml concentration. For vehicle control of SB-431542, the same volume of DMSO, for vehicle control of TGFβ-2, the same volume of 4mM HCl +0.1% BSA in 1xPBS solution is added in the culture. When both inhibitor and activator is needed to be used, only DMSO is added as vehicle control. Depending on the experiment, it is either added into the blast medium or the hemogenic endothelium medium. Depending on the experiment, the medium is kept for maximum 3 days before harvesting the cells.

Chapter3: Exploring the cellular heterogeneity during EHT

1. Introduction

In order to understand the underlying mechanism of EHT, one needs to identify the changes in cell characteristic throughout the transition. According to our current knowledge on hematopoietic and endothelial markers, we define the EHT as hemogenic endothelial (HE) cells transiting through pre-hematopoietic progenitor (Pre-HP) state towards to become hematopoietic stem/progenitor cells (HSPC)(Eilken, Nishikawa, & Schroeder, 2009; Lancrin et al., 2009). However, the cell populations isolated by using endothelial and hematopoietic markers are a lot more in number than the actual functional HE or pre-HP cells (Boisset et al., 2014; Lancrin et al., 2009b) which is possibly due to cellular heterogeneity. In this project, I aim to define the HE and pre-HP populations by comprehensive gene expression profiling ultimately to find exclusive markers of each populations.

1.1. Current markers to identify populations:

Specifying genes for the endothelial cells to have hematopoietic capacity have been the focusing point for a long time. In theory, hemogenic endothelial cells have cell surface endothelial markers VE-Cadherin, Flk-1, Tie2/Tek and also the early hematopoietic lineage markers CD41, C-Kit, CD45 (Eilken et al., 2009b; Ferkowicz, 2003; Lancrin et al., 2009a; W. Li et al., 2005; Mikkola, Fujiwara, Schlaeger, Traver, & Orkin, 2003; Zovein et al., 2008). Combination of those markers let us enrich hemogenic endothelial cells among all endothelial cells. However finding a putative marker of hemogenic endothelium is still an unachieved goal.

Runx1 has been the mostly studied gene for regulation of EHT. Although its expression is vital for the successful EHT, not all Runx1 expressing endothelial cells are going through the transition. Additionally, Runx1 is expressed in non-hemogenic tissues such as olfactory epithelium, spinal ganglia, maxillary processes (T. North et al., 1999)

and various stages of murine life, not only during embryonic development. Several studies done for the Runx1 function in hematopoiesis, identified two promoters are activated during developmental hematopoiesis(Enid Yi Ni Lam et al., 2009; Nottingham et al., 2007) indicating very specific regulation of Runx1 activity in HE or Pre-HP cells (Bee et al., 2010; Sroczynska, Lancrin, Kouskoff, et al., 2009b). Regarding that specific function, reporter cell and mouse lines are generated to trace the Runx1 proximal and distal promoter activity to mark cells initiated EHT (Sroczynska, Lancrin, Kouskoff, & Lacaud, 2009a). The staining of Runx1 proximal promoter with endothelial markers is so far the only specific marker for the hemogenic endothelium population.

In early studies, Sca1/Ly6a has been used as an isolating marker for HSCs in the bone marrow (Spangrude, Heimfeld, & Weissman, 1988) and fetal liver (Huang & Auerbach, 1993). Sca1/Ly6a expression in endothelial cells is recently claimed to be marking hemogenic endothelial, which will give rise to only HSC (M. F. T. . de Bruijn et al., 2002). Recent study with CBFB deficient mice with induced rescue under the promoters of Tie2 or Sca1 genes show that hemogenic endothelial cells with erythroid/myeloid progenitors (EMP) or HSC forming potential can be separated. This study brings an important argument as EMP forming hemogenic endothelium can be labeled with Tie2 promoter, at the same time HSC forming hemogenic endothelium can be labeled with Sca1/Ly6a promoter, which indicates separate hemogenic endothelial cells related with particular progenitor function (Chen et al., 2011). However the neither Ly6a nor Tie2 is putatively labeling these specific hemogenic endothelial cells (Figure 3.1.A).

SRY-related HMG box (SOX) family, F sub group of transcription factors were one of the claimed hemogenic endothelium markers. Sox7, Sox17, and Sox18 are the 3 transcription factors belong to that subgroup. Sox7 has role in primitive parietal endoderm differentiation (Futaki, Hayashi, Emoto, Weber, & Sekiguchi, 2004). Sox7 is

found to be expressed transiently in Flk-1+ mesoderm, then Sox7 expression is down regulated towards hematopoiesis. When Sox7 is over-expressed in HP cells, it blocks their maturation. When Sox7 is knocked down, number of hematopoietic and endothelial precursors are decreased (Gandillet et al., 2009). Sox7 and Sox18 were shown to be redundant especially in regulation of angiogenesis and vasculogenesis (Sakamoto et al., 2007). Sox18 is transiently expressed during hematopoiesis, unlike Sox7, its expression is high on CD41+ HP cells. When Sox18 is over-expressed in HP cells, it blocks maturation and induce proliferation (Serrano, Gandillet, Pearson, Lacaud, & Kouskoff, 2010). Studies on zebrafish show also knock down of Sox7 and Sox18 show defective vasculogenesis and angiogenesis, although hematopoiesis is claimed not be affected (Chung, Ma, Fung, & Leung, 2011). Lastly, Sox7 is expressed in endothelial cells including hemogenic endothelium and plays role in sustaining endothelial gene expression such as VE-cadherin (Costa et al., 2012). Consequently its expression does not discriminate between hemogenic and non hemogenic endothelial cells.

Sox17 is important for definitive endoderm specification(Kanai-Azuma et al., 2002). Its expression is found weak during hematopoietic specification and HSCs. But over-expression of Sox17 in HPs increases apoptosis rate (Serrano et al., 2010). The studies in zebrafish show also expression of Sox17 in the intermediate cell mass. Knock down of Sox17 results in reduced primitive erythrocytes but not affected definitive hematopoietic cells (Chung et al., 2011). It is shown to be important for maintenance in fetal HSCs(Kim, Saunders, & Morrison, 2007). Also it is expressed in intra-aortic clusters and ectopic expression of Sox17 increases self-renewal of clusters in vivo and in vitro (Nobuhisa et al., 2014). In parallel with its role in HSC maintenance, Sox17 is claimed to be marking hemogenic endothelial cells too (Clarke et al., 2013).

Sox7, Sox17 and Sox18 are all suggested to have important role for balancing the cell fate decision between proliferation and differentiation, but cumulative analysis of

studies during hematopoiesis indicates cell type specific expression of each(Serrano et al., 2010) (Figure3.1.B). Although Sox7 and Sox18 have overlapping expression during mesoderm specification to hemogenic endothelium, Sox7 is highly expressed in Flk-1+ hemangioblast cells (Gandillet et al., 2009) while Sox18 is expressed more abundantly in CD41+ HP cells (Serrano et al., 2010). On the other hand, Sox17 is shown to be expressed highly in intra-aortic clusters (Nobuhisa et al., 2014) and HSCs (Clarke et al., 2013) (Figure 3.1.C).

Lastly retinoic acid signaling is suggested to be regulating HSC formation from HE cells. Retinal aldehyde expressing endothelial cells are claimed to be hemogenic endothelium, which will give rise to HSCs (Chanda, Ditadi, Iscove, & Keller, 2013). Although the sorting of aldehyde receptor expressing cells together with VE-Cadherin+ and Runx1+ gates, isolate the cells with HSC potential; single staining of aldehyde receptor expression does not specify the hemogenic endothelium (Figure 3.1.D).

In conclusion, the studies in the search of identification of hemogenic endothelium helped to enrich the cells with hematopoietic potential within the endothelial population, when it is used in combination with endothelial and early hematopoietic markers. However the claimed marker proteins; Runx1, Ly6a, Sox7, Sox17, Sox18, retinoid acid receptors are not exclusively expressed in the hemogenic endothelial cells. Furthermore, while hemogenic endothelial cells become pre-hematopoietic progenitor as the next step during EHT process, the claimed marker proteins are not sufficient to distinguish HE from pre-HP cells.

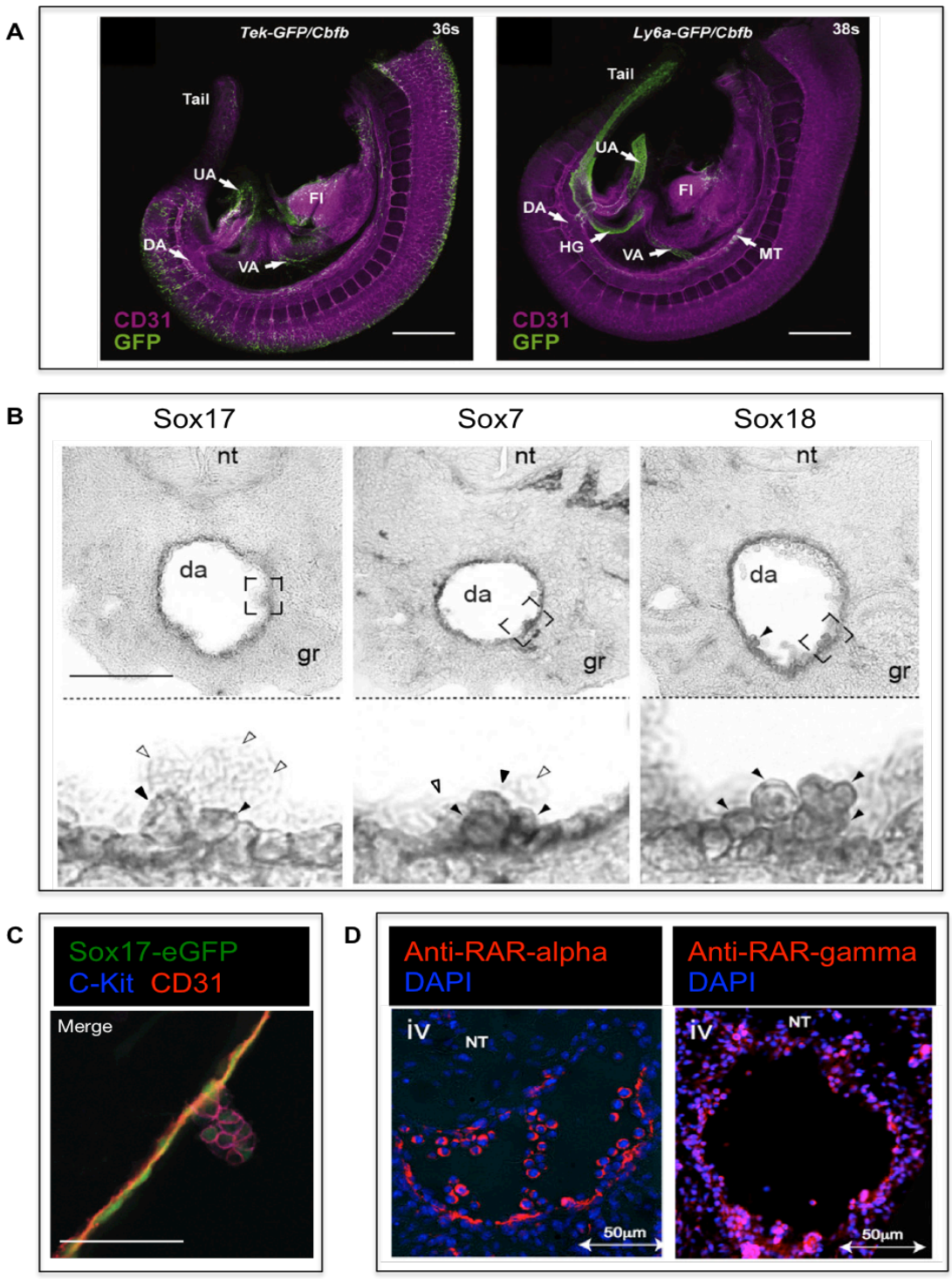

Figure 3.0.1 ***Markers reported to be labeling hemogenic endothelium in previous studies.*** *A.* ***E10.5 whole mount immunofluorescence staining of transgenic mouse lines. (Adapted from figure 6 of Chen et al., 2011, Cell Stem Cell)*** *B.* ***E10.5 AGM in situ hybridization staining of Sox17, Sox7 and Sox18. (Adapted from figure 4 of Nobuhisa et. al. 2014, Mol. And Cell. Bio.)*** *C.* ***E10.5 intra-aortic hematopoietic cluster of Sox17 GFP/+ mouse staining with C-kit and CD31. (Adapted from figure 2.b of Clarke et. al. 2013, Nature Cell Biology)*** *D.* ***E11.5 AGM of retinoic acid receptors staining (Adapted from figure 1 of Chanda et. al. 2013, Cell)***

1.2. Functional heterogeneity within marked populations:

Independent studies claim to identify hemogenic endothelial cells depending on their combination of cell surface markers and transgenic reporter genes. However the marked cells out-number the actually functional hemogenic endothelium or pre-HP populations, which is only possible to be confirmed in functional assays. Due to non-consensual definitions of cell types and lack of combinatorial study for all markers, it is difficult to draw a definitive conclusion about cell type specific expression of these markers.

Not all marked hemogenic endothelial cells are going through the EHT and not all marked pre-HP cells have the same hematopoietic potential. The *in vitro* studies showed that only 1 in 79 endothelial cells could give rise to differentiated HP cells (Lancrin et al., 2009). The hematopoietic cells composing the intra-aortic clusters (IAHCs) are showing differential expression of some markers, which initially thought to be related with hematopoietic maturity. Among 500-600 IAH cells in E10.5 AGM (Figure 3.2.A), only 1 HSC is found which is confirmed to give rise to all types of hematopoietic cells upon in vivo transplantation (Boisset 2014). At E11.5 the intra-aortic cluster forming cells decrease (Figure 3.2.B) but cells with HSC capacity may increase up to 11 cells. The rest of the cells are showing limited hematopoietic lineage potency.

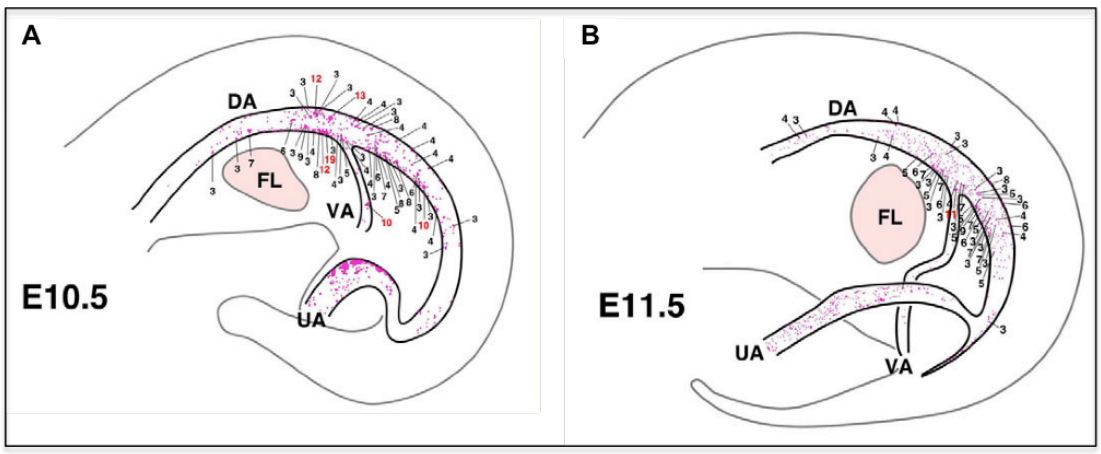

Figure 3.0.2 ***Mapping of C-Kit+ intra-arterial hematopoietic clusters in*** *A.* ***E10.5 and*** *B.* ***E11.5 embryos. (Adapted from figure 2 of Yokomizo et. al. 2010 Development)***

Previous studies on marked HE and Pre-HP populations suggested the presence functional heterogeneity (Boisset et al., 2014; Lancrin et al., 2009). Partially it might be related with the lack of exclusive marker of those populations. It may also be the reflection of population with basic potential, which can only become functional upon an extrinsic signal to trigger differentiation. If we can identify highly homogeneous population and visualize its frequency in AGM and YS hematopoiesis in time course, we can enlighten the heterogeneous EHT.

1.3. Our approach and hypothesis

Cell identity can be defined by gene expression profile and functional protein repertoire. Up until recently, material needed for gene expression analysis wouldn't be enough from one cell. The microfluidics technology developed in the last few years made it possible to do single cell qRT-PCR and single cell total mRNA sequencing.

2. Results:

2.1. The establishment of the single cell qRT-PCR technique

The single cell qRT-PCR for 96 genes is a technique established in the last few years (Sthalberg 2010). Comparing with the conventional qRT-PCR, it requires extra steps and precautions due to the low amount of RNA material to begin with. The optimization of the technique and later the verification of the results with expectation is the vital part of this project.

The establishment of the technique was based on two aspects; the variety of cell types and the panel of genes. In vitro differentiation of mES cells allows us to sort population of cells within its controlled timing during EHT. Our knowledge of gene expression change can be classified for endothelial and hematopoietic genes. All together, expected gene expression pattern of relatively known cell types became our guide to test the technique.

2.2. Selection of first samples to test: Sorted cell populations derived from in vitro differentiation system

For the selection of cell types, I used the mES cell differentiation protocol on the Runx1 +/hCD4 cell line generated previously (Sroczynska 2009). In this cell line human CD4 gene is knocked-in in the proximal promoter of the Runx1 to trace hematopoietic specific expression of Runx1 via hCD4 specific antibody (Figure 3.3.A). It makes an ideal reporter cell line to isolate hemogenic endothelial (HE) population, which is not distinguishable from the non-hemogenic endothelial (NonHE) phenotype by expression of endothelial markers (such as VE-Cadherin), yet not transcribing the hematopoietic markers. Further in EHT, HE cells start to express early hematopoietic markers like CD41, giving rise to pre-hematopoietic progenitor (pre-HP) cells. Those cells lose their endothelial markers and gain round morphology and finally become hematopoietic progenitor (HP) (Figure3.3.B). In order to isolate all of the populations, day1.5 of blast culture was chosen to be the best time point because populations from all stages of EHT are found approximately in equal proportions. VE-Cadherin is used as endothelial marker, CD41 is used as early hematopoietic marker and the hCD4 is used as Runx1 expression reporter to isolate NonHE, HE, Pre-HP, and HP populations (Figure3.3.C).

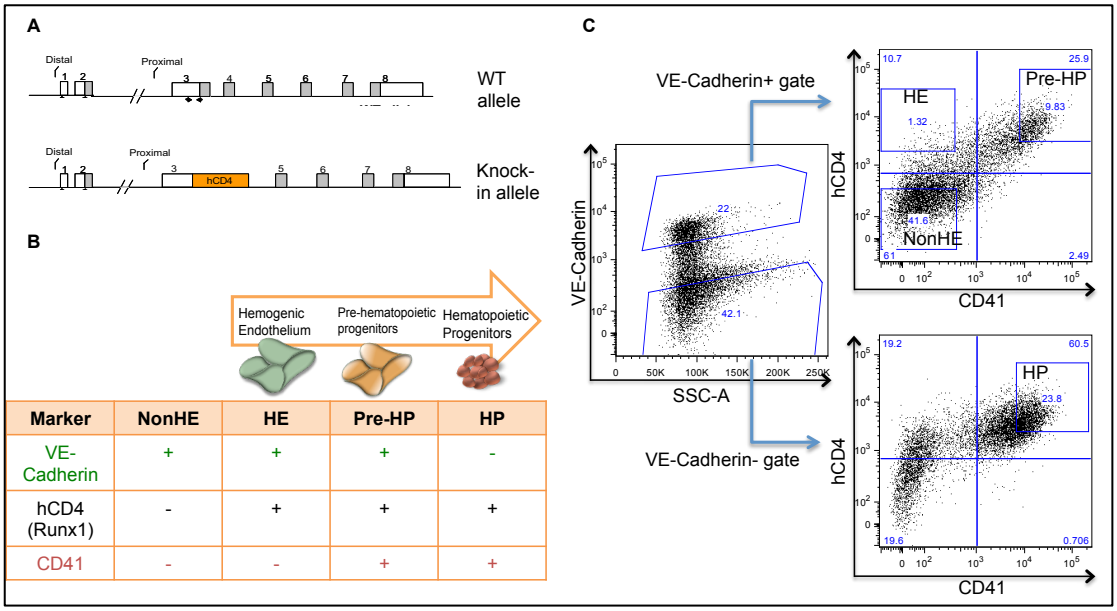

Marker	NonHE	HE	Pre-HP	HP
VE-Cadherin	+	+	+	-
hCD4 (Runx1)	-	+	+	+
CD41	-	-	+	+

Figure 3.0.3 ***The strategy to isolate cell populations by using Runx1 hCD4/+ cell line****. A. The cell line has one WT and one hCD4 knock-in Runx1 alleles. (adapted from Sroczynska 2009) B. The markers and corresponding populations are depicted as they are expected to appear during EHT. C. The sample sorting strategy for isolation of the 4 populations.*

2.3. Choice of 96 genes to check expression in single cells

The selection of genes has to be distinctive enough to spot the separate populations and also has to be extensive enough to conclude about the nature of the populations. The largest microfluidics chip allows us to run qPCR for 96 genes in 96 single cells. Considering the loss of endothelial phenotype and gain of hematopoietic features during EHT, we decided to choose two large sets of endothelial and hematopoietic marker genes. We included also a list of transcription factors having role in developmental hematopoiesis. The addition of epithelial to mesenchymal transition (EMT) and TGFβ/BMP pathway related genes is more regarding the other project in my thesis. Lastly, one reference gene (Ppia)(Handschumacher, Harding, Rice, Drugge, & Speicher, 1984) was selected to see equal mRNA material among different single cells (Table 3.1). I have tested Hprt1, H2afz and Ppia primers for qPCR study with cells isolated form ES cell culture, which claimed to have stable gene expression for ES cells (Mamo, Gal, Bodo, & Dinnyes, 2007). Only the Ppia primers gave the most consistent Ct values for different samples, therefore we added Ppia into the primer panel for the single cell study.

Among 96 genes, there are 39 genes as the transcriptional effectors of Runx1 and Gfi1, which we thought important for EHT regulation. Recently, we have shown that Gfi1 and Gfi1b are down-stream targets of Runx1, which decreases the endothelial gene expression in hemogenic endothelial cells during the transition (Lancrin 2012). The Runx1 KO cells fail in forming functional hematopoietic progenitors through EHT. However induced Gfi1 or Gfi1b expression, in the absence of Runx1 can rescue the emergence of round hematopoietic progenitors. In parallel, the double Gfi1 and Gfi1b KO mouse has hematopoietic progenitors, which cannot detach from the endothelial layer during EHT in yolk sac. This indicates the crucial role of Gfi1 and Gfi1b function in repression of endothelial gene expression and morphology.

Since Gfi1 is a direct binding target of Runx1 and plays an important role in the loss of endothelial characteristics, the genes whose expression is regulated by both Runx1 and Gfi1 took our attention as a potential marker for hemogenic endothelium. To reveal the transcriptional change when Runx1 or Gfi1 is expressed in Runx1 KO cells, previously Christophe Lancrin performed two sets of mRNA microarray experiments (unpublished data). Surprisingly there were 7 up-regulated and 32 down-regulated genes by both Runx1 and Gfi1 activity. Confirmation of the expression pattern change of 39 genes upon Runx1 and Gfi1 activity was done by conventional qRT-PCR. We found that the majority of the fold changes gathered from Runx1 and Gfi1 microarray experiments have consistent pattern in the conventional qRT-PCR experiments (Figure 3.4 for Runx1 experiments, Figure 3.5 for Gfi1 experiments).

Gene classification	Gene names
Housekeeping gene (1)	PPIA
Genes regulated by Runx1 and Gfi1 (39)	ADCY4, ATP2A3, CACNA2D1, CDH5, COL4A2, COL4A5, DCAF12L1, DPYSL3, ENPP1, EPS8, ESAM, FAM122B, FBN1, FLRT2, FMO1, GDPD5, GPR126, GRIA4, LAD1, LAT, LGR5, MEIS2, MET, MYB, MYOM1, NOTCH1, NPR1, PALLD, PCDH12, PDZD2, PLCD1, PPP1R16B, PTPRB, PTPRM, SAMD4, SASH1, SHE, SLA, UPP1
TGFB-BMP pathway related genes (22)	ACVR1, ACVR1B, ACVR2A, ACVR2B, ACVRL1, BMP4, BMPR1A, BMPR2, ENG, SMAD1, SMAD2, SMAD3, SMAD4, SMAD5, SMAD6, SMAD7, SMAD9, TGFB1, TGFB2, TGFB3, TGFBR1, TGFBR2
EMT related genes (11)	ACTA2, CDH2, SERPINE1, SNAI1, SNAI2, TGFB1, TGFB2, TGFB3, TGFBR1, TGFBR2, CTNNB1
Endothelial genes (17)	CDH5, CLDN5, ENG, ERG, ESAM, FBN1, GPR126, KDR, MEIS2, NOTCH1, NPR1, PCDH12, PTPRB, PTPRM, RAMP2, SOX7, TEK
Hematopoietic genes (22)	EPO, EPOR, GATA1, GATA2, GFI1, GFI1B, HBB-B1, HBB-BH1, ITGA2B, ITGAM, ITGB3, KIT, LMO2, LYL1, MPO, MYB, PTPRC, RUNX1, SFPI1, SLA, TAL1, THPO
Transcription factors (16)	ERG, FLI1, GATA1, GATA2, GFI1, GFI1B, LMO2, LYL1, MEIS2, MYB, RUNX1, SFPI1, SNAI1, SNAI2, SOX7, TAL1

Table 63.1 ***The list of 96 genes selected for single cell qRT-PCR, and their classification related with their reason of choice.***

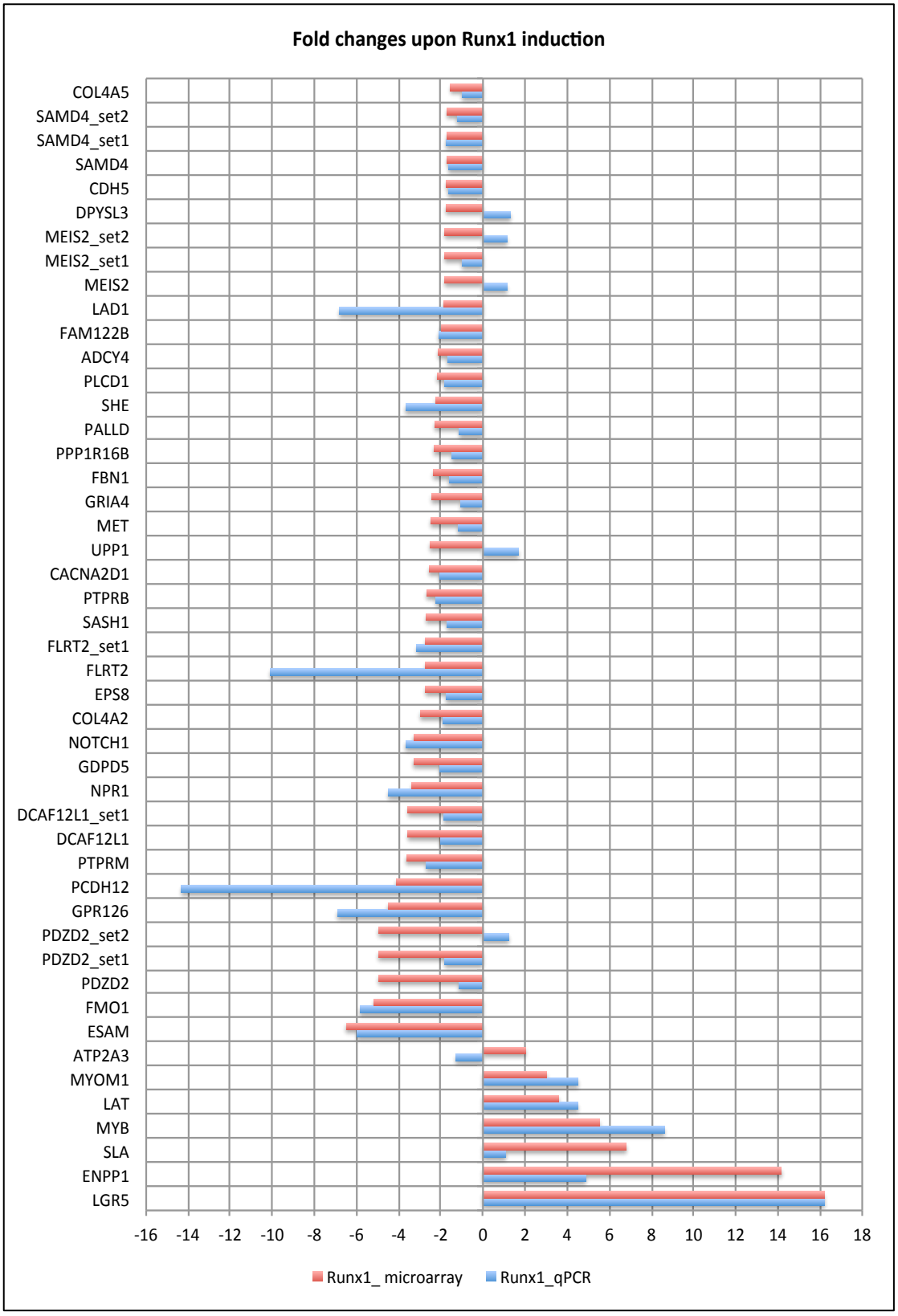

Figure 3.0.4 ***The fold changes of the 39 genes in induced Runx1 expressed cells versus Runx1 knock-out cells. The red bars represent the mRNA microarray and the blue bars represent the qRT-PCR fold change values.***

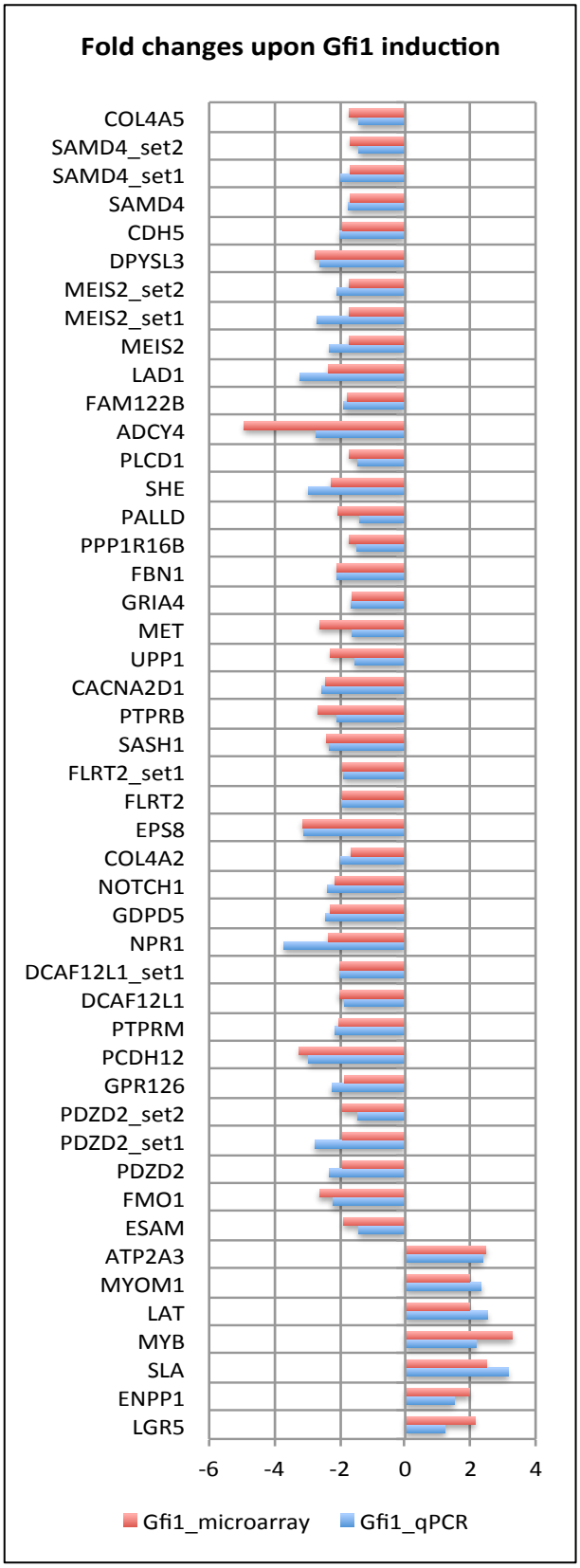

Figure 3.0.5 ***The fold changes of the 39 genes in induced Gfi1 expressed cells versus Runx1 knock-out cells. The red bars represent the mRNA microarray and the blue bars represent the qRT-PCR fold change values.***

2.4. The first single cell qRT-PCR results of blast culture isolated cells

The first two experiments of single cell qRT-PCR were done with sorted 4 populations (Figure3.6.B) from blast day 1.5 culture of Runx1 hCD4/+ cell line. NonHE, HE, Pre-HP and HP cell populations are defined according to their VE-cadherin, hCD4/Runx1, CD41 expression as it is explained before (Figure3.3). After removal of the samples with no expression of the 96 genes, called outliers, 135 single cell samples were left. The global Z score expression value of 96 genes for each single cell is represented in hierarchical clustering of samples (on the horizontal axis) and the genes (on the vertical axis) (Figure 3.6.A). The sample clustering done by the algorithm in general does not fully overlap with the sorted population identity, although HP cells are clearly distant from HE and NonHE cells. The principal component analysis of the results shows the similarity of cells belong to 4 populations within 2 principal components (Figure 3.6.C). In contrast the expected EHT course of action among populations is represented as distribution of cells in the PCA score plot. The NonHE cells are overlapping with the HE cells; HE cells are overlapping with Pre-HP cells and Pre-HP cells are overlapping with HP cells, while the distance between endothelial and hematopoietic cloud is evident (Figure 3.6.C).

To identify gene expression pattern in detail, each gene expression value was investigated among 4 populations by violin plots. The expression profile of single cells within a population can be visualized as a distribution of Log2 expression values in the violin plots. The common effectors of Gfi1 and Runx1, 39 genes (Figure 3.7), were checked as comparison with the microarray and qPCR data (Figure 3.4 and Figure 3.5). Among the 7 up-regulated genes, 5 of them (Atp2a3, Myom1, Myb, Sla, Enpp1) show higher expression in HP population than in NonHE, HE and Pre-HP populations. Among 32 down-regulated genes, 26 genes (Adcy4, Cdh5, Col4a2, Col4a5, Dcaf12l1, Dpysl3, Eps8, Esam, Fbn1, Fmo1, Gdpd5, Gpr126, Met, Meis2, Notch1, Npr1, Palld, Pcdh12, Pdzd2, Plcd1, Ptprb, Ptprm, Ppp1r16b, Samd4, She, Upp1) show lower expression in HP

population than in the others. It is also interesting to see some genes have a fashion of gradual decrease or increase in the expected fashion of EHT: NonHE, HE, Pre-HP and HP.

The violin plot of endothelial genes show the expected pattern of gradual or sudden expression decrease in the order of EHT from NonHE to HP. Among 18 endothelial genes, all but 2 (Pecam1, Cldn5) show the lower expression towards EHT (Figure 3.8.A). On the contrary, among 22 hematopoietic genes, only 11 genes (Epor, Gata1, Gfi1b, Hbb-b1, Hbb-bh1, Itgb3, Mpo, Myb, Runx1, Sla, Sfpi1) show expression increase towards EHT (Figure 3.8.B). The other hematopoietic genes either don't vary significantly among populations, or don't follow the expected increase during the EHT course.

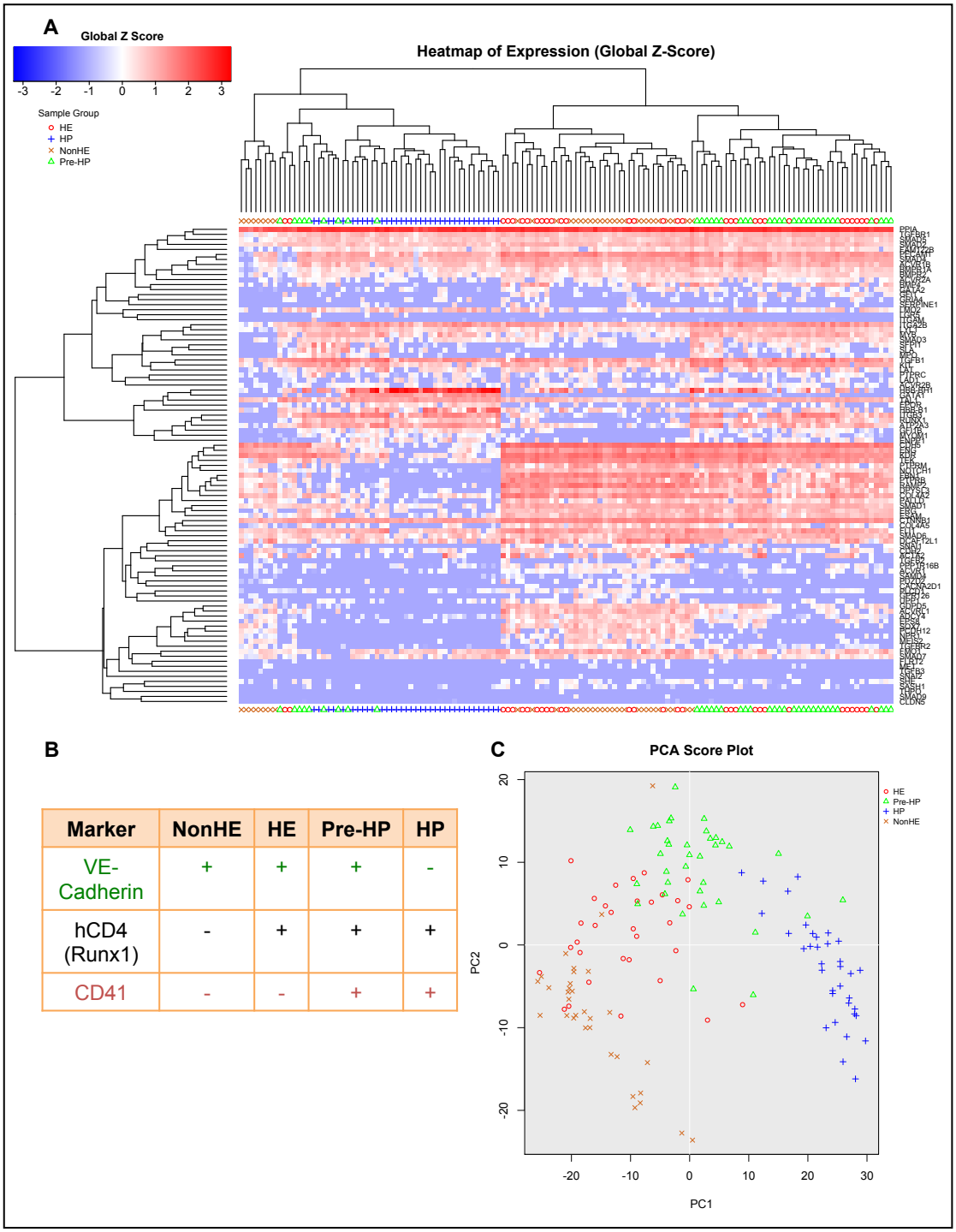

Marker	NonHE	HE	Pre-HP	HP
VE-Cadherin	+	+	+	-
hCD4 (Runx1)	-	+	+	+
CD41	-	-	+	+

Figure 3.0.6 ***Single cell qRT-PCR analysis of sorted 4 populations from blast day1.5 culture of Runx1 hCD4/+ cell line.*** *A.* ***Hierarchical clustering of cells sorted as 4 populations with their expression level of 96 genes. The expression level is represented as global Z score, (blue) low to (red) high.*** *B.* ***The sorted population according to 3 markers expression, VE-Cadherin as endothelial, hCD4/Runx1 as EHT initiation, CD41 as early hematopoietic markers.*** *C.* ***Principal component analysis score plot of cells with their sorted population identity.***

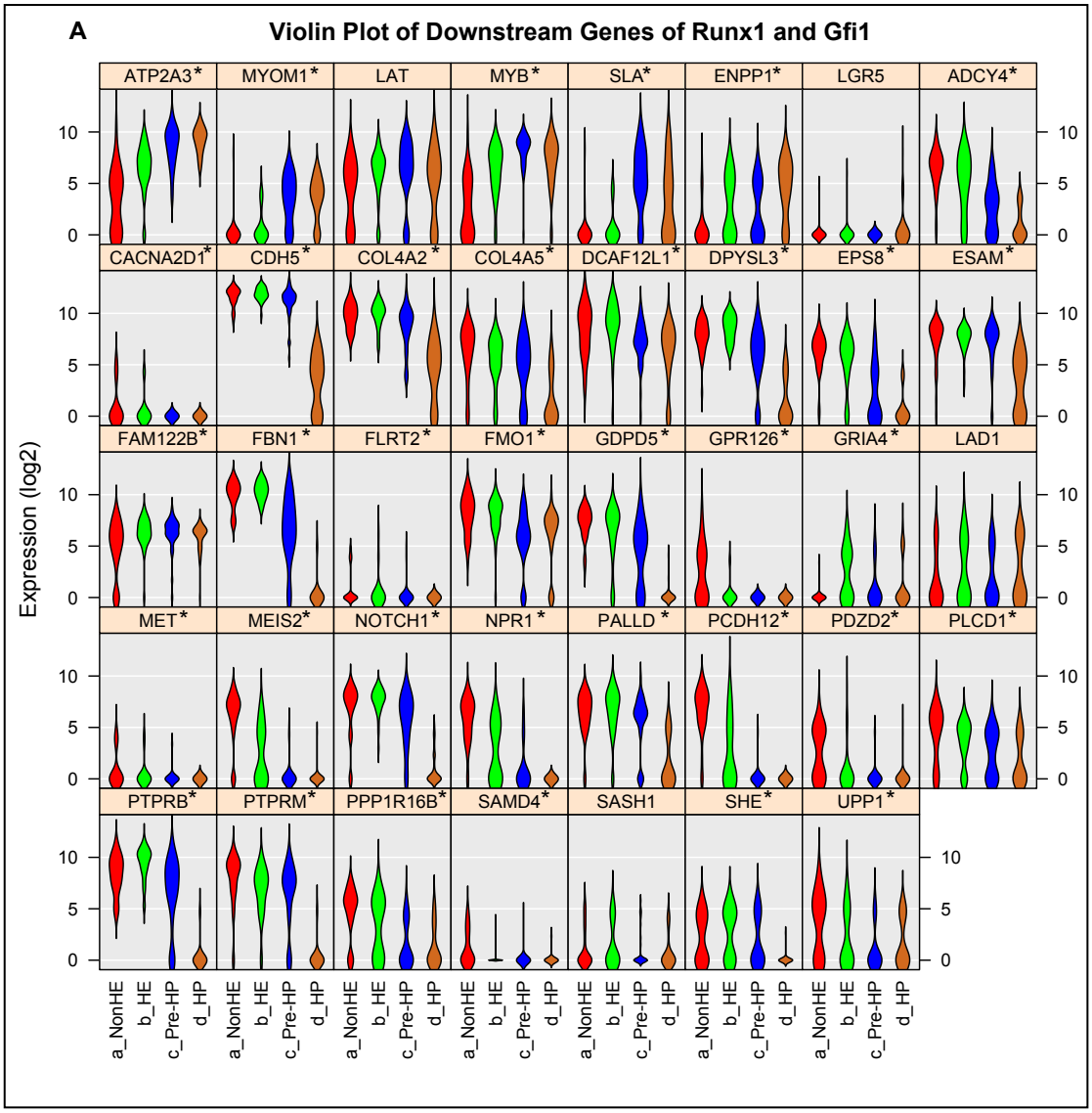

Figure 3.0.7 ***Violin Plots of 4 populations and the expression of 39 genes regulated by Runx1 and Gfi1. Among the gene expression values within populations, the genes with ANOVA p value is lower than 0.05 are indicated with * next to the gene name. The first 7 (Atp2a3, Myom1, Lat, Myb, Sla, Enpp1, Lgr5) are the common up-regulated genes by Runx1 and Gfi1; the rest 32 genes are the common down-regulated ones.***

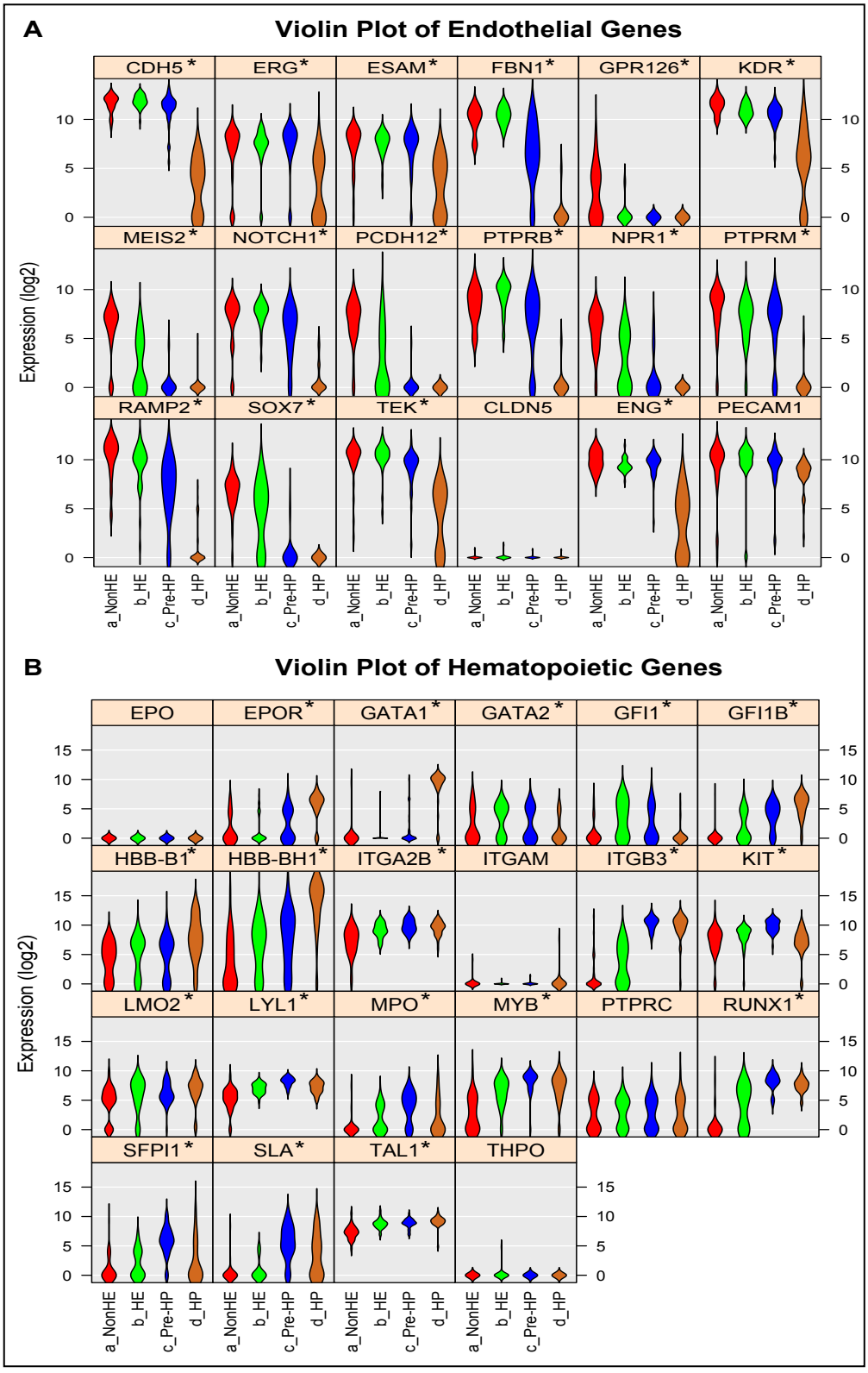

Figure 3.0.8 ***Violin Plots of 4 populations with the expression of*** *A.* ***endothelial genes and*** *B.* ***hematopoietic genes. Among the gene expression values within populations, the genes with ANOVA p value is lower than 0.05 are indicated with * next to the gene name. The genes are listed in alphabetical order.***

2.5. Investigation of in vivo endothelial to hematopoietic transition by single cell qRT-PCR technique

In order to explore the in vivo EHT at the single cell level, we decided to isolate hemogenic endothelial cells and pre-hematopoietic progenitors from two hematopoietic tissues: yolk sac (YS) and aorta-gonad mesonephros (AGM) (Figure 3.9.A). YS is the region where first hematopoietic progenitors emerge and AGM is the first tissue where the HSCs appear. Therefore the comparison of cells isolated from these two tissues will be valuable to understand the differences of hematopoietic programs. Also to address the timing of EHT in these two tissues, we decided to isolate cells from E9.0, E10.5 and E11.0 mouse embryos. Since we do not have a Runx1 hCD4 reporter mouse line, we used only VE-Cadherin and CD41 markers to sort. We aim to sort all VE-Cadherin positive cells, with CD41 expression level: negative, medium or high. I sorted 32 cells per population per time point and tissue (except for E9.0 AGM, I managed only to get 9 cells due to its very low frequency) (Figure 3.9.B). We have run 6 micro-fluidics chips (96 single cells *96 genes) with the AGM and YS derived cells.

2.5.1. The identification of subpopulations from mouse embryo derived cells

EHT can be analyzed at single cell level as a step-wise transition of specific cell types. The cell types can be visualized in the single cell qRT-PCR as subpopulations depending on the shared gene expression pattern. By combining the expression values of cells collected from YS and AGM within 3 time points, I aim at identifying all cell types during EHT with high resolution.

All 6 chip run results were combined in analysis and samples with no expression of the 96 genes, defined as outliers, were removed. After removal of outliers, there were 510 single cells in total for YS and AGM within 3 time points (Figure 3.10.A). For the unbiased analysis of hematopoiesis within two tissues, we decided to combine the data from 510 cells to check its sample annotations afterwards. Because I will address the TGFB/BMP pathway in the chapter 4, I removed the 22 genes (Table 3.1) related with it

from this analysis. The hierarchical clustering of the merged data from all tissues and time points is shown in Figure 3.10.B. In the hierarchical clustering, 6 sample clusters were defined (Figure 3.10.B).

The violin plots visualize the distribution of gene expression within a population. In figure 3.11.A, the violin plots of endothelial genes for each sample cluster is shown. For SC_2 (green), SC_4 (orange) and SC_5 (purple), all endothelial genes have high expression values. In comparison with them, SC_3 (blue) has lower but still positive expression profile of endothelial genes. SC_6 (pink) cells have lower endothelial expression and for some genes (Npr1, Ptprm, Ramp2, Sox7) there is a bi-modal (both low and high) expression profile indicating heterogeneity within the population. In contrast to all, SC_1 (red) cells have either no or lower expression of endothelial genes (Cdh5, Esam, Notch1, Eng, Pecam1) compared with the other sample clusters. Although all of the cells were sorted through VE-Cadherin positive gate, SC_1 cells show almost no VE-Cadherin (also known as Cdh5) gene expression. It might be explained by SC_1 cells bearing VE-Cadherin protein on the cell surface but switched off its gene expression. In summary, SC_1 has almost no; SC_3 and SC_6 have intermediate; SC_2, SC_4, SC_5 have high endothelial gene expression profile (Figure 3.11.A).

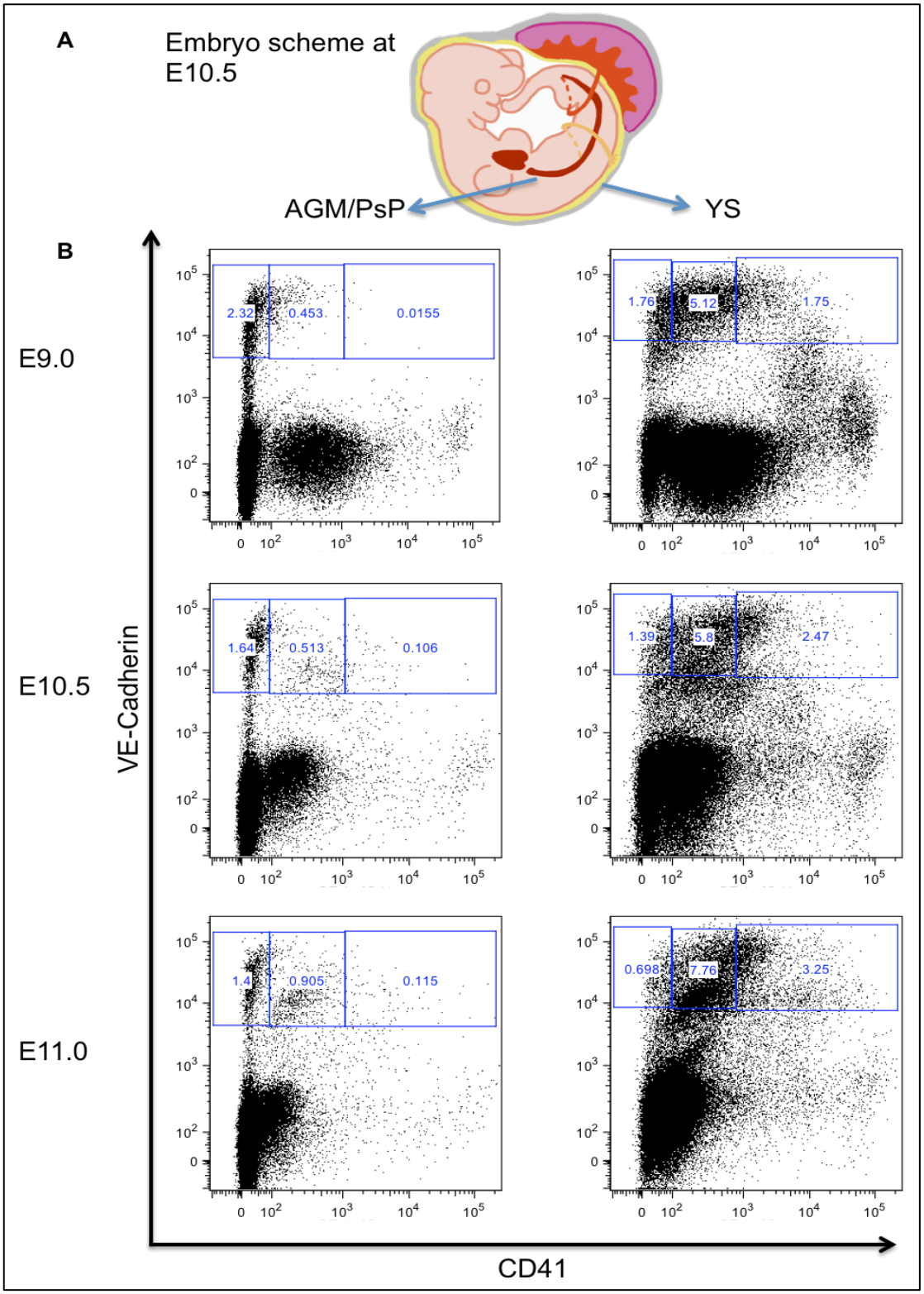

Figure 3.0.9 ***Single cell sorting of isolated cells from AGM and YS tissues at stages of E9.0, E10.5 and E11.0 mouse embryos.*** *A.* ***The representative scheme of E10.5 mouse embryo, to show AGM and YS localization.*** *B.* ***The FACS plots used for sorting of single cells from 3 time points and 2 tissues. VE-Cadherin and CD41 staining was applied to sort 3 cell populations (VE-Cadherin+, CD41 negative /intermediate /high) from each time point and tissue.***

The violin plots of hematopoeitic genes for all sample clusters are shown in Figure 3.11.B. Unlike the endothelial genes in figure 3.11.A, hematopoietic gene expressions are not following a common up/down regulation. This might be due to the fact that some hematopoietic genes up-regulated in only specific population of cells depending on the progress of EHT. Population SC_1 and SC_6 show high expression of Itgam, Itgb3, Myb, Ptprc, Runx1, Sfpi1 and Sla. Despite that similarity with SC_1, only SC_6 show high expression of Gata2, Gfi1, Gfi1b, Kit, Mpo, Tal1; while SC_1 does not present distinctive expression for other hematopoietic genes.

A

Time point and tissue	CD41neg	CD41mid	CD41hi	Total cell count
E9.0 AGM	27	29	9	65
E9.0 YS	31	28	30	89
E10.5 AGM	31	29	30	90
E10.5 YS	25	31	31	87
E11.0 AGM	29	29	31	89
E11.0 YS	31	30	29	90
Total cell count	174	176	160	510

B

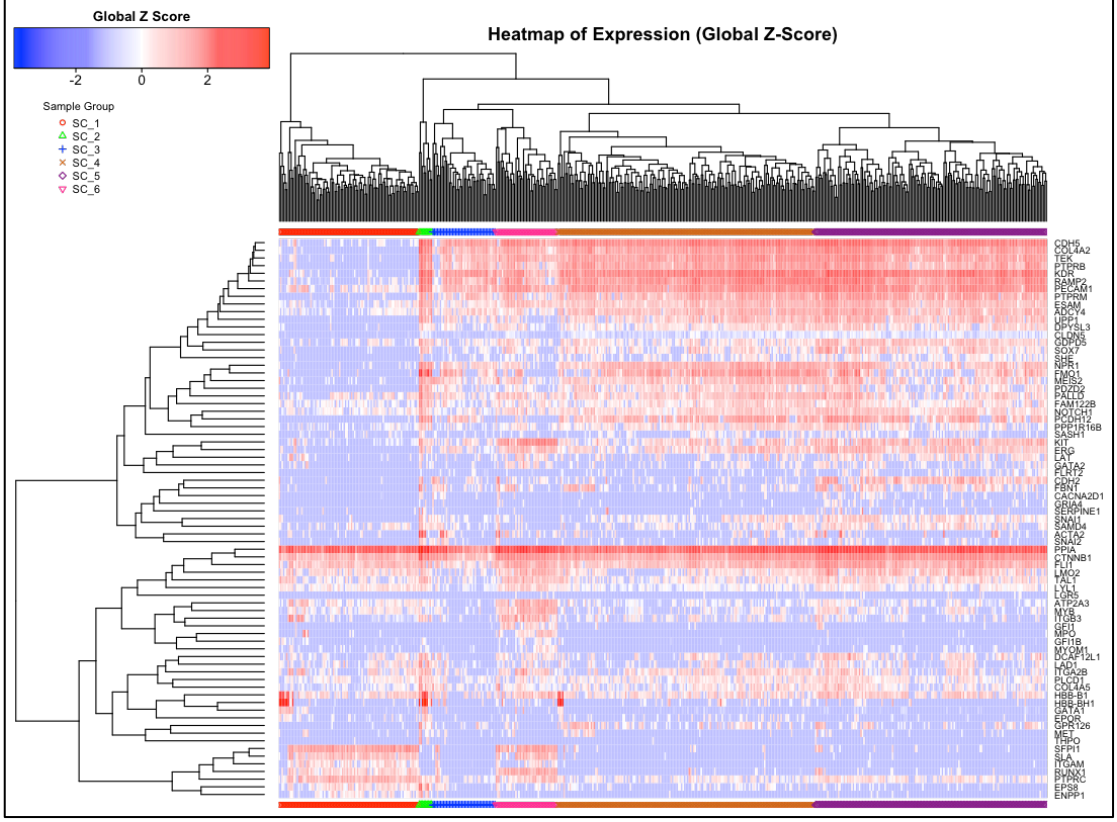

Figure 3.0.10 ***Single cell analysis of merged cells isolated from YS and AGM from all time points****. A. The number of cells isolated from each tissue, each time point and each CD41 sorting gate is indicated. B. The hierarchical clustering of all isolated cells from mice with 74 genes expression values. The sample clustering with a distance threshold of 0.62 identified 6 clusters.*

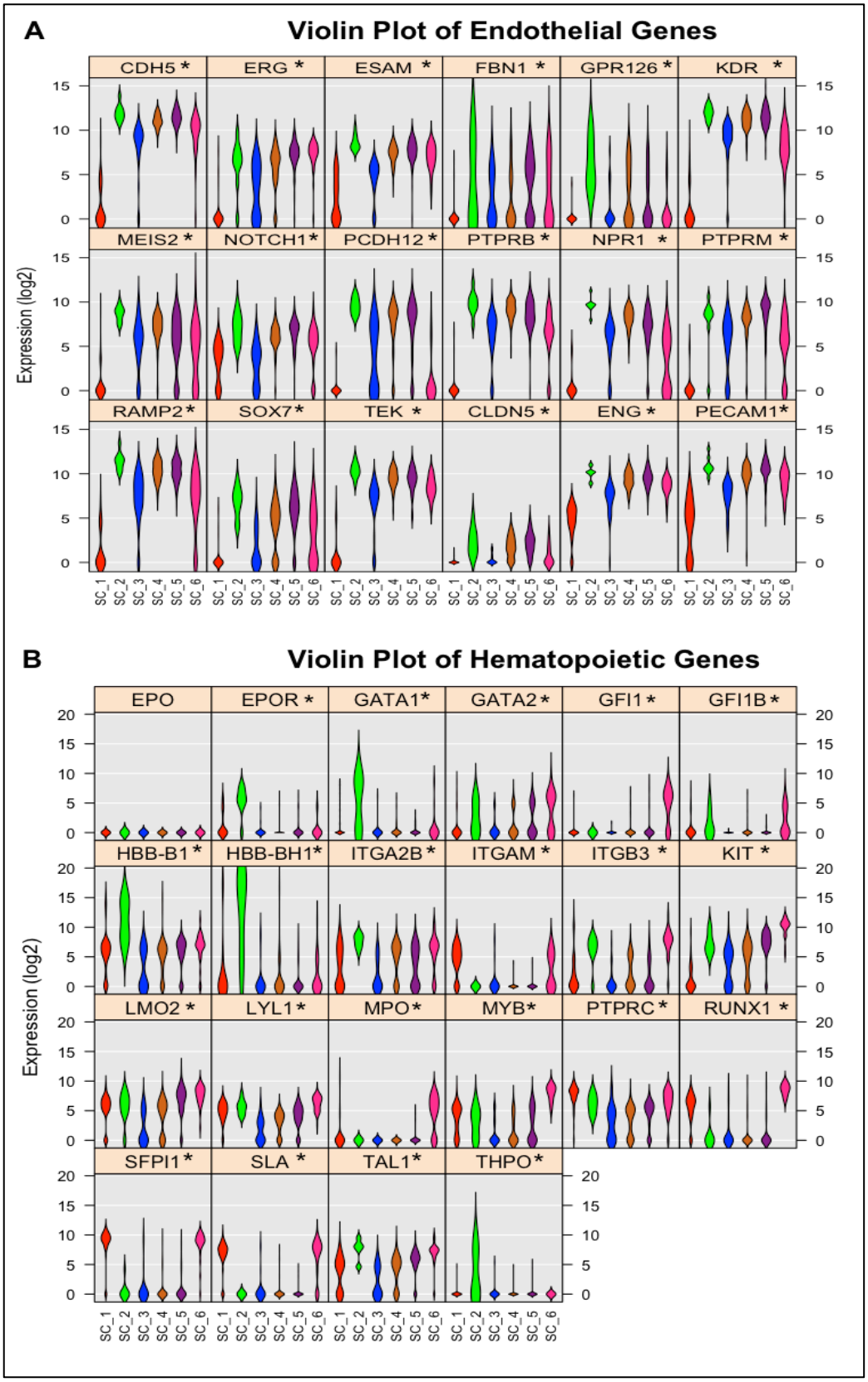

Figure 3.0.11 ***The violin plots of gene expression of*** *A.* ***endothelial genes and*** *B.* ***hematopoietic genes within sample clusters. Among the gene expression values within populations, the genes with ANOVA p value is lower than 0.05 are indicated with * next to the gene name. The genes are listed in alphabetical order.***

SC_3, SC_4 and SC_5 present a highly similar low or none expression profile for all hematopoietic genes, however SC_5 has slightly higher values for genes Gata2, Kit, Lmo2, Lyl1, Myb, Tal1 and SC_4 has a few cells expressing Hbb-b1 and Hbb-bh1. It is important to emphasize the either no expression or bi-modal expression pattern for the aforementioned genes within these populations. It may due to heterogeneity especially within SC_5 population.

Lastly SC_2 population seems to express some hematopoietic genes (Epor, Gata1, Gata2, Gfi1b, Hbb-b1, Hbb-bh1, Itga2b, Itgb3, Kit, Lmo2, Lyl1, Myb, Ptprc, Tal1, Thpo) at high levels. Interestingly Runx1, Sfpi1, Sla , Itgam are not expressed but Epor, Gata1, Hbb-b1, Hbb-bh1; which are the genes related to the erythroid lineage are expressed at the highest level in the SC_2 compared to other populations.

All together endothelial and hematopoietic gene expression profiles give us a clue about the identity of 6 sample clusters. According to Figure 3.11.A and B, SC_3, SC_4, SC_5 populations have dominant endothelial profile. SC_3 can be separated by lower endothelial genes while SC_5 is particular with co-expressing some key hematopoietic genes. In that terms, SC_5 might contain hemogenic endothelial cells, while SC_3 and SC_4 are closer to non-hemogenic endothelial cells.

On the other hand, SC_1, SC_2 and SC_6 have gene expression profiles close to hematopoiesis with separate characteristics. SC_1 is clearly not expressing endothelial genes and express some hematopoietic genes including Runx1. Since we sorted VE-Cadherin presenting cells in their surface, cells composing SC_1 should be the cells close to the the final step of the EHT. SC_6 is interesting with both strong endothelial gene expression and some hematopoietic genes similar to SC_1. Regarding that, SC_6 appears to be the cells with common gene expression profile of SC_5 and SC_1.

Above all, the most interesting population is SC_2 with very high expression of both endothelial genes and some erythroid related marker genes (Hbb-b1, Hbb-bh1, Epor, Gata1, Thpo) without expressing Runx1, Sfpi1 and Sla. Since such a population with erythroid-endothelial profile has not been identified before, it requires further confirmation.

Previously we have seen that isolated cells from blast culture day 1.5 has a pattern of expression in parallel with the progression in EHT for 39 genes regulated by Runx1 and Gfi1. Commonly up-regulated 7 genes have higher expression and some down-regulated genes have lower expression from HE towards HP population (Figure 3.7). In order to check expression level of 39 genes within sample clusters of mouse embryo isolated cells, I analyzed the expression of 39 genes (Figure 3.12). According to the previous analysis with endothelial and hematopoietic genes, in vivo EHT steps might follow the sequence SC_4➔ SC_5 ➔SC_6 ➔ SC_1. In this sense, when I analyze the 39 genes' expression change from SC_4, SC_5, SC_6 to SC_1, I saw the up-regulation of Atp2a3, Myom1, Lat, Myb, Sla, Enpp1. Among the other 32 genes, most of them (Adcy4, Cdh5, Col4a2, Col4a5, Dcaf12l1, Dpysl3, Esam, Fam122b, Fbn1, Fmo1, Gdpd5, Meis2, Notch1, Npr1, Palld, Pcdh12l1, Pdzd2, Ptprb, Ptprm, Samd4, She, Upp1) showed down-regulation in the hypothesized direction from SC_4, SC_5, SC_6 to SC_1. The expression of the 39 genes in vivo correlates with what we've found in vitro. However we found some discrepancies such as Eps8, which increases when the cells become progressively hematopoietic. Another example is Atp2a3 whose expression is reduced in the SC_1 population compared to SC_6. In general these 39 genes may be useful to classify the cells during the EHT.

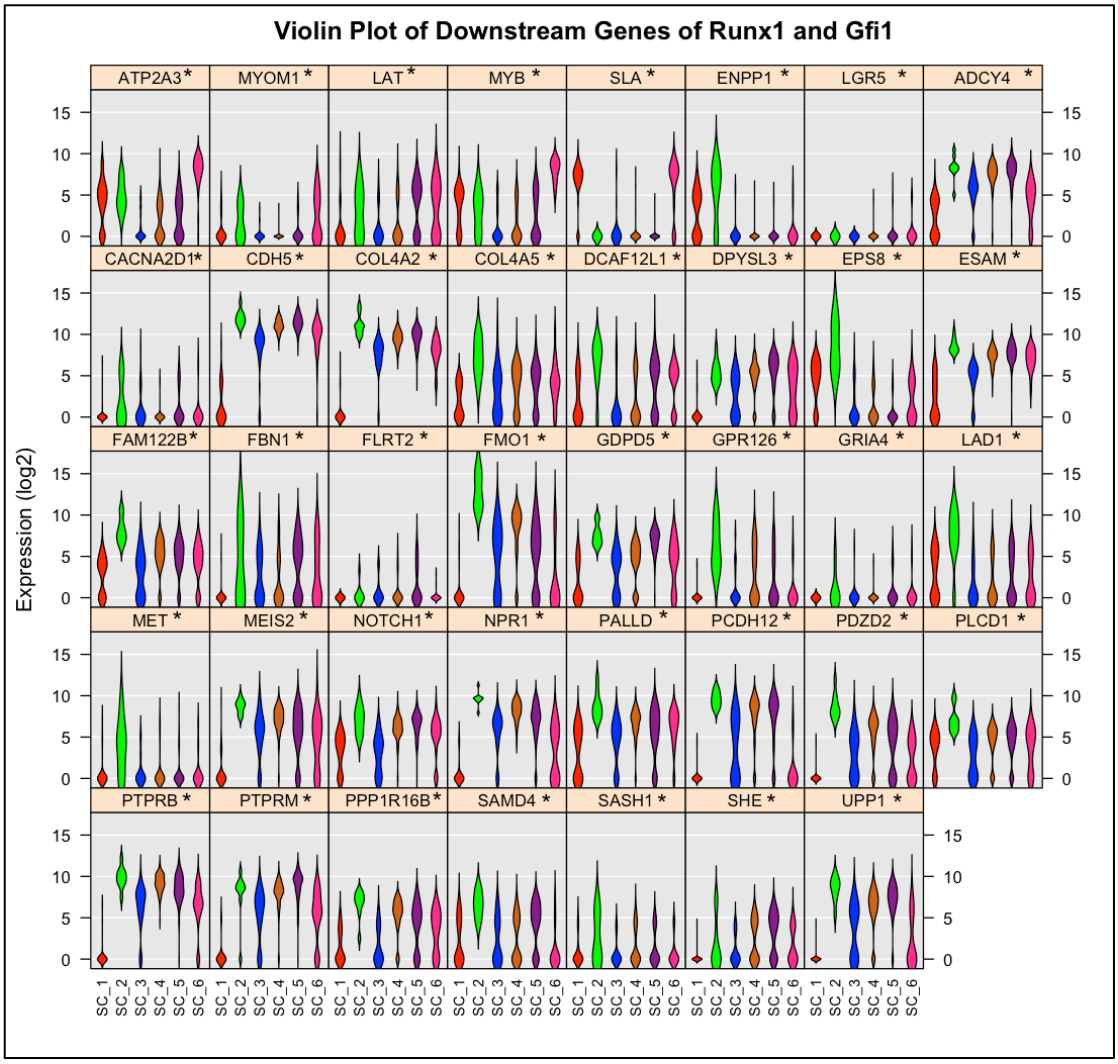

Figure 3.0.12 ***The violin plots of the 39 genes commonly regulated by Runx1 and Gfi1 within sample clusters. Among the gene expression values within populations, the genes with ANOVA p value is lower than 0.05 are indicated with * next to the gene name. The first 7 (Atp2a3, Myom1, Lat, Myb, Sla, Enpp1, Lgr5) are the commonly up-regulated genes by Runx1 and Gfi1; the rest 32 genes are the commonly down-regulated ones.***

The initial sorting idea with CD41 negative, intermediate and high annotations is based on the expectation of gradual increase in CD41 expressing cells during the transition from HE to Pre-HP. Since CD41 is an early hematopoietic marker, it would be expected to have correlation with the EHT progression. To see this correlation, I calculated the CD41 composition of each sample clusters in terms of their initial CD41 gate related names and presented with principal component analysis (Figure 3.13).

Principal component analysis is a method to project the 96 dimensional data into 2 strongest principal components, which is helpful to see the sample clustering relations. PCA Score Plot of all sample clusters show that SC_3, SC_4, SC_5 and SC_2 cells look closer while SC_1 is far from them and SC_6 is dispersed in between SC_1 and SC_5. The sample clusters are represented in PCA score plot with corresponding CD41 annotation composition. Surprisingly, SC_1, the sample cluster with the most hematopoietic signature, is composed of only 42% of CD41hi and 58% of CD41mid. SC_6, the transitory population on the other hand, is composed of 93% of CD41hi, which is the highest proportion for CD41hi cells and 7% CD41mid. Surprisingly endothelial clusters, SC_3, SC_4 and SC_5 have also contribution from CD41 hi and mid cells. SC_3 has 57% and SC_5 has 58% contribution from CD41neg cells, which can be related with their endothelial phenotype. However, the other endothelial population SC_4 show almost equal contribution from all CD41 annotated cells, which was not expected and will be addressed later in the discussion. Lastly, SC_2 has contribution from all CD41 annotated cells as well and 45% of it is from CD41hi cells, which is fitting its endothelial-erythroid phenotype.

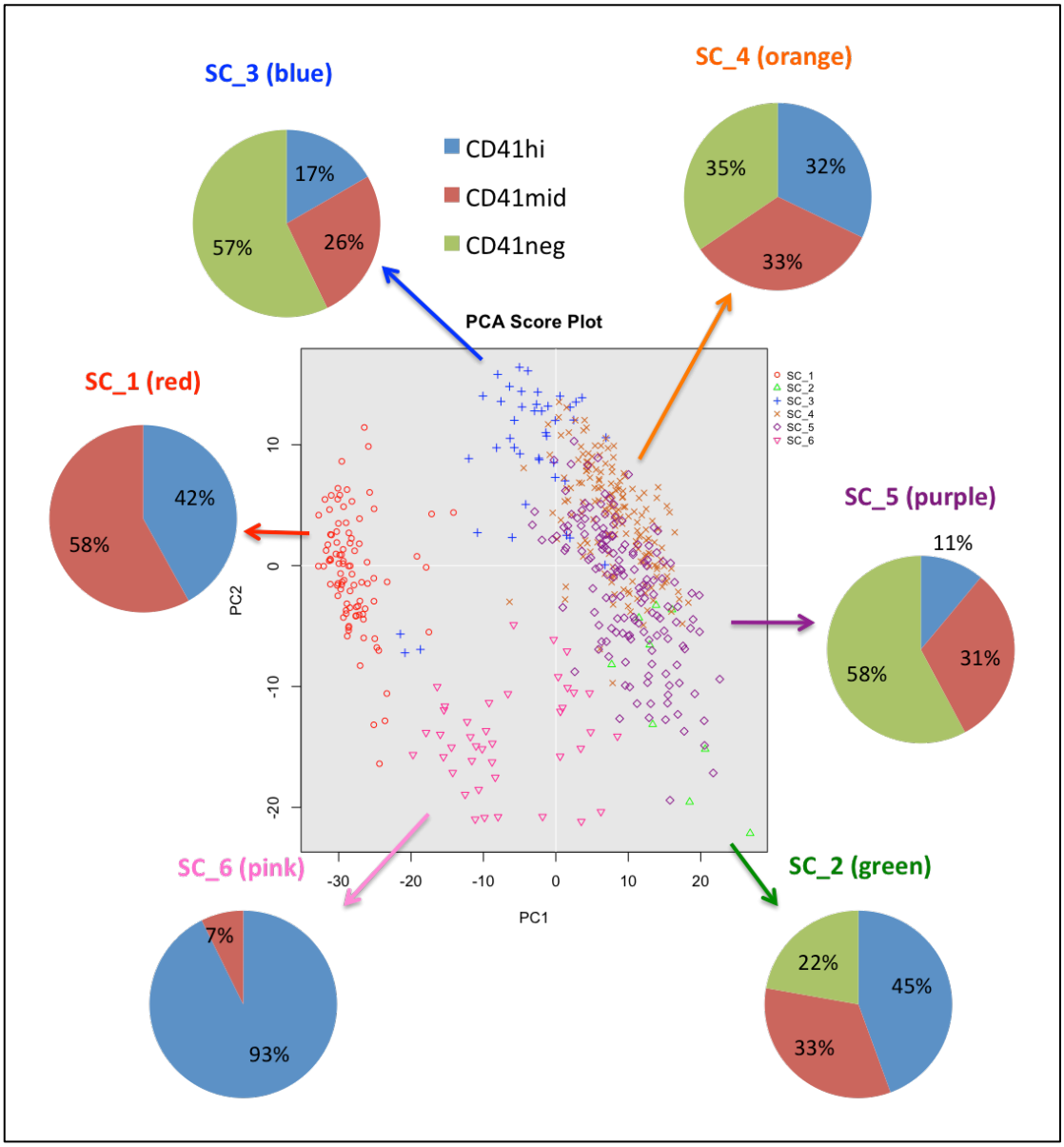

Figure 3.0.13 ***The PCA plot and CD41 annotation composition for each sample cluster***

2.5.2. Investigating the tissue origin of the sample clusters

The identified sample clusters are defined in the merged data, but the abundance of each cell population might be different depending on the tissue origin. The hematopoiesis in YS and AGM has been compared in several studies and often AGM is referred as the first hematopoietic site to support de novo HSC emergence. One explanation would be the tissue microenvironment as YS and AGM have very distinct

cellular environment, which may influence the hematopoietic capacity of the emerging progenitors. Another explanation would be the different nature of the endothelial cells forming the YS vasculature compared to the ones in the dorsal aorta. To answer this question, I checked the tissue origin for each sample cluster considering also the CD41 annotations (Figure 3.14). The CD41 annotations are shown in bar plots and number of cells detected within that group, and the total percentage for AGM or YS origin is shown in the adjacent pie chart. The SC_1, SC_5, SC_6 populations are highly composed of cell isolated from AGM, regardless of their CD41 annotation. SC_3 and SC_4 populations, on the other hand, mostly composed of cells isolated from YS. SC_2 is a small population composed of cells derived only from YS.

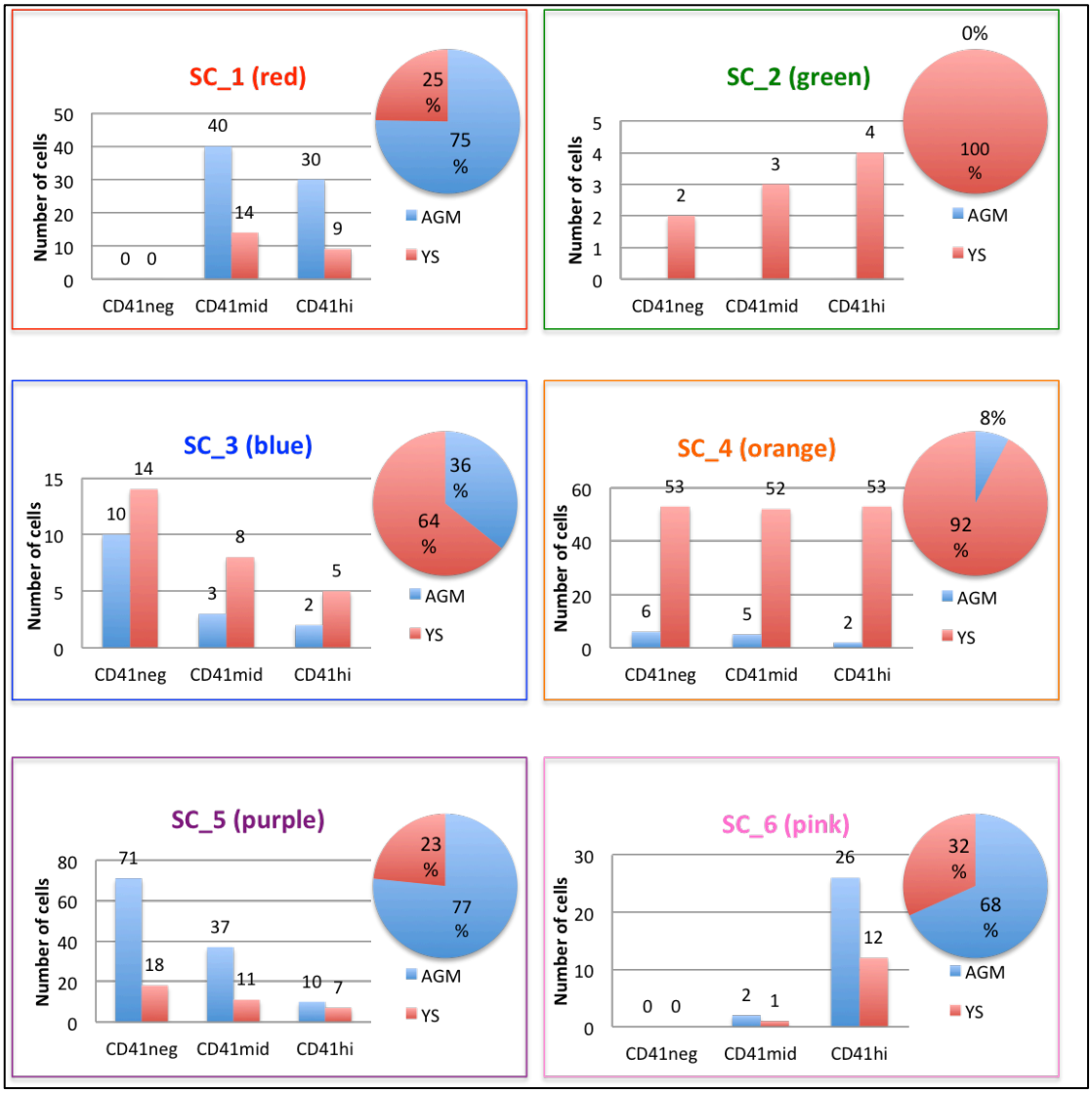

Figure 3.0.14 ***The cluster composition according to the tissue of origin. The bar plots are representing the number of cells detected from AGM (blue) and YS (red) with CD41 annotations in the sample cluster. The adjacent pie chart is representing the frequency of tissue origin contributing in corresponding sample cluster.***

2.5.3. Investigating at which embryonic stage the sample clusters can be found

Another difference between AGM and YS hematopoiesis is the timing. The YS is the first site of hematopoiesis, which provides the first erythroid cells at around E7.5-E8.0 in the mouse embryo. Afterwards the YS can also form myeloid-erythroid progenitors. On the other hand, hematopoiesis in the AGM starts much later, at around E9. The blood flow starts after the initiation of the heartbeat at E8.25. Since we sorted VE-cadherin positive cells, we assume the circulating mature HPs have been excluded and only cells

associated with the endothelial lining were included in our analysis. This is important not to have cells mixed from another tissue or time point. In order to see the time of origin for each population, I calculated the composition of time points with the tissue origin (Figure 3.15)

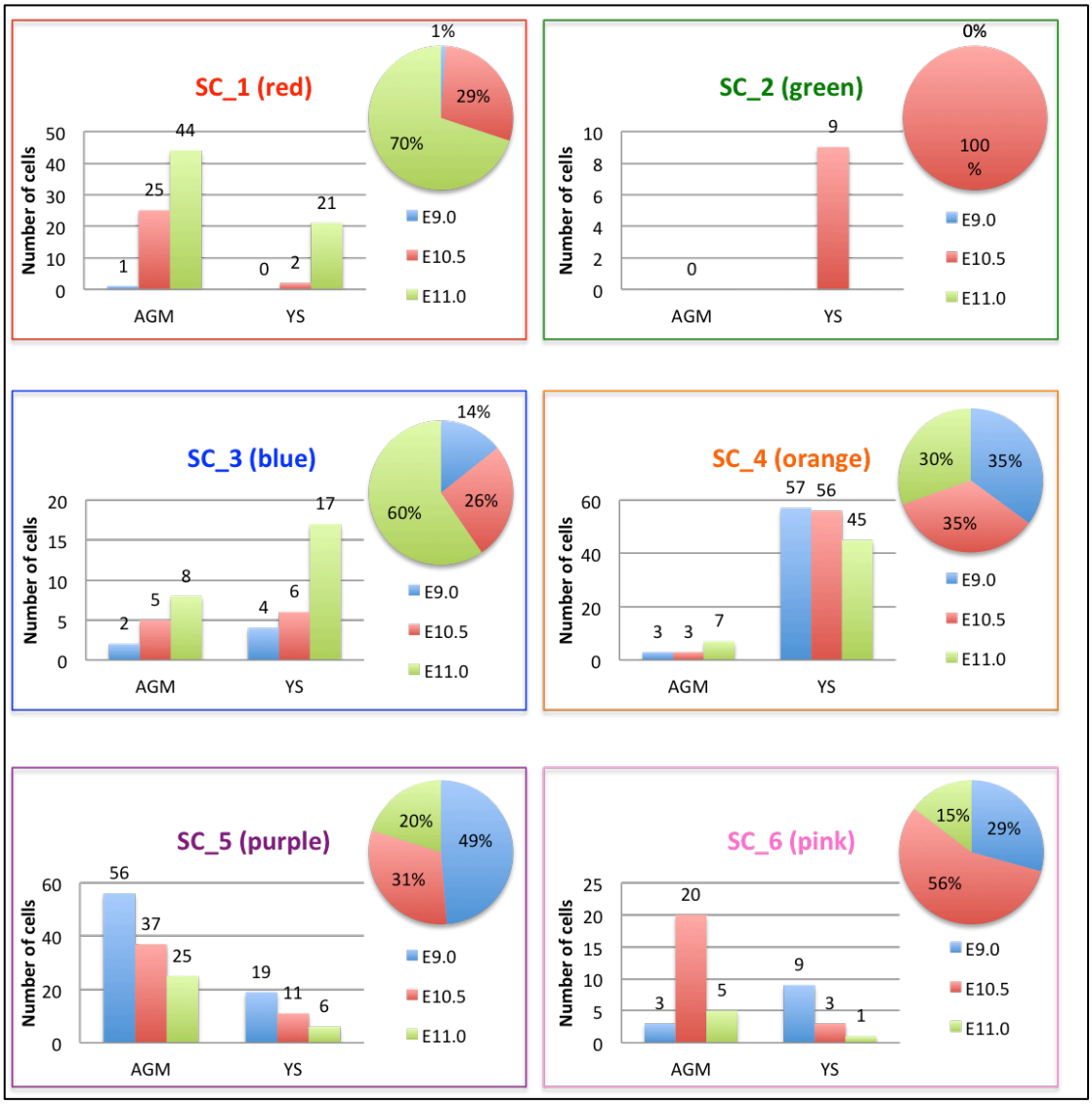

Figure 3.0.15 ***The cluster composition according to the embryonic stage. The bar plots are representing the number of cells detected at E9.0 (blue), E10.5 (red) and E11.0 (green) embryonic stage with tissue annotations in the sample cluster. The adjacent pie chart is representing the frequency of time point origin contributing in the regarding sample cluster.***

SC_1 population is mostly composed of cells found at E11.0 and second most at E10.5, regardless of the tissue origin. Since SC_1 is representing the cells with the clearest hematopoietic profile, the number of cells increasing over time is fitting the expectation. SC_3 has similar pattern of having higher contribution at later time points. SC_5 is just the reverse, as the highest percentage is from E9.0 time point. It makes sense as it might be the population with HE potential, so its frequency may drop when it differentiates into hematopoietic cells. Interestingly SC_2 population is composed of only E10.5 YS origin cells. SC_4 population is almost equally contributed from all 3 embryonic stages. Lastly, the SC_6 population can be found at all time points in AGM and YS. For AGM derived SC_6 cells, E10.5 is the time point at which they are the most frequent. For YS, E9.0 is the time point with the highest frequency, while its frequency decreases towards E11.0. That may be consistent with the early blood formation in the yolk sac.

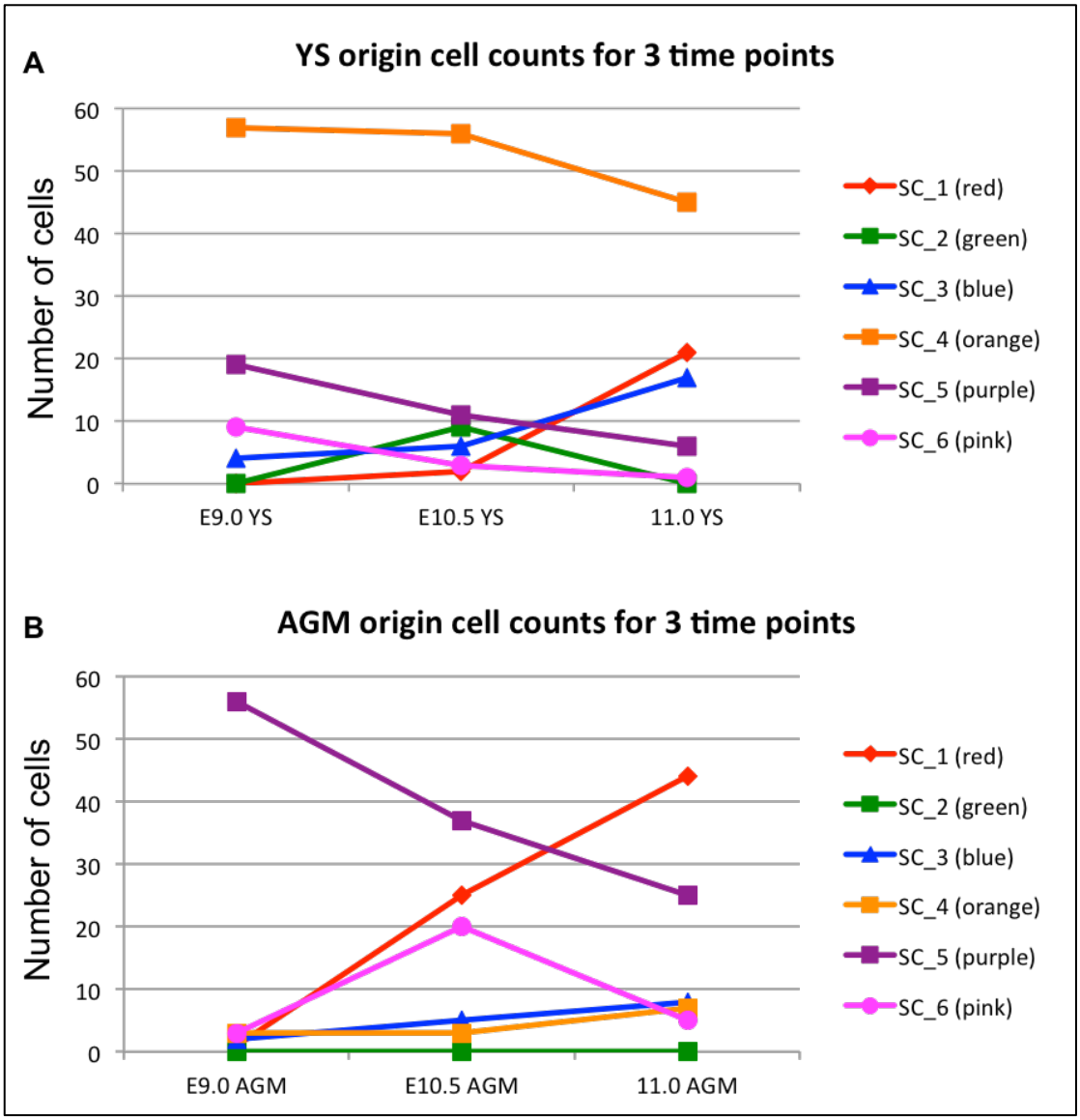

Figure 3.0.16 ***The dot plots of cell counts of annotated sample clusters within*** *A.* ***YS and*** *B.* ***AGM for all time points.***

To visualize the calculated cell counts for each tissue and time point, I made the bar point of cell counts for sample clusters from YS (Figure 3.16.A) and AGM (Figure 3.16.B). According to that, the numbers of cells for each sample clusters within YS time points show small variations compared with AGM. Among the endothelial clusters, SC_4 population is the dominant of YS. The cell count for SC_1 is increasing from E10.5 to E11.0 time points, while SC_5, SC_6 and SC_4 composing cell counts are lowering. This is fitting with the expected pattern of less endothelial cells and more hematopoietic

progenitors when the time passes. Since SC_2 population is only found in the E10.5 YS, it may represent a very small population appearing in a very short time window.

For cells derived from AGM, all sample clusters exhibit change in cell count within time points, except SC_2 which is not existing in AGM. In AGM, the dominant endothelial cell population is SC_5 and its cell counts decrease from E9.0 to E11.0 time points. In parallel, the SC_1 cells are increasing in number from E9.0 to E11.0 stages. The opposing trend of SC_5 cell counts decrease and the SC_1 cell counts increase is fitting the expected pattern of EHT as the hemogenic endothelial cells are giving rise to hematopoietic progenitors. As the intermediate population between SC_5 and SC_1, SC_6 is found highest at E10.5 AGM tissue then it is decreased at 11.0. Surprisingly SC_6 is found dominantly at the E10.5 AGM, which might again indicate tightly regulated transient population emerging for a very short time window.

3. Discussion:

Up to now, the studies on EHT made the general frame of the process and its importance in the emergence of blood progenitor cells. Combined usage of well known hematopoietic and endothelial markers allowed us to enrich cell populations going through EHT. Gene loss/gain of function studies explained the important mechanisms on EHT regulation. However the conventional techniques become limited to gain precise information about the cell identity change during EHT, because it is happening to very rare cells and in a short time window during vertebrate development. Besides the scarcity of the cells, functional heterogeneity is detected within the labeled populations. With the recent advances of the single cell transcriptional analysis, it is now possible to gain detailed gene expression profile of those cells. Additionally we can gain information about the regulatory genes functioning in specific cells. By utilizing the single cell gene expression technique, in this chapter I aimed to dissect the cell identity change during EHT in detail.

3.1. The establishment of single cell qRT-PCR technique for our cells

The initial run with sorted NonHE, HE, Pre-HP, and HP populations from blast culture day1.5 worked as we expected, which confirms that the technique is functioning well. The selection of 96 genes is differentially expressed to allow sufficiently the identification of subpopulations. Indeed, the sample clustering made by the algorithm (Figure 3.6.A) is similar to sorting identity of the cells (Figure 3.6.B) but not identical, which indicates cellular heterogeneity within sorted populations. In the PCA score plot (Figure 3.6.C) it was clear that NonHE cells are projected close to HE and HE is close to Pre-HP and Pre-HP is close to HP, which is very similar expected pattern of appearance during EHT. This indicates our selection of genes can monitor the transition stages in detail. The cellular heterogeneity regardless of its marker verifies our starting point that combination of VE-Cadherin, CD41, and Runx1 proximal promoter marker is not enough to isolate pure populations.

The commonly up/down regulated genes by Runx1 and Gfi1 might be good candidates to monitor the EHT stage. Previously, by mRNA microarray and conventional qRT-PCR, we have identified 39 genes commonly regulated by both Runx1 and its direct target Gfi1. Regarding the overlapping transcriptional regulation role of Runx1 and Gfi1, the common targets of them might reveal the set of gene expression change during EHT. Therefore we checked the 39 genes' expression for the sorted populations at single cell level. The violin plots shows that 5 genes out of 7 up-regulated and 22 out of 32 down-regulated genes are fitting to the expected pattern, in the order of populations as EHT (Figure 3.7). That suggests that Gfi1 and Runx1 at the single cell level could regulate the majority of the 39 genes. Some genes don't fit the expected fashion of regulation, which might be related with the cells harvested at day1.5 blast culture for single cell work, which was different for the samples used for the microarray and conventional qPCR analyses. Since we found 27 genes fitting the expected gene expression change, we can use them as a reference point to detect the stage of cells during the transition.

In addition to the 39 genes, the list of endothelial and hematopoietic genes are also fitting the expected pattern of gene expression regulation. Since endothelial cells are gaining hematopoietic characteristics and losing endothelial ones during EHT, within the population order from NonHE to HE, then to Pre-HP, and then to HP, it is expected to have lower endothelial markers and higher hematopoietic markers. When the populations in EHT order is checked, the violin plot of endothelial genes (Figure 3.8.A) are showing down-regulation pattern (except for Cldn5) and hematopoietic genes (Figure 3.8.B) are showing up-regulation pattern in general (except for Epo, Itgam, Thpo). In conclusion, the initial run with blast culture day 1.5 isolated cells showed that our list of genes are sufficient to identify sub-populations fitting the EHT progression.

3.2. Analysis of EHT in AGM and YS by using single cell qRT-PCR technique

The EHT is happening in AGM and YS, the two main hematopoietic sites during embryogenesis; but the emerging cells types and its timing is very different for each tissue. Therefore, investigating the gene expression profile of the cells isolated from YS and AGM within time points E9.0, E10.5 and E11.0, would help us to understand EHT progression for these tissues. Regarding that aim, our approach was to sort VE-Cadherin positive and CD41 negative (CD41neg) or intermediate (CD41mid) or high (CD41hi) expressing cells for each tissue of 3 time points (Figure 3. 9).

3.2.1. Identification and characterization of sample clusters

The data for all time points and tissue of origin was merged to identify sample clusters common for all (Figure 3. 10.A). The hierarchical clustering without the TGFβ/BMP related genes, form gene clusters and 6 sample clusters (Figure 3.10.B). The endothelial (Figure 3.11.A), hematopoietic (Figure 3.11.B) and 39 genes commonly regulated by Runx1 and Gfi1 (Figure 3.12) gene expression was visualized in violin plots. Depending on the high endothelial gene expression and lack of hematopoietic gene expression, SC_3 (blue), SC_4 (orange), SC_5 (purple) would define populations with more prominent endothelial phenotype. SC_2 (green) is a population with strong endothelial gene expression as well as mature erythroid marker expression. On the other hand SC_1 (red) has very clear hematopoietic gene expression profile and no endothelial gene expression. Finally, SC_6 (pink) is representing a cell profile in between SC_5 and SC_1 by expressing very similar endothelial markers with SC_5 but also some hematopoietic markers.

A detailed analysis for each sample cluster is useful to identify them, as it is simplified in the Figure 3.17.A. SC_3 seems to have no hematopoietic gene expression and the endothelial gene expression is lower than SC_4 and SC_5 populations. Therefore

SC_3 would represent a population with weaker endothelial phenotype. Another endothelial population, the SC_5 is distinguishable from SC_4 with lower expression of some endothelial markers (Gdpd5, Sox7, Npr1, Fmo1, Meis2) and higher expression of some hematopoietic markers (Kit, Erg) (Figure 3.17.A). Therefore SC_5 may represent a population with hemogenic endothelium potential.

SC_6 is the population having expressed endothelial genes together with key hematopoietic genes. The endothelial signature is lower than SC_5 for the genes Cdh5, Col4a2, Tek, Ptprb, Kdr, Ramp2, Pecam1, Gdpd5, Sox7, Npr1, Fmo1, and Meis2. Additionally some hematopoietic genes (Kit, Erg, Atp2a3, Myb, Itgb3) are expressed higher than SC_5. Above all, the signature SC_6 is more prominent with the highest Runx1 expression among other sample clusters, together with other key hematopoietic markers (Sfpi1, Sla, Itgam, Ptprc) (Figure 3.17.A). Those hematopoietic markers emphasize on the initiation of the EHT but there is not yet expression of mature hematopoietic markers.

It is interesting to observe no endothelial gene expression at all in SC_1 population, while it is also sorted within VE-Cadherin positive gate. SC_1 cells are supposed to have the protein on the cell surface, but the VE-Cadherin gene expression seems to be down regulated. Since there are 93 cells in SC_1, rather than a technical error, it might be due to recently switched off VE-Cadherin gene expression. Indeed the previous studies supported the fact that some circulating cells at E10.5 stage may have VE-Cadherin on their membrane as a reminiscence of its endothelial origin (Taoudi 2005) but not expressing the gene anymore (Zovein 2008).

Among all sample clusters, SC_2 is the smallest but also the most interesting sample cluster. It is surprising to see the expression of very mature erythroid cell type related genes (Hbb-b1, Hbb-bh1) coexpressed together with several endothelial genes but not with Runx1, which is the key regulator of EHT (Figure 3.17.A).

A

Gene expression summary table of sample clusters

Gene Name	SC_3	SC_5	SC_6	SC_1	SC_4	SC_2
CDH5	++	+++	++	-	+++	+++
COL4A2	++	+++	++	-	+++	+++
TEK	++	+++	++	-	+++	+++
PTPRB	++	+++	++	-	+++	+++
KDR	++	+++	++	-	+++	+++
RAMP2	++	+++	++	-	+++	+++
PECAM1	++	+++	++	-	+++	+++
GDPD5	+	++	+	-	+	++
SOX7	+	++	+	-	+	++
NPR1	+	++	+	-	+++	+++
FMO1	+	++	+	-	+++	+++
MEIS2	+	++	+	-	+++	+++
KIT	+	++	+++	-	+	+
ERG	+	++	++	-	+	+
ATP2A3	-	+	++	+	+	+
MYB	-	+	++	+	+	+
ITGB3	-	+	++	+	+	+
HBB-B1	-	+	+	+/+++	+/+++	+++
HBB-BH1	-	-	-	-/+++	-/+++	+++
SFPI1	-	-	++	++	-	-
SLA	-	-	++	++	-	-
ITGAM	-	-	+	+	-	-
RUNX1	-	-	++	+	-	-
PTPRC	+	+	+	++	+	+

B

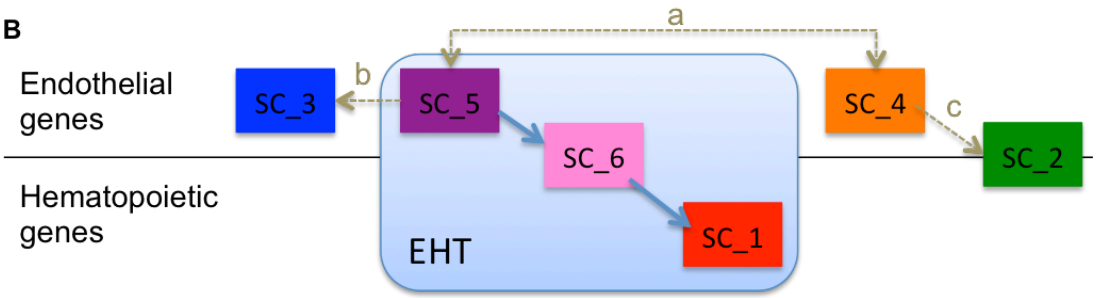

Figure 3.0.17 ***Single cell gene expression summary for in vivo sample clusters****. A. Simplified gene expression data for some endothelial (green tones) and hematopoietic (orange and red tones) genes varying between sample clusters. The list of genes clustered closely (as in Figure 3.10.B) shown within the dark borders. Mark explanation: no expression (-), low expression (+), intermediate expression (++), high expression (+++), bimodal expression as the dominant expression sign is the first before the*

slash (+/) while it has some cells with very highly expression within the same sample cluster (+/+++ or -/+++) *B.* ***Proposed model of sample cluster differentiation relations, according to their endothelial and hematopoietic gene composition. EHT progression is shown as transition from SC_5 to SC_6 and then to SC_1 populations. Additional proposed differentiation relation is shown as dashed lines (a) between SC_4 and SC_5 populations, (b) for differentiation of SC_5 to SC_3, and (c) for differentiation of SC_4 to SC_2.***

3.2.2. CD41 protein is not the direct marker of cell progression during EHT

Since CD41 is the early hematopoietic marker expressed during EHT, we hypothesized that cells would express more CD41 protein on the membrane as it goes through EHT. To test this hypothesis, we sorted VE-Cadherin positive cells with CD41 negative, intermediate or high gates and then check CD41 annotation within the previously identified sample clusters. Unexpectedly, the CD41 protein doesn't increase gradually from endothelial to hematopoietic sample clusters (Figure 3.13). It seems like CD41 hi expression is more abundant in transiting SC_6 cells (93% from CD41hi), while CD41 mid expression is marking the more mature hematopoietic SC_1 cells (58% from CD41mid).

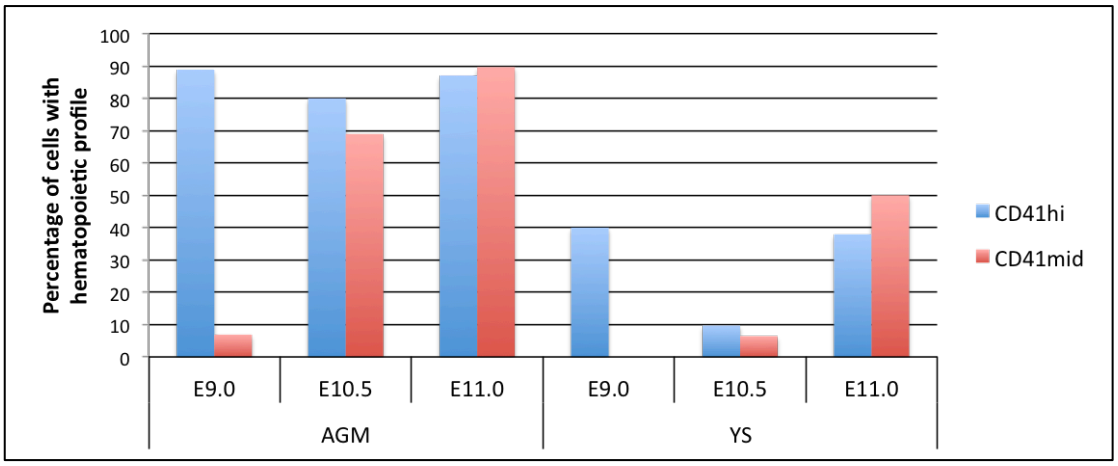

Figure 3.0.18 ***The percentage of cells with hematopoietic profile among CD41mid and CD41hi annotated cells. The hematopoietic profile is assessed such that the cells expressing (Ct value is lower than 24) at least 2 of the major hematopoietic genes (Sla, Itgam, Runx1, Sfpi1) are accepted hematopoietic. The ratio of hematopoietic cell count within the total acquired cell count for each CD41 fraction is calculated and converted to a percentage.***

It is shown in Figure 3.13 that the endothelial sample clusters (SC_3, SC_4, SC_5) have contribution from all CD41 annotations, although CD41 negative is the most abundant for SC_3 (57% from CD41neg) and SC_5 (58% from CD41neg). SC_4 is an exception as it is almost equally contributed from all CD41 annotations. It might be explained by finding of SC_4 mostly (92%) in YS derived cells, where the cells show more common features regardless of CD41 annotation. As shown in figure 3.18, we found that between 60 and 90% of CD41+ cells in the YS are not expressing any hematopoietic genes. This is very surprising, as CD41 has so far always been considered as an exclusive hematopoietic marker. We can see that this non hematopoietic expression is mostly seen in the YS as in the AGM (apart from CD41mid at E9), between 80 and 90 % of CD41 positive cells are also expressing hematopoietic genes.

3.2.3. Sample clusters show different abundance within AGM and YS

Although most sample clusters are detected in the two tissues, the abundance of each cluster is changing (Figure 3.14). For AGM, the most abundant endothelial cluster is SC_5 (purple), which is decreasing from E9.0 to E11.0 (Figure 3.16). At the same time, the SC_1 (red) population is increasing from E9.0 to E11.0 and the transiting SC_6(pink) population is at the highest frequency at E10.5 (Figure 3.16).

The YS is in general showing more equilibrated and stable count for sample clusters, in comparison with AGM (Figure 3.16). For YS, the most abundant endothelial population is SC_4 (orange) (92% of SC_4 is from YS) while the other SC_5 (purple) exists (23% of SC_5 is from YS) but not as high frequency as SC_4 (Figure 3.14). The frequency of both SC_4 and SC_5 drops from E10.5 to E11.0. On the other hand, SC_1(red) hematopoietic population increases a lot from E10.5 to E11.0 (Figure 3.16). SC_3 (blue) population is also more abundant in YS as 64% of it from YS (Figure 3.14)

In summary, SC_5, SC_6 and SC_1 have the highest contribution from AGM, although they exist also in YS. Interestingly SC_2(green) population is found only in YS at day E10.5. Moreover, SC_3 and SC_4 are highly abundant in YS (Figure 3.16).

3.2.4. Detection of sample clusters within 3 time points revealed the differentiation path

For the in vivo analysis of EHT progress, the population abundance change can reflect the transition stage. If the sample cluster abundance is increasing or decreasing between time points E9.0 to E10.5 and E11.0, it may indicate that one type of cell giving rise to another one. By using this approach, here I propose a model for YS and AGM EHT process.

The SC_5 (purple), SC_6 (pink), SC_1 (red) cells are found both in YS and AGM, SC_5 cells have strong endothelial gene expression profile as well mild Kit and Erg expression, which might indicate hemogenic potential. Later, SC_6 has very similar but less endothelial in addition to strong hematopoietic gene expression. SC_6 is distinctive with highest Kit and Runx1 expression, which suggests an already triggered EHT program. Lastly, SC_1 has no endothelial gene expression, lower Runx1, Myb, Itgb3 but strong hematopoietic gene expression related with blood maturation, such as Sfpi1, Sla, Ptprc. Within the SC_1, there are very few cells expressing mature erythroid markers Hbb-b1. Since for both YS and AGM, the cell counts for SC_5 decreases while SC_1 is increasing from E9.0 to E11.0, I propose the presentation of EHT as transition of SC_5 to SC_6 intermediate cells and then to SC_1 more hematopoietic committed cells (Figure 3.17.B).

Recently A. Medvinsky's group proposed a characterization of 3 different cell populations based on their marker expression. (Rybtsov 2011, Rybtsov 2014). According to that model, Pro-HSC is the most immature cells with VE-Cadherin, Runx1, CD41 and C-Kit expression. Pre-HSC type I is one step further than Pro-HSC by

expressing CD41 lower, and pre-HSC type II is more mature with CD43 and CD45 low expression. When the pre-HSC type II differentiate to HSC, it expresses CD45 and CD43 high but not CD41 anymore. If we consider a direct relation with the gene expression and the availability of that protein on cell surface for labeling, we may refer to the model suggested by Medvinsky's group. With that approach, SC_5 may include a small population of hemogenic endothelial cells due to the high endothelial profile but very few Runx1+ cells. SC_6 may include the pro, pre type I and pre type II HSCs depending on the tissue and the time point. SC_1 may match with a population pre-HSC type II because of high Ptprc (CD45) expression. However this interpretation needs to be confirmed by functional analysis for each population.

The SC_4 and SC_5 samples seem very similar in terms of endothelial gene expressions, yet there are some differences to make the clusters. Since SC_5 has Kit expression and lower expression of endothelial genes Nrp1 and Meis2 than SC_4 which might indicate that SC_5 has capacity to become hematopoietic. However it does not eliminate the possibility of one giving rise to the other population as drawn in dashed lines in Figure 3.17.B.a.

The SC_3 (blue) population is identified as low endothelial gene expression and for both YS and AGM, the cell counts for SC_3 increases gradually towards E11.0. Since its gene expression pattern looks similar to the pattern of SC_4, I proposed that SC_3 cells might be derived from SC_4 in a form of less endothelial gene expression as shown in dashed lines in Figure 3.17.B.b. However, Ppia (the reference gene) expression level for some cells within the SC_3 is un-expectedly low. Such low expression have to be double checked in order to eliminate the possibility of a technical error, before inferring about the biological meaning of the SC_3 cells.

The SC_2 cells are very interesting with both strong endothelial and erythroid gene expression profile, which was never reported before. Those cells are detected only at

E10.5 of YS. The SC_2 endothelial gene expression profile is similar to SC_4 and there are very few cells within SC_4 expressing Hbb-b1 and Hbb-bh1 erythroid genes like SC_2 (Figure 3.17.A). Considering these similarities in gene expression, I propose that SC_2 cells might be derived from SC_4 population only for very short time window between E9.0 to E10.5 of YS (Figure 3.17.B.c).

4. Conclusion and Future directions:

With the new advances on the microfluidics mechanical controlling units, it is possible to run mid-throughput qPCR reactions on cDNA material harvested from single cells. (Ståhlberg, Rusnakova, Forootan, Anderova, & Kubista, 2013). The technique has been used to perform an extensive gene expression profiling studies on blastocyst stage embryos to reveal fate decisions at single cells (Guo et al., 2010), early kidney development of mouse (Brunskill et al., 2014), and early emergence of lymphomyeloid restricted progenitors in mouse hematopoiesis (Böiers et al., 2013). It has been a very powerful technique also to reveal gene regulatory networks (Moignard et al., 2013) and cell surface repertoire (Guo et al., 2013) in adult mouse hematopoietic lineage, as well as the fate change profiling during EHT (Swiers et al., 2013). Recently it was used in combination with site specific transcriptional activators to reveal regulatory networks, to understand the role of Sfpi1 in developmental hematopoiesis (Wilkinson et al., 2014).

The difference between AGM and YS hematopoiesis has been a debate topic for a long time (Lassila, Eskola, Toivanen, Martin, & Dieterlen-Lievre, 1978) (Tanaka et al., 2012). There is a consensus for AGM as the only site for generation of HSCs with long-term functional repopulation capacity, in addition to the multi-potent progenitors (Boisset et al., 2010; Chen et al., 2011; a Medvinsky & Dzierzak, 1996). On the other hand YS is the site for the first HP emergence, forming the primitive erythroid cells, followed by erythroid myeloid and lymphoid progenitors (Lux et al., 2008; Palacios & Imhof, 1993; Samokhvalov et al., 2007). Although the hematopoiesis at both AGM and YS

depends on the transition of hemogenic endothelial cell to HSPC (Boisset et al., 2010; W. Li et al., 2005), the hematopoietic program at each site is initiated at different time during embryogenesis. YS hematopoiesis is initiated at around E7.5 and actively generating HPs until E11.0, while AGM hematopoiesis is started at E9.5 and continues until E12.0 (Palis, Robertson, Kennedy, Wall, & Keller, 1999). Despite all those studies, the difference of hematopoietic programs for both tissues could not be analyzed at the single cell level, until today.

In this project, we used the single cell qRT-PCR technique to explore the hematopoietic program of AGM and YS at the single cell level. We aimed at identification of cell types during the course of EHT for both AGM and YS tissues. In order to capture all types of cell appearing during EHT, we chose to collect cells from time points E9.0, E10.5 and E11.0. A similar study done previously by Swiers G. et al., with single cells isolated from all big arteries (AGM, vitelline and umbilical arteries together) using a set of 20 endothelial and hematopoietic affiliated genes (and 4 reference genes) while we used a panel of 96 genes. With the help of Runx1 +23 GFP enhancer-reporter transgenic mouse line, they separated the hemogenic endothelium (HE) from the other endothelial cells (NonHE). They isolated NonHE, HE, CD41+ HP cells and CD45+ HP cells to follow the EHT course (Swiers et al., 2013). However their study neglects the fact that even sorted populations have cellular heterogeneity, which is actually seen as sub-populations within their hierarchical clustering of sorted populations. Also by combining the cells from AGM, umbilical and vitelline arteries, they lose the information about tissue specificity. In terms of expression change of certain genes (Gata2, Tal1, Gfi1, Sfpi1 and Myb), our proposed model of EHT confirms the transition within their sorted populations. On top of it, our study provides data about YS hematopoiesis and makes it possible to compare the hematopoietic programs initiated within hemogenic endothelium of the two tissues.

The transition model I proposed for EHT (SC_5 → SC_6 → SC_1) has shared gene expression profile with the populations introduced in Wilkinson et. al. and Swiers et. al. However, for all three studies, it is solely based on the gene expression data, whose biology needs to be confirmed. For future experiments, isolation of that populations and confirming the hematopoietic lineage commitment capacity will be precious to conclude about the initial cell identity. Finding the corresponding sample clusters within the embryo (AGM would have higher population frequencies) would be possible by using reporter cell/mouse lines for that gene. Alternatively, among 96 genes, some cell surface proteins (such as Itgb3) can be used for antibody labeling if the gene expression is directly correlated with protein expression.

Lastly, SC_2 is an interesting sample cluster, which was not discovered before. Despite the fact that there are only 9 cells, all isolated from E10.5 YS, it may still reflect a biologically relevant population. To confirm that cells co-expressing endothelial and erythroid genes exist, we need to isolate it using another method. Following that approach, we used the mir144/451-eGFP mouse line (Rasmussen et al., 2010), which expresses GFP specifically in the erythroid lineage. In the FACS analysis of E10.5 YS derived cells from mir144/451$^{+/GFP}$ embryos, we found a very small VE-Cadherin+ GFP+ population, which would fit the only 9 cells found in SC_2 (Irina Pinheiro, data not shown). As a next step, we will run single cell qRT-PCR of those isolated cells to check gene expression profile and see if it matches with the SC_2 profile. In parallel, we will test its functional hematopoietic lineage potential by performing in vitro hematopoietic commitment assay with the sorted VE-Cadherin+ GFP+ cells. If the results confirm the endothelial and erythroid function of these cells, it will be the first-time identification of erythroid lineage commitment at endothelial stage. Under the circumstances that we confirm the existence of such rare population detectable only for a short time in the YS, one may speculate that these cells can be the endothelial cells already committed to

erythroid lineage with previously proposed Runx1 independent EHT program (Lacaud G. 2002)

Single cell qRT-PCR is a powerful technique to analyze the expression of 96 genes in the same cell, however some aspects of the results have to be confirmed by other methods. Since 96 genes are chosen in customized manner, there is a bias introduced by the choice of genes. Within the samples, there might be cells, which cannot be distinguished by the expression level of 96 chosen genes. Single cell mRNA sequencing would offer a great solution to get the un-biased gene expression profiling. By aiming at identification of distinguished sub-populations, we analyzed VE-Cadherin positive cells isolated from AGM. Through collaboration with Sarah Teichmann's lab in EMBL EBI, we followed the C1 (Fluidigm) single cell mRNA sequencing protocol. The initial results are promising as we identified sub-populations with distinctive gene expression profile. In the future, we are planning to compare those sub-populations with the ones found in single cell qRT-PCR. Furthermore, the distinctive genes of sub-populations have a potential use as a marker gene related with that population. Therefore, identified genes will be confirmed for labeling specific cells in vivo and in vitro.

Gene expression can be a good indication of cell type, but sometimes the post-transcriptional regulations and post-translational modifications become the determining factor for having the functional protein in the cell. Therefore the protein expression analysis would be needed for population analysis during EHT. Lyoplate monoclonal antibody panel is the collection of 176 mouse antibodies provided by BD. This experiment would not have been possible using embryonic cells because of the small quantity of material per embryo. To bypass this problem, I used the in vitro ES cell differentiation system and I managed to generate a large cell numbers sufficient to screen these 176 antibodies on cells derived from blast day 1.5 culture. I selected the list of antibodies with overall labeling frequency within 4-80%. In order to focus on finding

a marker for hemogenic endothelium, I chose 15 antibodies showing differential expression within VE-Cadherin positive cells. Lastly I confirmed that 13 of them has similar expression pattern in AGM and YS derived cells at E10.5 embryos. In the future, I will test the enrichment of hematopoietic commitment of the cells isolated from E10.5 isolated AGM and YS samples. If any of the 13 antibodies show enrichment of hematopoietic potential, I will check the gene expression profile of those cells in the search of a match between the sample clusters discussed in this chapter.

In the future, by combining the information gained by C1 single cell mRNA sequencing and lyoplate antibody screening, I aim to find a good marker for isolation of the sample clusters SC_5, SC_6 and SC_1. After isolation of the corresponding populations, my ultimate aim is to confirm their lineage capacity in hematopoietic commitment assays.

Chapter 4: The role of TGFβ Pathway in EHT

1. Introduction:

1.1. EndMT and its similarity with EHT

Endothelial cells can have high plasticity during development and can transit through a migratory cell type. Endothelial to mesenchymal transition (EndMT) is a key developmental event, which is first identified in endocardial cushion formation. Initial studies with chicken and rat developing heart tissue suggested the endothelial cells are transforming into mesenchymal cells and migrating towards the region called cardiac jelly (Markwald, Fitzharris, & Manasek, 1977). Formed cardiac jelly composed of extracellular matrix elements and mesenchymal cells surrounded by endothelial layer, which all together named as endocardial cushion. Endocardial cushion is preceding the heart valves (Maron & Hutchins, 1974), therefore EndMT is vital for heart development.

On top of its essential role in development, the EndMT may also play an important role in tissue fibrosis and cancer metastasis in adult organism. The fibrotic diseases are due to accumulation of fibroblasts and extracellular matrix into the site of injury. Such as in cardiac fibrosis, endothelial origin cells are giving rise to fibroblasts thorough EndMT (Zeisberg, Tarnavski, et al., 2007). Similarly EndMT is found to contribute to kidney fibrosis (Zeisberg, Potenta, Sugimoto, Zeisberg, & Kalluri, 2008), pulmonary fibrosis (Arciniegas, Neves, Carrillo, Zambrano, & Ramírez, 2005) , and intestinal fibrosis(Rieder et al., 2011). Similarly carcinoma associated fibroblasts can promote tumor progression and EndMT is claimed to have role in emergence of activated fibroblasts from nearby endothelial cells (Zeisberg, Potenta, Xie, Zeisberg, & Kalluri, 2007).

Upon detection of the EndMT initiating signal, the cells are delaminated from the endothelial layer. Following this, the mesenchymal markers such as αSMA and FSP1 are

replacing the endothelial markers such as VE-Cadherin, CD31. The endothelial cells are losing their apical-basal polarity, endothelial marker expressions, tight junctions and adhesions within endothelial layer, resulting in a migratory cell type (Potenta, Zeisberg, & Kalluri, 2008).

1.2. General remarks of TGFB signaling

Transforming growth factor beta (TGFβ) signaling pathway is the driver of many cellular events underlying various developmental regulations. The pathway consists of three main players: TGFβ superfamily ligands, cell membrane-bound receptors and the effector molecules in the cell (SMAD transcription factors). The series of kinase event is initiated upon binding of a ligand on a homodimer of type II TGFβ receptor. This binding recruits a TGFβ receptor type I homodimer to form all together a hetero-tetrameric complex and the type II receptors phosphorylate the type I receptors. Phosphorylated type I receptors become active and then they phosphorylate and activate a group of receptor regulated SMAD (R-SMAD) proteins. The phosphorylated R-SMADs later form heterodimers with common-mediator SMAD proteins (Co-SMADs) and localize into nucleus where they act on target genes in means of transcription activation. Another type of SMAD proteins, Inhibitory SMAD (I-SMAD), can block the phosphorylation of R-SMADs, which cuts off the down-stream relay of the signal (Evangelia Pardali & Ten Dijke, 2012)

The cellular response might be different depending on the types of ligand binding to receptors (Goumans et al., 2002; Evangelia Pardali & Ten Dijke, 2012). TGFβ superfamily protein ligands include TGFβ isoforms, activins, bone morphogenetic proteins (BMPs). In endothelial cells, all TGFβ isoforms bind to TGFBR2 (also known as TβRII), which then recruits TGFBR1 (also known as ALK5). This receptor complex then phosphorylates Smad2 and Smad3 (Figure4.1.A). Instead of TGFβ, if BMP is available as a ligand, it binds to different type II receptors, BMPRII or ActRII; then different type I

receptors, ALK1/2/3/6. These type I and type II receptors form a different complex, which relays the signal through Smad1/5/8 (Figure4.1.B). The type of Smad proteins localized in the nucleus will determine the target gene for transcription. In summary two sets of signaling events can be activated depending on the ligand availability in the environment and receptor availability in the cell.

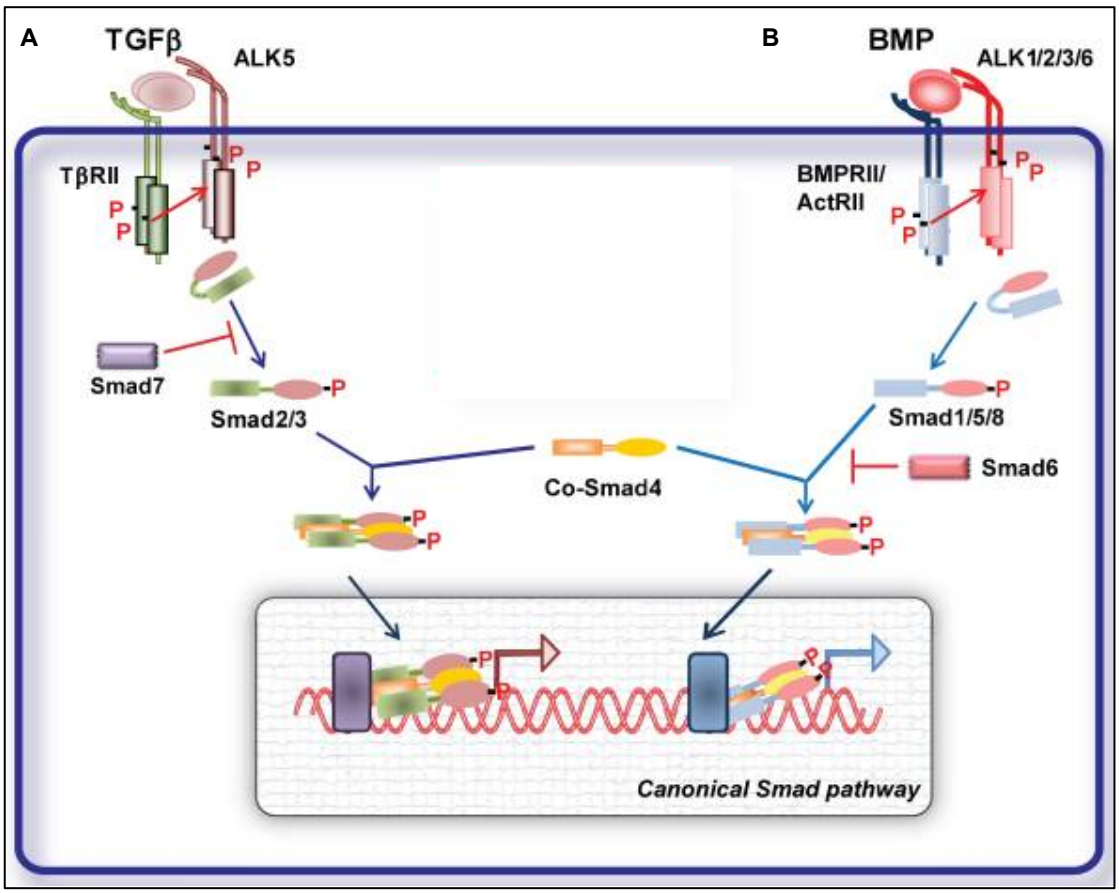

Figure 4.0.1 ***Simplified TGFβ signaling pathway showing two sets of kinase reactions resulting in different gene transcription initiation. Image is adapted from Pardali, E., & Ten Dijke, P. (2012) International Journal of Biological Sciences. A. TGFβ family proteins trigger the signaling cascade through TGFBR2, TGFBR1 (ALK5), SMAD2/3. B. BMP family proteins trigger the signaling cascade through BMPRII, ACTRII, ALK1/2/3/6, SMAD1/5/8.***

1.3. TGFβ pathway in EndMT

There are several signaling mechanisms controlling EndMT and TGFβ pathway is one of the important regulators involved in both developmental and pathologic cases. TGFβ1, as a cardiac fibrosis promoting ligand, induces EndMT therefore increases

number of fibroblasts, whose effect can be reversed by introducing BMP-7 (Zeisberg, Tarnavski, et al., 2007). TGFβ1 also increases the rate of EndMT in primary endothelial cell lines, generating more fibroblast cells. Similarly high TGFβ1 labeling overlaps in the areas of FSP1 expressing fibroblasts in tumor tissues (Zeisberg, Potenta, et al., 2007). Smad7, which is a negative regulator of TGFβ signaling, inhibits EndMT mediated renal fibrosis (Lan et al., 2003). Smad3, an R-Smad family protein, deficiency on the other hand can be protective against renal fibrosis(Inazaki et al., 2004; Sato, Muragaki, Saika, & Roberts, 2003).

A very comprehensive study of TGFβ pathway in regulation of EndMT was done on the fibrodysplasia ossificans progressiva (FOP) disease (Medici et al., 2010). FOP patients suffer from ectopic bone formation in soft tissues after acute inflammation. A genotypic study showed a mutation in Alk2 (also known as Acvr1) gene causes constitutively active receptor type I for TGFβ signaling (Shore et al., 2006). Further Medici et al. confirmed the role of active Alk2 on FOP disease by using either a mouse model with constitutively active Alk2 or by treating the normal endothelial cells with TGFβ2 or BMP4. The result is the same for both cases as the endothelial cells transited to mesenchymal, stem-like cell phenotype, later they can differentiate into osteoblasts. In summary, this study links the TGFβ/Alk2 signaling with activation of EndMT mechanism in a disease.

1.4. TGFβ pathway in hematopoiesis

Mouse studies suggested that the loss of function of TGFB signaling (either ligand, or receptor, or the effector proteins) causes deficiencies in hematopoiesis. Two groups generated TGFB1 null mouse and reported that rare viable TGFB1-/- mice have excess inflammatory response, leading to death within one month after birth. (Kulkarni et al., 1993; Shull et al., 1992). The deficient phenotype related with the hematopoiesis was noticed when TGFB1-/- mouse embryos are investigated prior than E10.5 (Dickson et

al., 1995). At E9.5 of TGFB1-/- embryos, endothelial cells are less adherent yet they can form the yolk sac and the embryo proper vasculature but not enough of capillary vessels. This can be interpreted as the initial emergence of vascular endothelial precursors from hemangioblast is intact, however further differentiation of endothelial cells to support the vasculature is disrupted in TGFB1-/- embryos. In parallel at E9.5 there are less red blood cells in TGFB1-/- yolk sac then in a wild type littermate. This anemic phenotype is possibly caused by a deficiency in the yolk sac hematopoiesis. (Dickson et al., 1995).

Similar anemic phenotype is observed in other mouse knock-out studies of the pathway. Deletion of either the type I receptor ALK1 (Oh et al., 2000), or another type I receptor TGFBR1 (Larsson et al., 2001) or type II receptor TGFBR2 (Oshima, Oshima, & Taketo, 1996) or their binding partner Endoglin (D. Y. Li et al., 1999) or the signaling transducer Smad5 (Sankar et al., 1996) results in embryonic lethality with anemia. All these studies report the similar phenotype of weak, dilated vasculature that does not support a proper circulation, together with less blood cell emergence. In contrast to abnormal hematopoiesis phenotype, TGFBR1 -/- mouse hematopoietic stem cells show a completely normal hematopoietic differentiation capacity in vitro (Larsson et al., 2001). Additionally, when TGFBR1 is conditionally knocked out in adult mice; the isolated hematopoietic stem cells showed increased proliferation in vitro but normal self-renewal and differentiation in vivo (Larsson et al., 2003).

Runx1 protein, the key transcription factor of EHT, is interestingly found to be physically interacting with Smad proteins in various cell types. Affinity chromatography made from mouse megakaryoblastic cells revealed a physical interaction of Runx1 and Smad2 proteins (Yu et al., 2012) Another study reported that Smad3/4 proteins and Runx1 cooperatively bound on target DNA site to trigger transcription from immunoglobulin α constant region during B cell maturation (Y. Zhang & Derynck, 2000).

Similar interaction of Smad3/4 proteins with Runx1 plays the role of regulating human germ line IgA gene expression (E. Pardali et al., 2000) and induction of germline immunoglobulin Cα promoter (Hanai et al., 1999).

1.5. Hypothesis:

Considering the valuable findings from knock-out studies showing TGFβ signaling involvement in early hematopoiesis, we investigated the possible role of TGFβ pathway in the regulation of EHT. Furthermore, Runx1 interaction with Smad proteins in adult hematopoiesis may suggest a similar developmental regulation of Runx1 binding to target DNA during EHT. Putting together the previous findings about TGFβ signaling and hematopoiesis might suggest a regulatory mechanism of EHT.

The regulatory role of TGFβ signaling in EndMT is well studied and the recognition of TGFβ ligand in endothelial cells triggers a set of events activating EndMT. The loss of their endothelial phenotype and the gain of migratory features are the shared morphological changes between EndMT and EHT. Yet the resulting phenotype is mesenchymal cells in EndMT and hematopoietic cells in EHT. Due to the similarity in endothelial phenotype loss, I hypothesized that TGFβ signaling could be involved in a common molecular mechanism to regulate the initial endothelial phenotype loss in EndMT and EHT.

2. Results:

2.1. Expression analysis of TGFβ pathway related genes during EHT

If TGFβ signaling has a role in EHT regulation, the cells undergoing EHT should express the elements of the cascade. In order to check the expression level of TGFβ signaling related genes, we decided to analyze EHT populations isolated from embryos or in vitro culture. As we discussed in the previous chapter, there is cellular heterogeneity for rare cell types appearing within a short time window, therefore we decided to use single cell qRT-PCR technique instead of the conventional one. Among the 96 genes (Table 3.1) to be used in BioMark 96 x 96 microfluidics platform, 22 are TGFβ/BMP pathway related genes (Table 4.1).

Function	Name	Alternative names	Long name	Ensembl
Receptor Type I	Acvrl1	Alk1; Acvrlk1	activin A receptor, type II-like 1	ENSMUSG00000000530
	Acvr1	Alk-2; Acvr; Alk8; SKR1	activin A receptor, type 1	ENSMUSG00000026836
	Bmpr1a	ALK3; Bmpr; BMPR-IA	bone morphogenetic protein receptor, type 1A	ENSMUSG00000021796
	Acvr1b	Alk4; SKR2	activin A receptor, type 1B	ENSMUSG00000000532
	Tgfbr1	Alk-5; TbetaRI	transforming growth factor, beta receptor I	ENSMUSG00000007613
Receptor Type II	Bmpr2	BMP-2, BMPRII	bone morphogenic protein receptor, type II	ENSMUSG00000067336
	Acvr2a	ActRIIa, Acvr2, tActRII	activin receptor IIA	ENSMUSG00000052155
	Tgfbr2	TbetaRII, TbetaR-II	transforming growth factor, beta receptor II	ENSMUSG00000032440
	Acvr2b	ActRIIB	activin receptor IIB	ENSMUSG00000061393
Ligand	Bmp4	Bmp-4; Bmp2b; Bmp2b1	bone morphogenetic protein 4	ENSMUSG00000021835
	Tgfb1	Tgfb; Tgfb-1; TGFbeta1	transforming growth factor, beta 1	ENSMUSG00000002603
	Tgfb2	Tgfb-2; BB105277	transforming growth factor, beta 2	ENSMUSG00000039239
	Tgfb3	Tgfb-3	transforming growth factor, beta 3	ENSMUSG00000021253
Signal transducer	Smad1	Madh1, Madr1, Smad 1	SMAD family member 1	ENSMUSG00000031681
	Smad2	Madh2, Madr2, Smad 2	SMAD family member 2	ENSMUSG00000024563
	Smad3	Madh3; AU022421	SMAD family member 3	ENSMUSG00000032402
	Smad4	DPC4; Madh4	SMAD family member 4	ENSMUSG00000024515
	Smad5	Dwf-C; Madh5	SMAD family member 5	ENSMUSG00000021540
	Smad6	Madh6	SMAD family member 6	ENSMUSG00000036867
	Smad7	Madh7	SMAD family member 7	ENSMUSG00000025880
	Smad9	Madh8; Madh9; Smad8	SMAD family member 9	ENSMUSG00000027796

Table 7.4.1 ***List of TGFβ pathway related genes with their role in the pathway. The official names are in the second column and the alternative names in the third.***

To recapitulate EHT in vitro, I used a well-established mESC protocol (Sroczynska, Lancrin, Pearson, & Lacaud, 2009). In this protocol, first mES cells were cultured for 3 days to generate embryoid bodies and the hemangioblast equivalent cells defined by Flk1 expression were sorted to start blast culture. By day 1.5 of blast culture, the NonHE, HE, Pre-HP and HP populations characterized by the combined staining pattern of VE-Cadherin, hCD4/Runx1 and CD41 (see Figure 3.3). The FACS isolated populations

can be further tested for hematopoietic differentiation capacity in hemogenic endothelium culture.

As it is explained in detail in chapter 3, to analyze the EHT in vivo, I decided to isolated VE-Cad+ cells expressing different levels of CD41 from AGM and YS tissues, which are the main EHT sites in the embryo. In order to collect cells from all stages of EHT within VE-Cadherin+ and CD41 negative/intermediate/high gates (Figure 3.9), the AGM and YS tissues of embryos at E9.0, E10.5 and E11.0 time points was sorted by FACS at the single cell level. The single cell qRT-PCR was run and the raw data results of the AGM and YS tissues for all time points are merged for the combined analysis (Figure 3.10). Also only for this chapter, the raw data of AGM samples from different time points are merged. The same sample clusters characterized in the chapter 3 are kept for the analysis in this chapter. According to the proposed model in chapter 3, the SC_4 and SC_5 are the main endothelial populations, while the SC_5 includes hemogenic endothelial cells. SC_6 has shared endothelial phenotype with SC_5 but also express some hematopoietic genes like Runx1. Lastly the SC_1 is the population with no endothelial expression but genes related with more mature hematopoietic phenotype. In summary, the SC_4 and SC_5 might include the non-hemogenic endothelial cells and the EHT process is expected to be from hemogenic endothelial cells of SC_5 to SC_6 and then to SC_1. It is noteworthy that, since we did not sort VE-Cadherin-, CD41+ cells from the embryo derived samples, for the in vivo analysis we do not expect to have a sample cluster corresponding to HP from the in vitro data set.

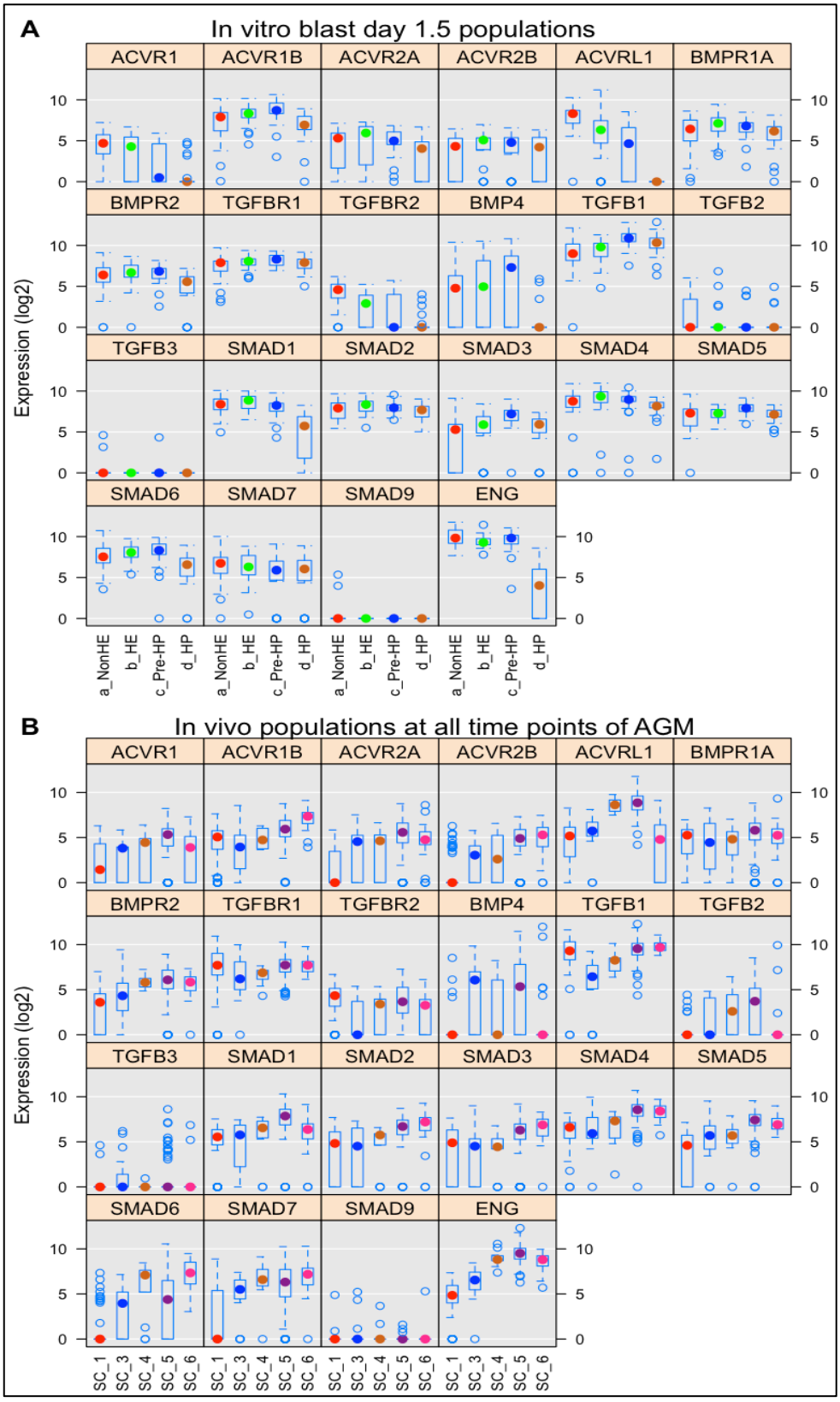

Figure 4.0.2 ***Single cell gene expression analysis of TGFβ pathway elements.*** *A.* ***Cells isolated from blast day 1.5 culture as it is explained in chapter 3*** *B.* ***Cell isolated from AGM of 3 time points (E9.0, E10.5, E11.0) with the sample clusters identified in chapter 3.***

First of all, we checked if we can detect the expression of the TGFβ pathway genes in NonHE, HE, Pre-HP and HP population isolated from in vitro blast day 1.5 culture (Figure 4.2.A) and previously identified endothelial populations from AGM section of E10.5 embryo (Figure 4.2.B). We observed that most of the TGFβ pathway related genes are expressed either at low level or not showing variance between populations. When we compare the populations in the direction of EHT, we saw a consistent pattern for both in vitro and in vivo of down-regulation of Acvrl1(ALK1), Tgfbr2, Eng, Bmp4 genes but no differential expression of Tgfbr1 (Alk5) (Figure 4.2). Previously it has been shown that both ACVRL1 (Alk1) and TGFBR1 (Alk5) are binding to TGFBR2 on human umbilical vessel endothelial cells (HUVEC). They suggested a model of angiogenesis control either via activation of Alk1 Smad1/5 signal transduction or via Alk5 activation triggering Smad2/3 signal transduction (Oh et al., 2000). We thought a similar balance could play role in endothelial cell differentiation towards hematopoiesis.

Since the expression of receptor type I and II is necessary for the signaling activity, we focused on the expression pattern of Acvrl1 (Alk1), Tgfbr1 (Alk5), and Tgfbr2. The box plot representation of gene expression values showed high Acvrl1 and Tgfbr1 expression, coupled with lower expression of Tgfbr2 on the cells with endothelial phenotype (NonHE, HE in Figure 4.3.A and SC_4, SC_5 in Figure 4.3.B). However when we cultured these endothelial cells isolated from blast day 1.5 in hemogenic endothelium culture for 2 days, we see dramatically decreased expression of Acvrl1 and obvious down-regulation of Tgfbr2 but almost no change of Tgfbr1 expression in descendent HP cells (Figure 4.3.C). Because it is technically challenging to trace the clonal progeny of hemogenic endothelial cells after EHT, we checked the gene expression level of AGM isolated cells with the previously identified sample clusters in the direction of EHT (SC_5 to SC_6 to SC_1 but no sample cluster equivalent of HP). Similar to in vitro results, SC_6 and SC_1 populations have lower Acvrl1 expression than SC_5 but there is no difference in Tgfbr1 and Tgfbr2 expression (Figure 4.3.D).

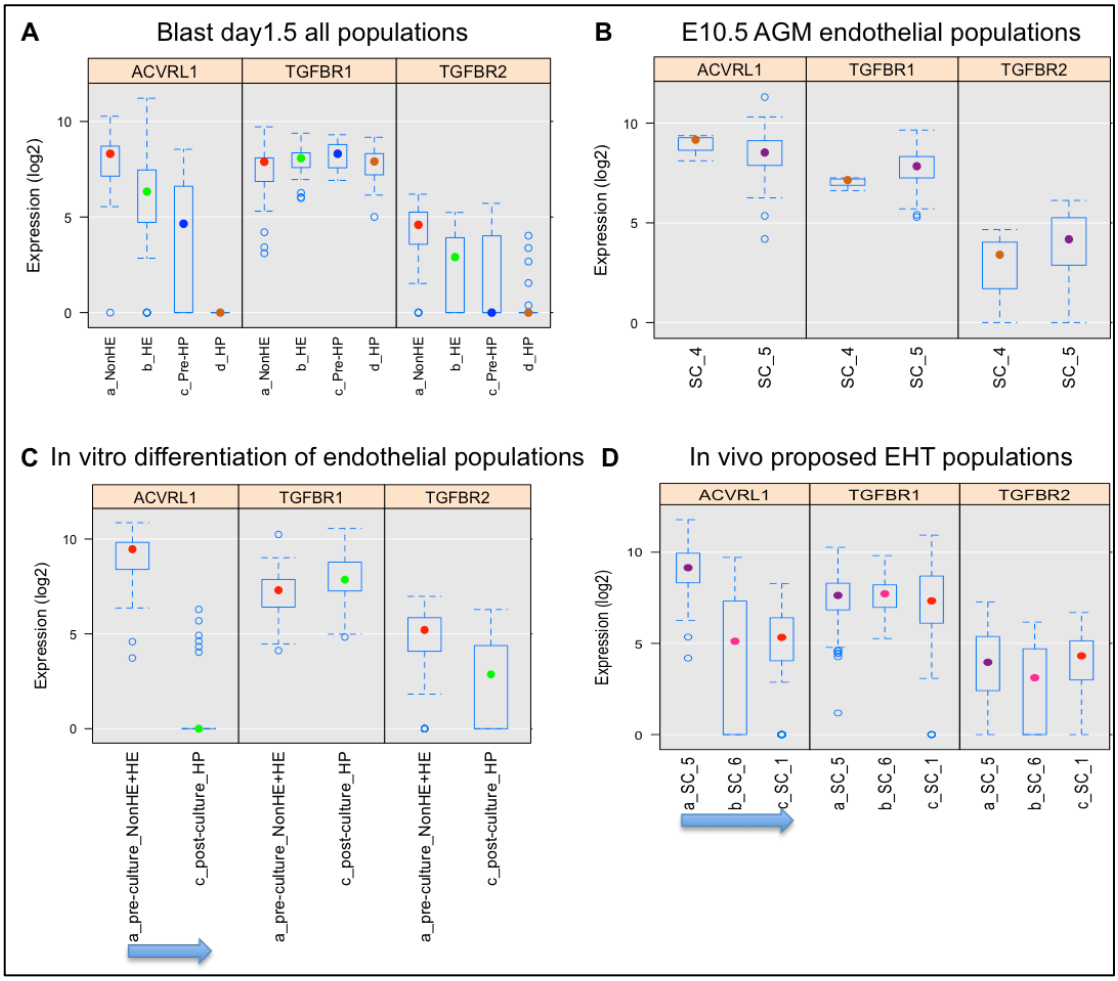

Figure 4.0.3 ***Box plot representation of single cell qRT-PCR results with log2 expression values of Acvrl1 (Alk1), Tgfbr1 (Alk5), Tgfbr2 genes.*** *A.* ***Populations from in vitro blast day1.5 culture were sorted as explained previously in Figure 3.6.*** *B.* ***Endothelial populations isolated from AGM of E10.5 embryos, sorted as explained previously in Figure 3.9 and populations are identified in Figure 3.10.*** *C.* ***NonHE+HE population isolated from blast day1.5 culture and HP population derived from the NonHE+HE population after the in vitro hematopoietic differentiation culture.*** *D.* ***In vivo YS and AGM derived populations according to the proposed model of EHT. The arrow indicates the expected EHT direction.***

2.2. Testing the effect of TGFβ activation and inhibition on EHT

EndMT can be triggered by ligand TGFβ2 (Medici et al., 2010). In order to activate the TGFβ signaling cascade, I added 5ng/ml of human recombinant TGFβ2 into the culture medium; or to inhibit the cascade, I added 10nM SB-431542, a small molecule inhibitor of ALK5. As a control, I used normal culture medium with the same amount of

suspension liquid 0.1%BSA + 4mM HCl for TGFβ2 or DMSO for SB431542 or without any addition. Since we did not acquire a different result with these 3 conditions, only DMSO added control was kept afterwards.

The cells were re-plated in hemogenic endothelium mix with either DMSO or 10nM SB431542 or 5ng/ml TGFβ2 for 3 days. The time-lapse images were taken for 3 days every 15 minutes. After three days of culture, the cells were examined for VE-Cadherin and CD41 expression by flow cytometry analysis. The harvested cells were also frozen to extract total RNA and perform mRNA microarray analysis (Figure4.4.A). Surprisingly, at the end of 3 days, there were more round cells in the condition with SB431542. On the other hand, in the presence of TGFβ2, there were very few round cells but more flat cells of mesenchymal morphology (Figure 4.4.B). The number of round cells during the 3 days of culture was quantified based on the live-cell imaging. The control with DMSO doesn't seem different morphologically (Figure 4.4.B) and also reflected in quantified number of round cells (Figure 4.4.C). It shows that there is a striking increase of round cells, presumably HP cells, in TGFβ inhibited condition compared to DMSO treated cells. On the contrary, TGFβ activation results in almost no round cells (Figure 4.4.C).

After 3 days of hemogenic endothelium culture, the cells are expected to have higher frequency of CD41+, VE-Cadherin- cells as in DMSO culture (Figure 4.5.A). The FACS analysis done after 3 days are showing a significant increase in CD41 positive frequency in condition with inhibitor while with the TGFβ activator CD41 positive frequency is dramatically lower. In contrast, VE-Cadherin frequency is significantly higher in TGFβ activator added condition than the control (Figure4.5.A&B).

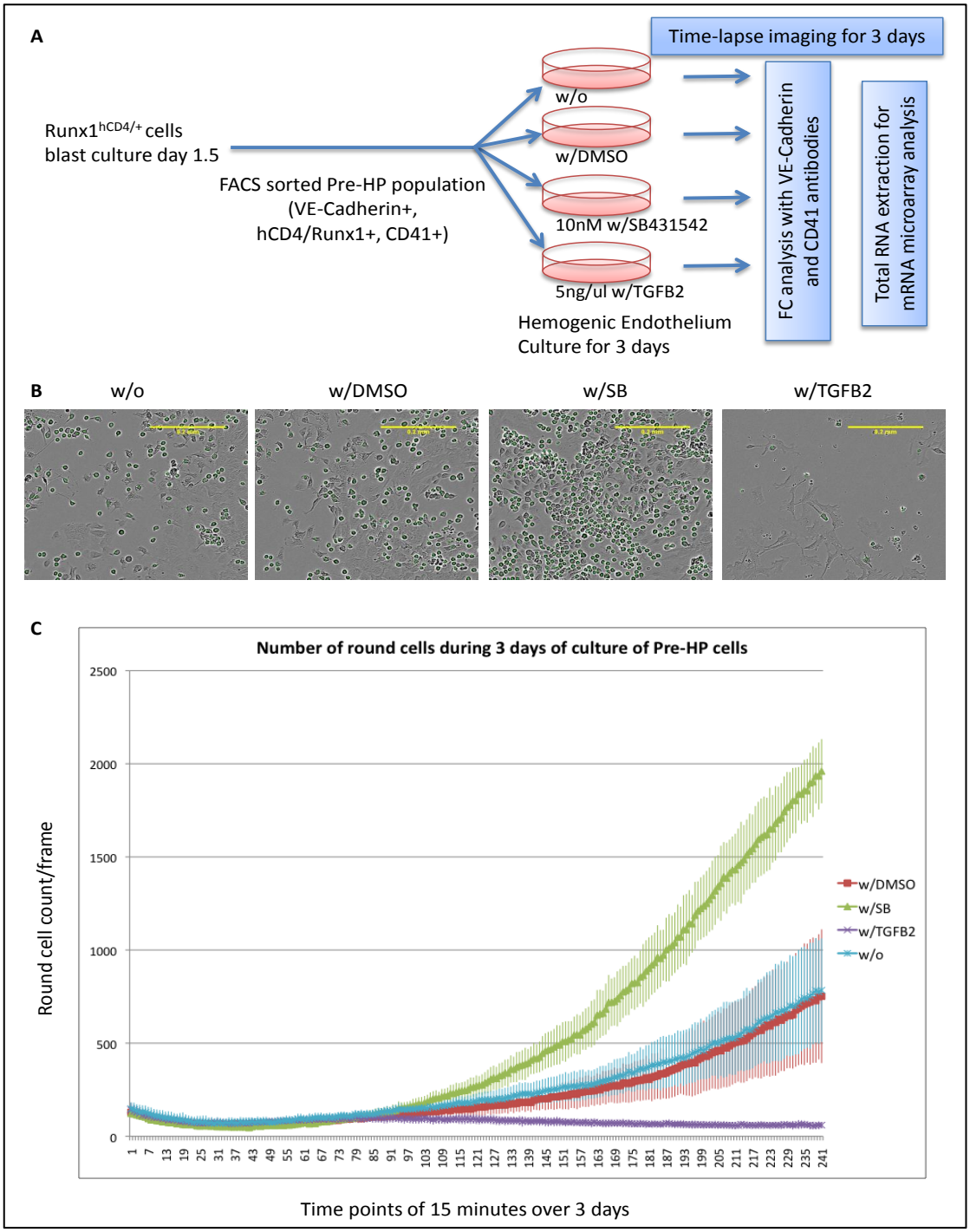

Figure 4.0.4 ***Culture of sorted Pre-HP population for 3 days in hemogenic endothelium culture.*** *A. The graphical representation of experimental flow. The samples are used for time-lapse imaging, FC analysis and mRNA microarray analysis.* ***B. The last image is taken with the incucyte microscope of each condition after 3 days of culture. The scale bar corresponds to 0.2µm. The green pseudo-color is indicating the round cells detected by the Cell Profiler software****. C. Number of round cells quantified based on the time-lapse imaging for 3 days. Nine images per culture condition were taken every 15 minutes over 3 days. Later round cell count was quantified, averaged for all 9 frames and error bars calculated as standard deviation of counts from 9 frames per condition.*

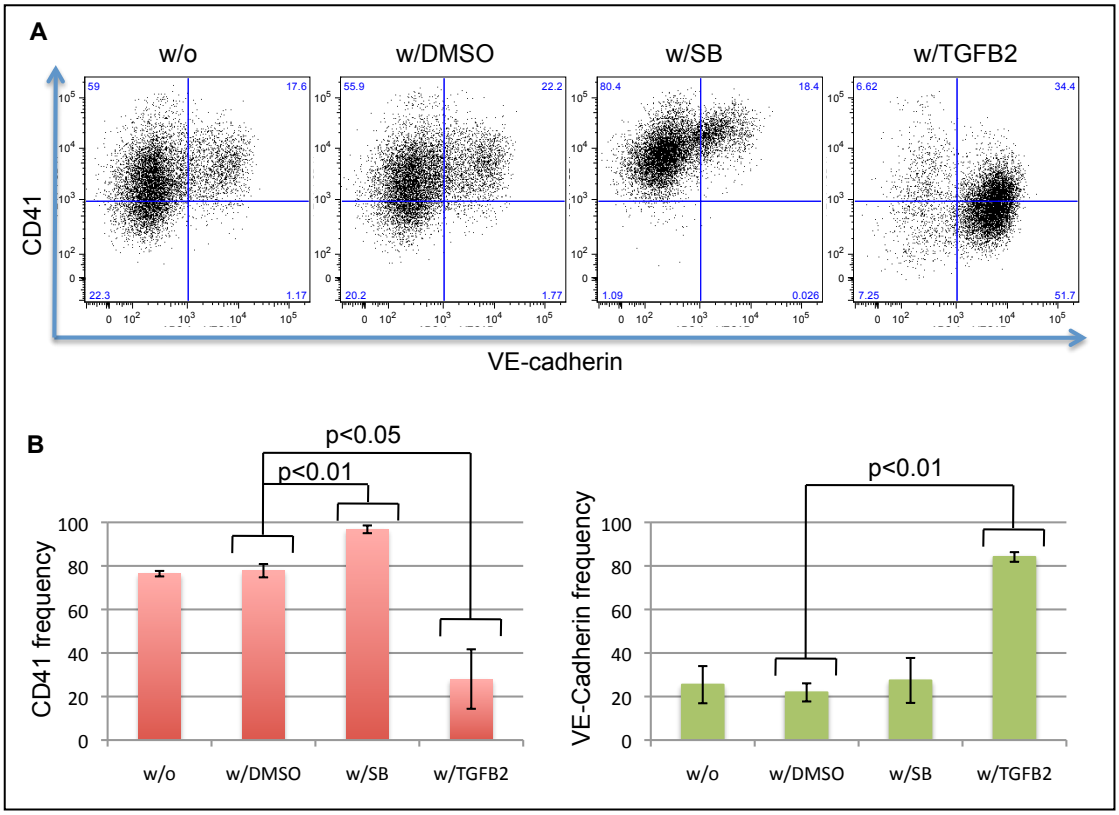

Figure 4.0.5 ***Flow cytometry result of cells after 3 days of culture in hemogenic endothelium medium with corresponding compound.*** *A.* ***Representative FC staining with VE-Cadherin and CD41 of samples harvested after 3 days of culture.*** *B.* ***Average CD41 and VE-Cadherin frequencies of FC results calculated from 3 independent experiments. The error bars represent standard deviation. Indicated p values are calculated with student t test. Non-indicated p values are higher than 0.05.***

2.3. TGFβ is promoting mesenchymal fate

Since the TGFβ2 treatment of Pre-HP cells give rise to a more smooth muscle like cell morphology dominance in the culture (Figure 4.4.B), we wanted to understand the resulting expression pattern after inhibiting the TGFβ pathway and activating it. We analyzed the mRNA microarray of the 3 sets of treated cells (Figure 4.4.A) with DMSO (control), with SB431542 (inhibitor) and with TGFβ2 (activator) as it is labeled in 3 different colors in Figure 4.6.A. We performed principal component analysis to compare the overall expression pattern after normalization. The control and inhibitor samples cluster very closely; on the other hand activator replicates cluster separately from them

(Figure 4.6.B), which suggests a completely different expression profile on TGFβ2 treatment versus control. Focusing on the comparison of activation versus control, we did hierarchical clustering of all 9 sample sets with the top 250 genes significantly changed expression in activation versus control. Figure 4.6.C shows close clustering of the samples from the same groups. It also depicts very similar expression pattern between control and inhibitor groups but the opposite pattern in activator group (Figure 4.6.C).

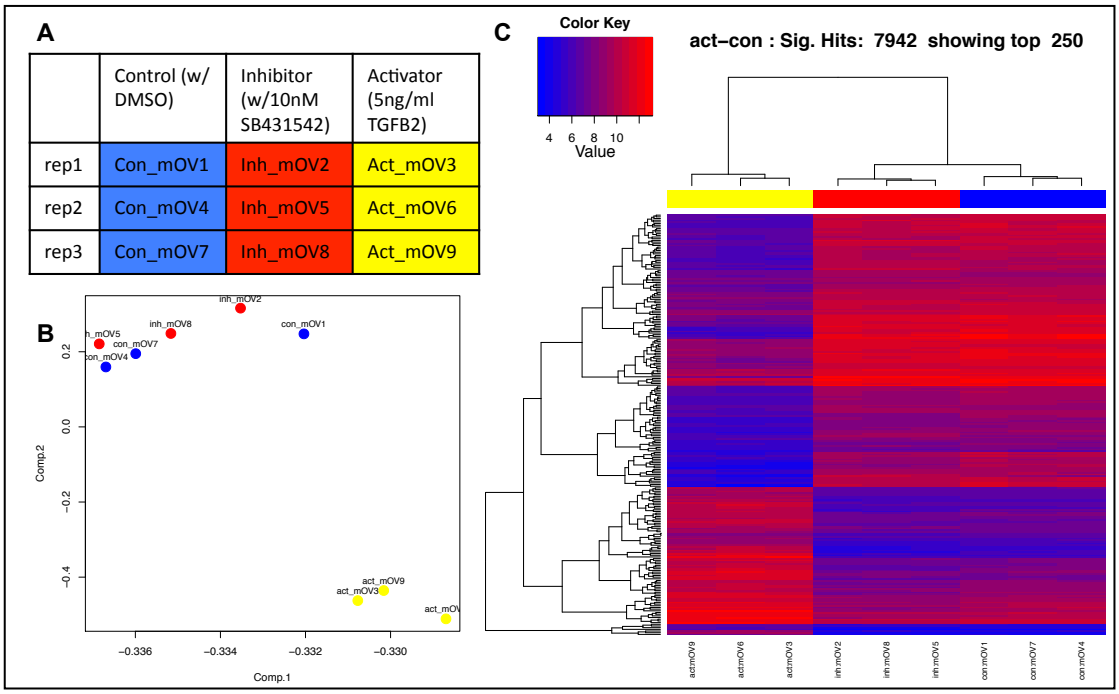

Figure 4.0.6 ***Microarray results of 3 days treated with DMSO, 10nM SB431542 (inhibitor), 5ng/ml TGFB2 (activator) as it is depicted in figure4.2.A.*** *A.* ***The sample annotation of 3 biological replicates of control (blue) , inhibitor (red), activator (yellow) samples shown.*** *B.* ***Principal component analysis is run for all samples after normalization.*** *C.* ***The hierarchical clustering of 9 samples based on the expression values of the most significant 250 genes from the activator versus control comparison.***

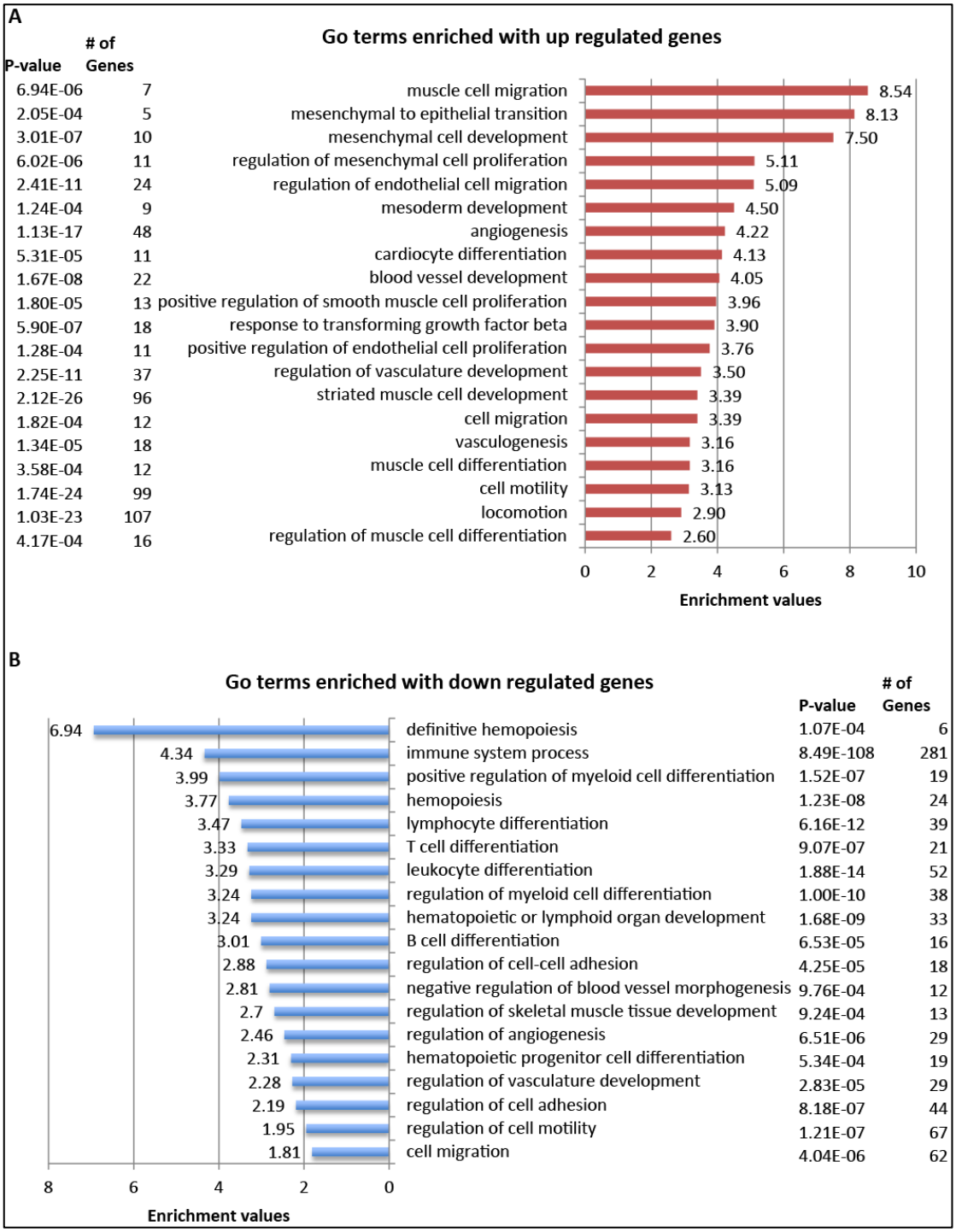

Figure 4.0.7 ***Gene Ontology (GO) analysis of biological processes for activator versus control sample set. The raw data is cleaned from the samples with adjusted p value lower than 0.01 and log2 fold change in between -1 and 1. The GO analysis is done with the shortened list in comparison with the background list from the raw data. Selection of significantly enriched biological process GO terms based on*** *A.* ***the up-regulated genes and*** *B.* ***the down-regulated genes on activator versus control.***

To understand the nature of the resulting cells upon treatment with TGFβ2, we analyzed the significantly up-regulated and down-regulated genes for gene ontology association with biological process terms. The top GO terms with high enrichment in up-regulated gene list seems to be associated with increased mesenchymal cell development, angiogenesis and endothelial cell migration (Figure 4.7.A). In contrast, the down-regulated gene list indicates GO terms related with decreased hematopoiesis, blood and immune cell differentiation, cell adhesion (Figure 4.7.B).

To conclude about the resulting cell phenotype after treatment, we checked the fold changes in sets known cell type related genes in microarray analysis. In general we see an increased expression of cardiac and muscle fate, mesenchymal fate, endothelial fate related genes after treatment with TGFβ2 (Figure 4.8.A). On the other hand, hematopoietic fate related genes are down-regulated after TGFβ2 treatment (Figure 4.8.B). The combination of the gene lists (Figure4.8.A&B) and GO terms (Figure4.7) for all 3 conditions; control versus inhibitor and control versus activator; gives a simplified view of gene expression pattern. The inhibition of TGFβ pathway with SB431542 treatment doesn't seem very different than control except for a higher expression of a short list of hematopoietic genes. On the other hand, activation by treating with TGFβ2 seems to promote a down-regulation of hematopoietic genes and an up-regulation of endothelial, mesenchymal, cardiac/muscle differentiation genes (Figure4.8.C).

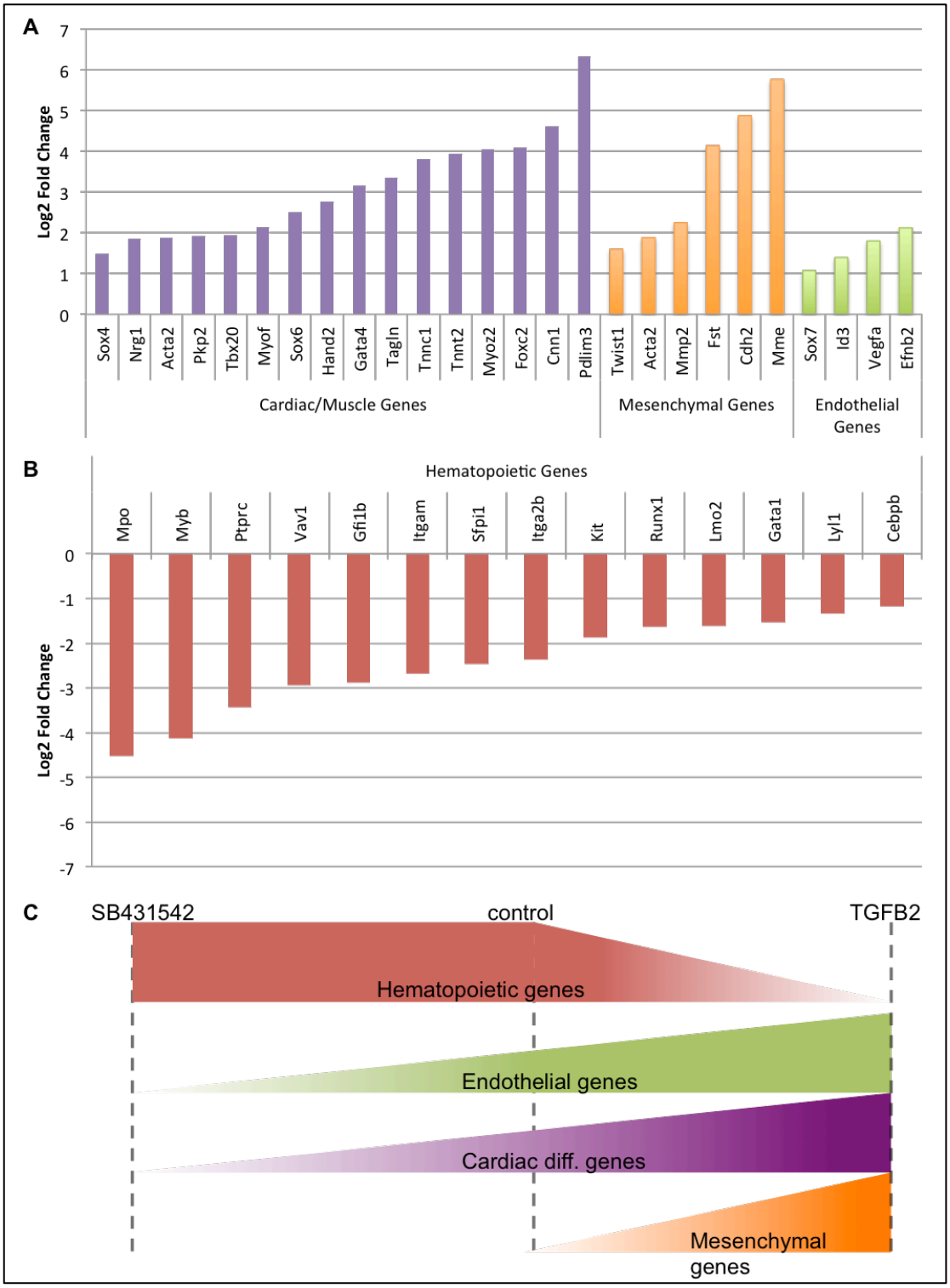

Figure 4.0.8 ***Cell type specific genes expression in microarray analysis. The bar plots of log2 fold change (higher then 1) in activator TGFβ2 versus control conditions .A. Selection of cardiac, muscle, mesenchyme, endothelium related genes are up regulated in activator and B. hematopoietic genes are down regulated in activator. C. Overview of expression of hematopoietic, endothelial, cardiac and mesenchymal fate related genes in 3 conditions.***

Lastly we decided to analyse EndMT related gene expression by using single cell qRT-PCR on the cells treated with DMSO, SB431542 and TGFβ2. These genes (Acta2, Cdh2, Snai1, Snai2, Serpine1) are markers of mesenchymal phenotype, which is expected to have increased expression as a result of EndMT. The analysis was done before and after the 2 days of hemogenic endothelium culture with sorted cell populations from day1.5 blast culture. The gene expression values are plotted as log2 expression values and box plots for each cell population. Treated endothelial and hemogenic endothelial cells with TGFβ2 showed higher expression of Acta2, Cdh2, Serpine1 genes in comparison with pre-culture cells and also with control or SB431542 treated cells. The Snai1 gene expression remains similar between samples while Snai2 expression is mostly not detected (Figure4.9).

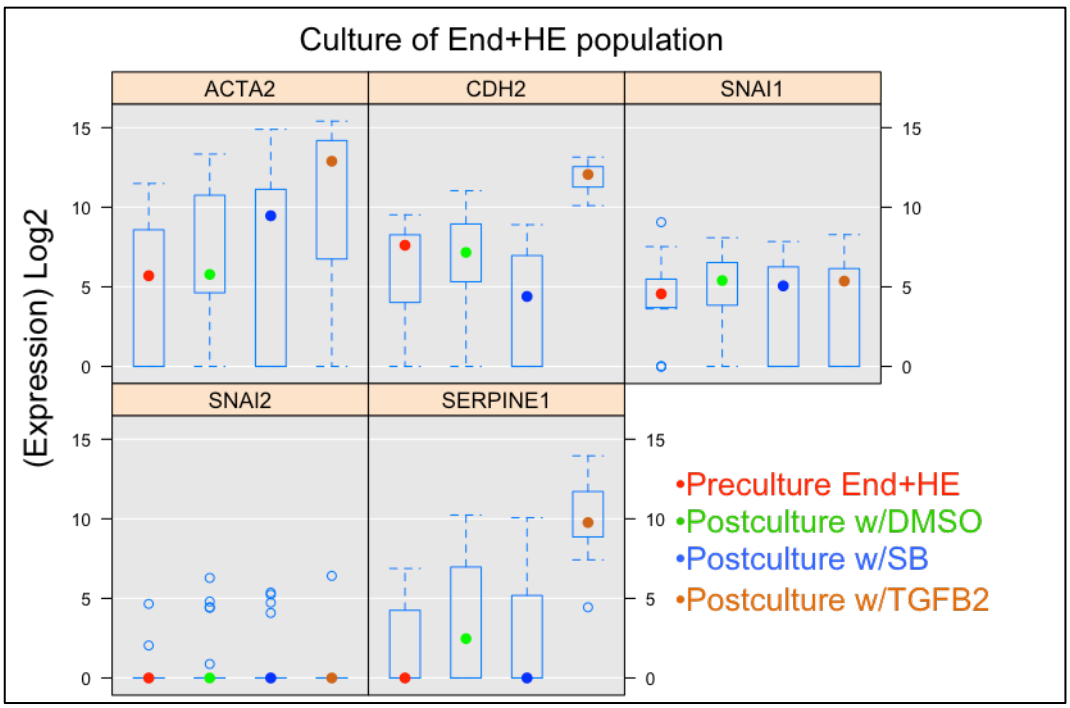

Figure 4.0.9 ***Single cell qPCR analysis of EndMT genes on samples after treatment with control, inhibitor, and activator. Before and after culture log2 expression values are shown as box plot graph. Sorted VE-Cadherin+, CD41- endothelial and hemogenic endothelium population is treated with DMSO, SB and TGFB2 for 2 days.***

3. Discussion:

Considering the similar loss of endothelial phenotype in EHT and EndMT, one could think of common signalling mechanisms regulating both endothelial transitions important during vertebrate development. The promoting role of TGFβ signalling in EndMT is a well-studied cellular regulation. Knowledge about TGFβ signalling in developmental hematopoiesis was promising for the idea of a possible role of this pathway in the regulation of EHT, but not specific enough to argue about regulation at the cell level. Here I hypothesized that TGFβ pathway is regulating the transition of endothelial cells towards hematopoiesis. I studied the cell type specific reaction for TGFβ signalling and combined the conventional molecular biology protocols with single cell gene expression techniques.

3.1. TGFβ receptors are expressed differentially during EHT

Firstly, we wanted to investigate if the cells going through EHT express the receptors of the TGFβ signaling, as it will be the first step to be responsive for the pathway activation. Considering the existence of the cellular heterogeneity even within sorted populations and the rareness of hemogenic endothelial cells we decided to study the gene expression at single-cell level to reveal TGFβ responsive cell type. By using single cell qPCR approach, we checked the gene expression of many signal transducer Smad proteins, type I and type II receptors (Table 4.1). Among them, the expression pattern of Acvrl1 (Alk1), Tgfbr1 (Alk5) and Tgfbr2 gave interesting results (Figure4.3). The endothelial cells isolated from both in vitro culture system (Figure4.3.A) and in vivo E10.5 AGM region (Figure4.3.B) showed high expression for Acvrl1, Tgfbr1 and mid expression of Tgfbr2. Interestingly, their expression levels change when the endothelial cells go through EHT, either after culture of those cells (Figure4.3.C) or only comparing the different subsets of endothelial cells going through EHT in vivo (Figure4.3.D). Both in vivo and in vitro experiments conclude that the receptor type I, Acvrl1 expression is

dramatically decreasing, and its binding partner type II receptor, Tgfbr2 is slightly reduced in cells going towards EHT. However, the other type I receptor, Tgfbr1 doesn't show an apparent gene expression change in the course of EHT. This result may indicate an initial role of Acvrl1 gene in endothelial cells but then it is down-regulated during EHT. This would reduce the TGFβ ligand binding to Acvrl1 while the cells would respond mostly via the Tgfbr1 changing the type of TGFβ response. While the inhibition of the pathway is positively regulating the EHT as we concluded in the first part, down-regulation of the crucial Acvrl1 gene might be a part of TGFβ pathway inhibitory program in the course of normal EHT.

3.2. TGFβ pathway activation is inhibiting EHT

Secondly, we tested the activation of TGFβ pathway by adding TGFβ2 ligand and inhibition by adding SB431542, an inhibitor of ALK5 receptor function (Figure4.4.A). Upon TGFβ2 treatment for 3 days, it resulted in a dramatic decrease of CD41 expressing, round, hematopoietic progenitor cell population (Figure 4.4 and Figure 4.5). Combining the same experiments with 3 biological replicates confirmed the results that TGFβ2 treatment is inhibiting EHT. On the other hand, treatment with inhibitor SB431542 gives rise to more round cells with CD41 expression (Figure 4.4 and Figure 4.5). All together, our data indicates that TGFβ inhibition is promoting EHT and resulting in more HP cells. A study done on human ES cell in vitro differentiation culture came up with the same results. When TGFβ inhibitor SB431542 is added, they observed generation of more HP cells (C. Wang et al., 2012). As an exploitation of these findings, the Alk5 inhibitor, SB431542, is also added into the culture medium to improve the in vitro hematopoietic differentiation system.

3.3. TGFβ pathway activation on endothelial cells promotes mesenchymal fate

Finally we analyzed the resulting gene expression pattern after cells are activated for TGFβ signaling, to get better understanding of the nature of TGFβ activated cells with

flat, adherent cell morphology. The microarray results of TGFβ activated versus control experiment indicates cardiac/muscle, mesenchymal, and endothelial cell-like gene expression profile (Figure 4.6, 4.7 and 4.8). Similar profile is also supported by higher expression of EndMT related Acta2, Cdh2, Serpine1 gene expressions in single cell qRT-PCR experiment (Figure4.9).

4. Conclusion and Future Directions

Our findings in general are indicating an inhibitory effect of TGFβ pathway in EHT, actually opposing our initial hypothesis. Here we provide evidence that actually TGFβ activation in endothelial cells through Tgfbr1 (Alk5) is giving rise to mesenchymal-like cell fate. On the other hand, inhibition of the pathway through Tgfbr1 (Alk5) is promoting EHT (Figure 4.10).

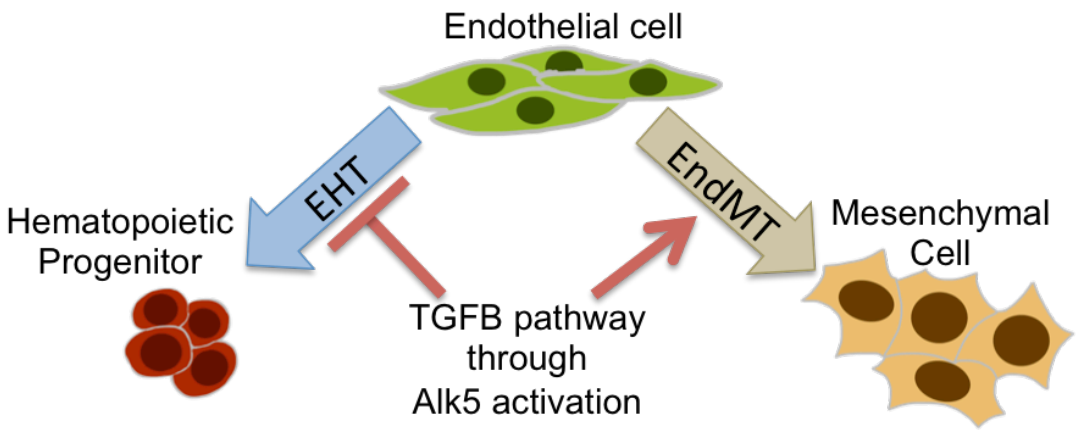

Figure 4.10 ***The proposed model about the regulatory role of TGFβ signaling on EHT and EndMT.***

For future directions, better understanding of the down-stream targets of the pathway inhibition and activation is needed. Specifically, a Western Blot and immuno-fluorescent staining for Smad proteins would be informative. Also a different inhibition system might be useful to eliminate possible un-specific binding effects of small molecule inhibitor SB431542. Finally it would be interesting to see the TGFβ inhibition

effect on EHT happening in vivo tissues. Triggering the pathway in a short time window for only hemogenic endothelial cells with no exclusive cell marker would be very challenging. An alternative test would be ex vivo AGM explant culture with the inhibitor SB431542 and testing the emergence of hematopoietic progenitors.

Activation of the mesenchymal cell fate through Alk5 would be interesting to investigate. Additional experiments to explore the cell fate decision upon TGFβ signal activation would enlighten the molecular mechanism of EndMT. With that aim, we are planning to explore the direct protein synthesis targets of TGFβ2 treatment after 6hours. Through a collaboration with Dr. Jeroen Krijsveld (EMBL Heidelberg) we successfully identified secreted proteins upon TGFβ activation and we are planning to identify the proteins changing after TGFβ activation in the intracellular compartment. The technique developed in Dr. Krijgsveld's lab made it possible to label the complete set of synthesized and secreted proteins by using amino-acids with different weight isotopes(Hughes & Krijgsveld, 2012). The comparison between proteome and cDNA microarray data would allow us to identify the direct targets of TGFβ activation.

Our study is putting forward the notion of exquisite regulation of endothelial cell transitions by TGFβ signaling towards mesenchymal or hematopoietic fate. Several articles in the literature have shown that the balance between which type I receptor activations seems to be a very delicate regulatory switch during development. Specifically for hematopoieisis, the role of Endoglin (Eng), the ancillary receptor of TGFβ family, has been studied widely. Eng $^{-/-}$ mESCs showed reduced hematopoiesis in the EB and blast culture (Perlingeiro, 2007), as well as in hematopoietic progenitor culture (Baik, Borges, Magli, Thatava, & Perlingeiro, 2012). This decreased hemangioblast and hematopoietic development of Eng$^{-/-}$ cells can be rescued by activation of Acvrl1 (Alk1), on the other hand Alk5 activation leads to the inhibition of hematopoiesis (L. Zhang et al., 2011) . As it was reported previously (Oh et al., 2000), different type I receptors

function through specific R-Smad transduction, which result in distinct differentiation programs. Another study on in vitro cultured mES cells showed the inhibitory effect of TGFβ1 and promoting effect of Activin A (another TGFβ family ligand) on hematopoiesis (Park et al., 2004). All together, our study confirm that TGFβ signalling through Alk5 is inhibiting hematopoiesis but our data is novel for showing the Alk5 inhibition during EHT with specifically on HE cells and its promoting effect toward mesenchymal phenotype. Here we also provide detailed gene expression when the down-stream mesenchymal or hematopoietic differentiation programs are triggered. This knowledge not only reveals a developmental mechanism but also hold a promise for future usage in stem cell manipulations.

General Conclusion and Future Perspectives

In the mouse development, the first hematopoietic progenitors are detected at E8 yolk sac. Those progenitor cells can only differentiate into primitive erythroid cells (Palis et al., 1999). Later during the development, at E10 stage, definitive hematopoietic progenitor cells with myeloid and lymphoid potential arise from the aorta-gonad-mesonephros (AGM) region (Medvinsky & Dzierzak, 1996). Cell tracing experiments show that both primitive and definitive hematopoietic progenitors are actually differentiated from endothelial cells (Jaffredo et al., 1998). These special endothelial cells bear not only endothelial markers and morphology but they also express early hematopoietic genes. Due to their distinctive features from other endothelial cells, they have been named hemogenic endothelium (HE) (Eilken et al., 2009). To become hematopoietic progenitors (HP), HE cells lose their endothelial features, while expressing hematopoietic markers coupled with some morphological changes such as detaching from the endothelial layer and having small and round shape. It is now well-accepted concept that the endothelial to hematopoietic transition (EHT) is a key developmental event leading to the formation of blood stem and progenitor cells during embryogenesis (Lancrin et al., 2009).

Understanding the cellular heterogeneity of cells during EHT is very important to decipher its molecular program. To achieve that aim, we used the single cell gene expression analysis approach. This technique allowed us to see the heterogeneity in transcriptional level. Such a detailed gene expression profiling on the EHT populations have never been achieved, due to the technical obstacles. Here we identified 6 populations in the embryonic hematopoiesis by using single cell qRT-PCR technique, which put forward exciting information about the cell characteristics. Based on the gene expression signature of those populations, in the future, we will identify definitive markers for isolation those populations. Moreover, by applying reverse genetic approach such as CRISPR/Cas9 (H. Wang et al., 2013), we can study the biological

functions of these genes during EHT. Ultimately, we aim to define those 6 populations and their relevant function in the mouse hematopoiesis.

Understanding the mechanism of endothelial to hematopoietic transition is interesting not only it generates one of the vital tissues of mammals, but it also holds a great potential of use in therapeutic applications, such as blood generation by differentiating induced pluripotent stem cells based on the information gathered about mechanism of EHT. Considering the fact that TGFβ signaling triggers a similar event during heart development called endothelial to mesenchymal transition (EndMT), we hypothesized that TGFβ activity should play a similar role in EHT as well. Our data suggest that the activation of the TGFβ pathway via Tgfbr1 (Alk5) is blocking the EHT but it is promoting the differentiation towards mesenchymal cell type, so it favors EndMT. Although both EndMT and EHT lead to a loss of endothelial cell identity and the generation of mobile cells, our study suggests that the TGF signaling has opposite effects on both.

Current literature defines the HE and PreHP cells roughly depending on a couple of surface markers and inform only about the role of a few transcriptional regulators during EHT. Yet, there are a lot of important scientific questions about the precise identity of the cells during EHT and their mechanism left un-answered. During my PhD period I sought out answers of these questions. I have searched for a connection between functional heterogeneity and heterogeneous gene expression patterns, which may reveal the stringent EHT program. Additionally, I have investigated the molecular mechanism through TGFβ signaling in terms of cell fate decision towards hematopoietic or mesenchymal cell type.

Bibliography

Adamo, L., Naveiras, O., Wenzel, P. L., McKinney-Freeman, S., Mack, P. J., Gracia-Sancho, J., … Daley, G. Q. (2009). Biomechanical forces promote embryonic haematopoiesis. *Nature*, *459*(7250), 1131–5. doi:10.1038/nature08073

Adamson, S. L., Lu, Y., Whiteley, K. J., Holmyard, D., Hemberger, M., Pfarrer, C., & Cross, J. C. (2002). Interactions between trophoblast cells and the maternal and fetal circulation in the mouse placenta. *Developmental Biology*, *250*(2), 358–73. doi:10.1006/dbio.2002.0773

Alvarez-Silva, M., Belo-Diabangouaya, P., Salaün, J., & Dieterlen-Lièvre, F. (2003). Mouse placenta is a major hematopoietic organ. *Development (Cambridge, England)*, *130*(22), 5437–44. doi:10.1242/dev.00755

Arciniegas, E., Neves, C. Y., Carrillo, L. M., Zambrano, E. a, & Ramírez, R. (2005). Endothelial-mesenchymal transition occurs during embryonic pulmonary artery development. *Endothelium : Journal of Endothelial Cell Research*, *12*(4), 193–200. doi:10.1080/10623320500227283

Baik, J., Borges, L., Magli, A., Thatava, T., & Perlingeiro, R. C. R. (2012). Effect of endoglin overexpression during embryoid body development. *Experimental Hematology*, *40*(10), 837–46. doi:10.1016/j.exphem.2012.06.007

Beaupain, D., Martin, C., & Dieterlen-Lièvre, F. (1979). Are developmental hemoglobin changes related to the origin of stem cells and site of erythropoiesis? *Blood*, *53*(2), 212–25. Retrieved from http://www.ncbi.nlm.nih.gov/pubmed/760851

Bee, T., Ashley, E. L. K., Bickley, S. R. B., Jarratt, A., Li, P., Sloane-Stanley, J., … de Bruijn, M. F. T. R. (2009). The mouse Runx1 +23 hematopoietic stem cell enhancer confers hematopoietic specificity to both Runx1 promoters. *Blood*, *113*(21), 5121–4. doi:10.1182/blood-2008-12-193003

Bee, T., Swiers, G., Muroi, S., Pozner, A., Nottingham, W., Santos, A. C., … de Bruijn, M. F. T. R. (2010). Nonredundant roles for Runx1 alternative promoters reflect their activity at discrete stages of developmental hematopoiesis. *Blood*, *115*(15), 3042–50. doi:10.1182/blood-2009-08-238626

Bertrand, J. Y., Chi, N. C., Santoso, B., Teng, S., Stainier, D. Y. R., & Traver, D. (2010). Haematopoietic stem cells derive directly from aortic endothelium during development. *Nature*, *464*(7285), 108–11. doi:10.1038/nature08738

Bertrand, J. Y., Kim, A. D., Teng, S., & Traver, D. (2008). CD41+ cmyb+ precursors colonize the zebrafish pronephros by a novel migration route to initiate adult hematopoiesis. *Development (Cambridge, England)*, *135*(10), 1853–62. doi:10.1242/dev.015297

Boisset, J.-C., Clapes, T., Klaus, A., Papazian, N., Onderwater, J., Mommaas-Kienhuis, M., … Robin, C. (2014). Progressive maturation towards hematopoietic stem cells in the mouse embryo aorta. *Blood*. doi:10.1182/blood-2014-07-588954

Boisset, J.-C., van Cappellen, W., Andrieu-Soler, C., Galjart, N., Dzierzak, E., & Robin, C. (2010). In vivo imaging of haematopoietic cells emerging from the mouse aortic endothelium. *Nature*, *464*(7285), 116–20. doi:10.1038/nature08764

Böiers, C., Carrelha, J., Lutteropp, M., Luc, S., Green, J. C. a, Azzoni, E., … Jacobsen, S. E. W. (2013). Lymphomyeloid Contribution of an Immune-Restricted Progenitor Emerging Prior to Definitive Hematopoietic Stem Cells. *Cell Stem Cell*, 535–548. doi:10.1016/j.stem.2013.08.012

Bradley, A., Evans, M., Kaufman, M. H., & Robertson, E. (1984). Formation of germ-line chimaeras from embryo-derived teratocarcinoma cell lines. *Nature*, *309*(5965), 255–6. doi:10.1038/309255a0

Brunskill, E. W., Park, J.-S., Chung, E., Chen, F., Magella, B., & Potter, S. S. (2014). Single cell dissection of early kidney development: multilineage priming. *Development (Cambridge, England)*, *141*(15), 3093–101. doi:10.1242/dev.110601

Burkert, U., von Rüden, T., & Wagner, E. F. (1991). Early fetal hematopoietic development from in vitro differentiated embryonic stem cells. *The New Biologist*, *3*(7), 698–708. Retrieved from http://www.ncbi.nlm.nih.gov/pubmed/1721533

Caprioli, a, Minko, K., Drevon, C., Eichmann, a, Dieterlen-Lièvre, F., & Jaffredo, T. (2001). Hemangioblast commitment in the avian allantois: cellular and molecular aspects. *Developmental Biology*, *238*(1), 64–78. doi:10.1006/dbio.2001.0362

Caprioli, A., Jaffredo, T., Gautier, R., Dubourg, C., & Dieterlen-Lièvre, F. (1998). Blood-borne seeding by hematopoietic and endothelial precursors from the allantois. *Proceedings of the National Academy of Sciences of the United States of America*, *95*(4), 1641–6.

Chanda, B., Ditadi, A., Iscove, N. N., & Keller, G. (2013). Retinoic acid signaling is essential for embryonic hematopoietic stem cell development. *Cell*, *155*(1), 215–27. doi:10.1016/j.cell.2013.08.055

Chen, M. J., Li, Y., De Obaldia, M. E., Yang, Q., Yzaguirre, A. D., Yamada-Inagawa, T., … Speck, N. A. (2011). Erythroid/myeloid progenitors and hematopoietic stem cells originate from distinct populations of endothelial cells. *Cell Stem Cell*, *9*(6), 541–52. doi:10.1016/j.stem.2011.10.003

Chen, M. J., Yokomizo, T., Zeigler, B. M., Dzierzak, E., & Speck, N. A. (2009). Runx1 is required for the endothelial to haematopoietic cell transition but not thereafter. *Nature*, *457*(7231), 887–91. doi:10.1038/nature07619

Choi, K., Kennedy, M., Kazarov, A., Papadimitriou, J. C., & Keller, G. (1998). A common precursor for hematopoietic and endothelial cells. *Development (Cambridge, England)*, *125*(4), 725–32.

Chung, M. I. S., Ma, A. C. H., Fung, T.-K., & Leung, A. Y. H. (2011). Characterization of Sry-related HMG box group F genes in zebrafish hematopoiesis. *Experimental Hematology*, *39*(10), 986–998.e5. doi:10.1016/j.exphem.2011.06.010

Clarke, R. L., Yzaguirre, A. D., Yashiro-Ohtani, Y., Bondue, A., Blanpain, C., Pear, W. S., … Keller, G. (2013). The expression of Sox17 identifies and regulates haemogenic endothelium. *Nature Cell Biology*, *15*(5), 502–10. doi:10.1038/ncb2724

Costa, G., Mazan, A., Gandillet, A., Pearson, S., Lacaud, G., & Kouskoff, V. (2012). SOX7 regulates the expression of VE-cadherin in the haemogenic endothelium at the onset of haematopoietic development. *Development (Cambridge, England)*, *139*(9), 1587–98. doi:10.1242/dev.071282

De Bruijn, M. F., Speck, N. a, Peeters, M. C., & Dzierzak, E. (2000). Definitive hematopoietic stem cells first develop within the major arterial regions of the mouse embryo. *The EMBO Journal*, *19*(11), 2465–74. doi:10.1093/emboj/19.11.2465

De Bruijn, M. F. T. ., Ma, X., Robin, C., Ottersbach, K., Sanchez, M.-J., & Dzierzak, E. (2002). Hematopoietic Stem Cells Localize to the Endothelial Cell Layer in the Midgestation Mouse Aorta. *Immunity*, *16*(5), 673–683. doi:10.1016/S1074-7613(02)00313-8

Dickson, M. C., Martin, J. S., Cousins, F. M., Kulkarni, A. B., Karlsson, S., & Akhurst, R. J. (1995). Defective haematopoiesis and vasculogenesis in transforming growth factor-beta 1 knock out mice. *Development (Cambridge, England)*, *121*(6), 1845–54.

Dieterlen-Lievre, F. (1975). On the origin of haemopoietic stem cells in the avian embryo: an experimental approach. *Journal of Embryology and Experimental Morphology*, *33*(3), 607–19. Retrieved from http://www.ncbi.nlm.nih.gov/pubmed/1176862

Doetschman, T. C., Eistetter, H., Katz, M., Schmidt, W., & Kemler, R. (1985). The in vitro development of blastocyst-derived embryonic stem cell lines: formation of visceral yolk sac, blood islands and myocardium. *Journal of Embryology and Experimental Morphology*, *87*, 27–45. Retrieved from http://www.ncbi.nlm.nih.gov/pubmed/3897439

Downs, K. M., & Gardner, R. L. (1995). An investigation into early placental ontogeny: allantoic attachment to the chorion is selective and developmentally regulated. *Development (Cambridge, England)*, *121*(2), 407–16. Retrieved from http://www.ncbi.nlm.nih.gov/pubmed/7768182

Drake, C. J., Brandt, S. J., Trusk, T. C., & Little, C. D. (1997). TAL1/SCL is expressed in endothelial progenitor cells/angioblasts and defines a dorsal-to-ventral gradient of vasculogenesis. *Developmental Biology*, *192*(1), 17–30. doi:10.1006/dbio.1997.8751

Durand, C., Robin, C., Bollerot, K., Baron, M. H., Ottersbach, K., & Dzierzak, E. (2007). Embryonic stromal clones reveal developmental regulators of definitive hematopoietic stem cells. *Proceedings of the National Academy of Sciences of the United States of America*, *104*(52), 20838–43. doi:10.1073/pnas.0706923105

Dzierzak, E., & Speck, N. a. (2008). Of lineage and legacy: the development of mammalian hematopoietic stem cells. *Nature Immunology*, *9*(2), 129–36. doi:10.1038/ni1560

Eichmann, A., Corbel, C., Nataf, V., Vaigot, P., Bréant, C., & Le Douarin, N. M. (1997). Ligand-dependent development of the endothelial and hemopoietic lineages from

embryonic mesodermal cells expressing vascular endothelial growth factor receptor 2. *Proceedings of the National Academy of Sciences of the United States of America*, *94*(10), 5141–6.

Eilken, H. M., Nishikawa, S.-I., & Schroeder, T. (2009a). Continuous single-cell imaging of blood generation from haemogenic endothelium. *Nature*, *457*(7231), 896–900. Retrieved from http://www.nature.com/doifinder/10.1038/nature07760

Eilken, H. M., Nishikawa, S.-I., & Schroeder, T. (2009b). Continuous single-cell imaging of blood generation from haemogenic endothelium. *Nature*, *457*(7231), 896–900. doi:10.1038/nature07760

Evans, M. J., & Kaufman, M. H. (1981). Establishment in culture of pluripotential cells from mouse embryos. *Nature*, *292*(5819), 154–6. doi:10.1038/292154a0

Faloon, P., Arentson, E., Kazarov, A., Deng, C. X., Porcher, C., Orkin, S., & Choi, K. (2000). Basic fibroblast growth factor positively regulates hematopoietic development. *Development (Cambridge, England)*, *127*(9), 1931–41.

Fehling, H. J., Lacaud, G., Kubo, A., Kennedy, M., Robertson, S., Keller, G., & Kouskoff, V. (2003). Tracking mesoderm induction and its specification to the hemangioblast during embryonic stem cell differentiation. *Development (Cambridge, England)*, *130*(17), 4217–27.

Ferkowicz, M. J. (2003). CD41 expression defines the onset of primitive and definitive hematopoiesis in the murine embryo. *Development*, *130*(18), 4393–4403. doi:10.1242/dev.00632

Futaki, S., Hayashi, Y., Emoto, T., Weber, C. N., & Sekiguchi, K. (2004). Sox7 plays crucial roles in parietal endoderm differentiation in F9 embryonal carcinoma cells through regulating Gata-4 and Gata-6 expression. *Molecular and Cellular Biology*, *24*(23), 10492–503. doi:10.1128/MCB.24.23.10492-10503.2004

Gandillet, A., Serrano, A. G., Pearson, S., Lie-A-Ling, M., Lacaud, G., & Kouskoff, V. (2009). Sox7-sustained expression alters the balance between proliferation and differentiation of hematopoietic progenitors at the onset of blood specification. *Blood*, *114*(23), 4813–22. doi:10.1182/blood-2009-06-226290

Garcia-Porrero, J. A., Godin, I. E., & Dieterlen-Lièvre, F. (1995). Potential intraembryonic hemogenic sites at pre-liver stages in the mouse. *Anatomy and Embryology*, *192*(5), 425–35.

Gekas, C., Dieterlen-Lièvre, F., Orkin, S. H., & Mikkola, H. K. a. (2005). The placenta is a niche for hematopoietic stem cells. *Developmental Cell*, *8*(3), 365–75. doi:10.1016/j.devcel.2004.12.016

Godin, I., Dieterlen-Lièvre, F., & Cumano, a. (1995). Emergence of multipotent hemopoietic cells in the yolk sac and paraaortic splanchnopleura in mouse embryos, beginning at 8.5 days postcoitus. *Proceedings of the National Academy of Sciences of the United States of America*, *92*(3), 773–7.

Godin, I. E., Garcia-Porrero, J. A., Coutinho, A., Dieterlen-Lièvre, F., & Marcos, M. A. (1993). Para-aortic splanchnopleura from early mouse embryos contains B1a cell progenitors. *Nature*, *364*(6432), 67–70. doi:10.1038/364067a0

Gordon-Keylock, S., Sobiesiak, M., Rybtsov, S., Moore, K., & Medvinsky, A. (2013). Mouse extraembryonic arterial vessels harbor precursors capable of maturing into definitive HSCs. *Blood*, *122*(14), 2338–45. doi:10.1182/blood-2012-12-470971

Goumans, M.-J., Valdimarsdottir, G., Itoh, S., Rosendahl, A., Sideras, P., & ten Dijke, P. (2002). Balancing the activation state of the endothelium via two distinct TGF-beta type I receptors. *The EMBO Journal*, *21*(7), 1743–53. doi:10.1093/emboj/21.7.1743

Grimes, H. L., Chan, T. O., Zweidler-McKay, P. A., Tong, B., & Tsichlis, P. N. (1996). The Gfi-1 proto-oncoprotein contains a novel transcriptional repressor domain, SNAG, and inhibits G1 arrest induced by interleukin-2 withdrawal. *Molecular and Cellular Biology*, *16*(11), 6263–6272.

Guo, G., Huss, M., Tong, G. Q., Wang, C., Li Sun, L., Clarke, N. D., & Robson, P. (2010). Resolution of cell fate decisions revealed by single-cell gene expression analysis from zygote to blastocyst. *Developmental Cell*, *18*(4), 675–85. doi:10.1016/j.devcel.2010.02.012

Guo, G., Luc, S., Marco, E., Lin, T.-W., Peng, C., Kerenyi, M. a, … Orkin, S. H. (2013). Mapping cellular hierarchy by single-cell analysis of the cell surface repertoire. *Cell Stem Cell*, *13*(4), 492–505. doi:10.1016/j.stem.2013.07.017

Haar, J. L., & Ackerman, G. a. (1971). Ultrastructural changes in mouse yolk sac associated with the initiation of vitelline circulation. *The Anatomical Record*, *170*(4), 437–55. doi:10.1002/ar.1091700406

Hanai, J. -i., Chen, L. F., Kanno, T., Ohtani-Fujita, N., Kim, W. Y., Guo, W. H., … Ito, Y. (1999). Interaction and functional cooperation of PEBP2/CBF with Smads. Synergistic induction of the immunoglobulin germline Calpha promoter. *The Journal of Biological Chemistry*, *274*(44), 31577–82. doi:10.1074/jbc.274.44.31577

Handschumacher, R. E., Harding, M. W., Rice, J., Drugge, R. J., & Speicher, D. W. (1984). Cyclophilin: a specific cytosolic binding protein for cyclosporin A. *Science (New York, N.Y.)*, *226*(4674), 544–7.

Huang, H., & Auerbach, R. (1993). Identification and characterization of hematopoietic stem cells from the yolk sac of the early mouse embryo. *Proceedings of the National Academy of Sciences of the United States of America*, *90*(21), 10110–4.

Huber, T. L., Kouskoff, V., Fehling, H. J., Palis, J., & Keller, G. (2004). Haemangioblast commitment is initiated in the primitive streak of the mouse embryo. *Nature*, *432*(7017), 625–30. doi:10.1038/nature03122

Hughes, C., & Krijgsveld, J. (2012). Developments in quantitative mass spectrometry for the analysis of proteome dynamics. *Trends in Biotechnology*, *30*(12), 668–76. doi:10.1016/j.tibtech.2012.09.007

Hwang, L. Y., Siegelman, M., Davis, L., Oppenheimer-Marks, N., & Baer, R. (1993). Expression of the TAL1 proto-oncogene in cultured endothelial cells and blood

vessels of the spleen. *Oncogene*, *8*(11), 3043–6. Retrieved from http://www.ncbi.nlm.nih.gov/pubmed/8414504

Inazaki, K., Kanamaru, Y., Kojima, Y., Sueyoshi, N., Okumura, K., Kaneko, K., … Nakao, A. (2004). Smad3 deficiency attenuates renal fibrosis, inflammation,and apoptosis after unilateral ureteral obstruction. *Kidney International*, *66*(2), 597–604. doi:10.1111/j.1523-1755.2004.00779.x

Jaffredo, T., Gautier, R., Eichmann, A., & Dieterlen-Lièvre, F. (1998). Intraaortic hemopoietic cells are derived from endothelial cells during ontogeny. *Development (Cambridge, England)*, *125*(22), 4575–83.

Kallianpur, A. R., Jordan, J. E., & Brandt, S. J. (1994). The SCL/TAL-1 gene is expressed in progenitors of both the hematopoietic and vascular systems during embryogenesis. *Blood*, *83*(5), 1200–8.

Kanai-Azuma, M., Kanai, Y., Gad, J. M., Tajima, Y., Taya, C., Kurohmaru, M., … Hayashi, Y. (2002). Depletion of definitive gut endoderm in Sox17-null mutant mice. *Development (Cambridge, England)*, *129*(10), 2367–79.

Keller, G., Kennedy, M., Papayannopoulou, T., & Wiles, M. V. (1993). Hematopoietic commitment during embryonic stem cell differentiation in culture. *Molecular and Cellular Biology*, *13*(1), 473–86.

Keller, G. M. (1995). In vitro differentiation of embryonic stem cells. *Current Opinion in Cell Biology*, *7*(6), 862–9.

Kennedy, M., Firpo, M., Choi, K., Wall, C., Robertson, S., Kabrun, N., & Keller, G. (1997). A common precursor for primitive erythropoiesis and definitive haematopoiesis. *Nature*, *386*(6624), 488–493.

Kim, I., Saunders, T. L., & Morrison, S. J. (2007). Sox17 dependence distinguishes the transcriptional regulation of fetal from adult hematopoietic stem cells. *Cell*, *130*(3), 470–83. doi:10.1016/j.cell.2007.06.011

Kissa, K., & Herbomel, P. (2010). Blood stem cells emerge from aortic endothelium by a novel type of cell transition. *Nature*, *464*(7285), 112–5. doi:10.1038/nature08761

Kissa, K., Murayama, E., Zapata, A., Cortés, A., Perret, E., Machu, C., & Herbomel, P. (2008). Live imaging of emerging hematopoietic stem cells and early thymus colonization. *Blood*, *111*(3), 1147–56. doi:10.1182/blood-2007-07-099499

Koushik, S. V, Wang, J., Rogers, R., Moskophidis, D., Lambert, N. A., Creazzo, T. L., & Conway, S. J. (2001). Targeted inactivation of the sodium-calcium exchanger (Ncx1) results in the lack of a heartbeat and abnormal myofibrillar organization. *FASEB Journal : Official Publication of the Federation of American Societies for Experimental Biology*, *15*(7), 1209–11.

Kulkarni, A. B., Huh, C. G., Becker, D., Geiser, A., Lyght, M., Flanders, K. C., … Karlsson, S. (1993). Transforming growth factor beta 1 null mutation in mice causes excessive inflammatory response and early death. *Proceedings of the National Academy of Sciences of the United States of America*, *90*(2), 770–4. doi:10.1073/pnas.90.2.770

Lacaud, G., Gore, L., Kennedy, M., Kouskoff, V., Kingsley, P., Hogan, C., … Keller, G. (2002). Runx1 is essential for hematopoietic commitment at the hemangioblast stage of development in vitro. *Blood*, *100*, 458–466. doi:10.1182/blood-2001-12-0321

Lam, E. Y. N., Chau, J. Y. M., Kalev-Zylinska, M. L., Fountaine, T. M., Mead, R. S., Hall, C. J., … Flores, M. V. (2009). Zebrafish runx1 promoter-EGFP transgenics mark discrete sites of definitive blood progenitors. *Blood*, *113*(6), 1241–9. doi:10.1182/blood-2008-04-149898

Lam, E. Y. N., Hall, C. J., Crosier, P. S., Crosier, K. E., & Flores, M. V. (2010). Live imaging of Runx1 expression in the dorsal aorta tracks the emergence of blood progenitors from endothelial cells. *Blood*, *116*(6), 909–914. Retrieved from http://www.bloodjournal.org/cgi/doi/10.1182/blood-2010-01-264382

Lan, H. Y., Mu, W., Tomita, N., Huang, X. R., Li, J. H., Zhu, H.-J., … Johnson, R. J. (2003). Inhibition of renal fibrosis by gene transfer of inducible Smad7 using ultrasound-microbubble system in rat UUO model. *Journal of the American Society of Nephrology : JASN*, *14*(6), 1535–48. doi:10.1097/01.ASN.0000067632.04658.B8

Lancrin, C., Mazan, M., Stefanska, M., Patel, R., Lichtinger, M., Costa, G., … Lacaud, G. (2012). GFI1 and GFI1B control the loss of endothelial identity of hemogenic endothelium during hematopoietic commitment. *Blood*. doi:10.1182/blood-2011-10-386094

Lancrin, C., Sroczynska, P., Serrano, A. G., Gandillet, A., Ferreras, C., Kouskoff, V., & Lacaud, G. (2010). Blood cell generation from the hemangioblast. *Journal of Molecular Medicine (Berlin, Germany)*, *88*(2), 167–72. doi:10.1007/s00109-009-0554-0

Lancrin, C., Sroczynska, P., Stephenson, C., Allen, T., Kouskoff, V., & Lacaud, G. (2009a). The haemangioblast generates haematopoietic cells through a haemogenic endothelium stage. *Nature*, *457*(7231), 892–5. doi:10.1038/nature07679

Larsson, J., Blank, U., Helgadottir, H., Björnsson, J. M., Ehinger, M., Goumans, M.-J., … Karlsson, S. (2003). TGF-beta signaling-deficient hematopoietic stem cells have normal self-renewal and regenerative ability in vivo despite increased proliferative capacity in vitro. *Blood*, *102*(9), 3129–35. doi:10.1182/blood-2003-04-1300

Larsson, J., Goumans, M. J., Sjöstrand, L. J., van Rooijen, M. A., Ward, D., Levéen, P., … Karlsson, S. (2001). Abnormal angiogenesis but intact hematopoietic potential in TGF-beta type I receptor-deficient mice. *The EMBO Journal*, *20*(7), 1663–73. doi:10.1093/emboj/20.7.1663

Lassila, O., Eskola, J., Toivanen, P., Martin, C., & Dieterlen-Lievre, F. (1978). The origin of lymphoid stem cells studied in chick yold sac-embryo chimaeras. *Nature*, *272*(5651), 353–4. doi:10.1038/272353a0

Lassila, O., Martin, C., Toivanen, P., & Dieterlen-Lièvre, F. (1982). Erythropoiesis and lymphopoiesis in the chick yolk-sac-embryo chimeras: contribution of yolk sac and intraembryonic stem cells. *Blood*, *59*(2), 377–81.

Li, D. Y., Sorensen, L. K., Brooke, B. S., Urness, L. D., Davis, E. C., Taylor, D. G., … Wendel, D. P. (1999). Defective angiogenesis in mice lacking endoglin. *Science (New York, N.Y.)*, *284*(5419), 1534–7.

Li, W., Ferkowicz, M. J., Johnson, S. A., Shelley, W. C., & Yoder, M. C. (2005). Endothelial cells in the early murine yolk sac give rise to CD41-expressing hematopoietic cells. *Stem Cells and Development*, *14*(1), 44–54. doi:10.1089/scd.2005.14.44

Lux, C. T., Yoshimoto, M., McGrath, K., Conway, S. J., Palis, J., & Yoder, M. C. (2008). All primitive and definitive hematopoietic progenitor cells emerging before E10 in the mouse embryo are products of the yolk sac. *Blood*, *111*(7), 3435–8. doi:10.1182/blood-2007-08-107086

Mamo, S., Gal, A. B., Bodo, S., & Dinnyes, A. (2007). Quantitative evaluation and selection of reference genes in mouse oocytes and embryos cultured in vivo and in vitro. *BMC Developmental Biology*, *7*, 14. doi:10.1186/1471-213X-7-14

Markwald, R. R., Fitzharris, T. P., & Manasek, F. J. (1977). Structural development of endocardial cushions. *The American Journal of Anatomy*, *148*(1), 85–119. doi:10.1002/aja.1001480108

Maron, B. J., & Hutchins, G. M. (1974). The development of the semilunar valves in the human heart. *The American Journal of Pathology*, *74*(2), 331–44. Retrieved from http://www.pubmedcentral.nih.gov/articlerender.fcgi?artid=1910766&tool=pmcentrez&rendertype=abstract

Martin, G. R. (1981). Isolation of a pluripotent cell line from early mouse embryos cultured in medium conditioned by teratocarcinoma stem cells. *Proceedings of the National Academy of Sciences of the United States of America*, *78*(12), 7634–8.

McGrath, K. E., Koniski, A. D., Malik, J., & Palis, J. (2003). Circulation is established in a stepwise pattern in the mammalian embryo. *Blood*, *101*(5), 1669–76. doi:10.1182/blood-2002-08-2531

Medici, D., Shore, E. M., Lounev, V. Y., Kaplan, F. S., Kalluri, R., & Olsen, B. R. (2010). Conversion of vascular endothelial cells into multipotent stem-like cells. *Nature Medicine*, *16*(12), 1400–6. doi:10.1038/nm.2252

Medvinsky, a, & Dzierzak, E. (1996). Definitive hematopoiesis is autonomously initiated by the AGM region. *Cell*, *86*(6), 897–906. Retrieved from http://www.ncbi.nlm.nih.gov/pubmed/8808625

Medvinsky, A. L., Samoylina, N. L., Müller, A. M., & Dzierzak, E. A. (1993). An early pre-liver intraembryonic source of CFU-S in the developing mouse. *Nature*, *364*(6432), 64–7. doi:10.1038/364064a0

Medvinsky, A., Rybtsov, S., & Taoudi, S. (2011). Embryonic origin of the adult hematopoietic system: advances and questions. *Development (Cambridge, England)*, *138*(6), 1017–31. doi:10.1242/dev.040998

Melchers, F. (1979). Murine embryonic B lymphocyte development in the placenta. *Nature*, *277*(5693), 219–21. doi:10.1038/277219a0

Mikkola, H. K. A., Fujiwara, Y., Schlaeger, T. M., Traver, D., & Orkin, S. H. (2003). Expression of CD41 marks the initiation of definitive hematopoiesis in the mouse embryo. *Blood*, *101*(2), 508–516.

Moignard, V., Macaulay, I. C., Swiers, G., Buettner, F., Schütte, J., Calero-Nieto, F. J., … Göttgens, B. (2013). Characterization of transcriptional networks in blood stem and progenitor cells using high-throughput single-cell gene expression analysis. *Nature Cell Biology*, *15*(4), 1–11. doi:10.1038/ncb2709

Murayama, E., Kissa, K., Zapata, A., Mordelet, E., Briolat, V., Lin, H.-F., … Herbomel, P. (2006). Tracing hematopoietic precursor migration to successive hematopoietic organs during zebrafish development. *Immunity*, *25*(6), 963–75. doi:10.1016/j.immuni.2006.10.015

Murray, P. D. F. (1932). The Development in vitro of the Blood of the Early Chick Embryo. *Proceedings of the Royal Society B: Biological Sciences*, *111*(773), 497–521. doi:10.1098/rspb.1932.0070

Müller, A. M., Medvinsky, A., Strouboulis, J., Grosveld, F., & Dzierzak, E. (1994). Development of hematopoietic stem cell activity in the mouse embryo. *Immunity*, *1*(4), 291–301. Retrieved from http://www.ncbi.nlm.nih.gov/pubmed/7889417

Nakano, T., Kodama, H., & Honjo, T. (1994). Generation of lymphohematopoietic cells from embryonic stem cells in culture. *Science (New York, N.Y.)*, *265*(5175), 1098–101. Retrieved from http://www.ncbi.nlm.nih.gov/pubmed/8066449

Nobuhisa, I., Osawa, M., Uemura, M., Kishikawa, Y., Anani, M., Harada, K., … Taga, T. (2014). Sox17-mediated maintenance of fetal intra-aortic hematopoietic cell clusters. *Molecular and Cellular Biology*, *34*(11), 1976–90. doi:10.1128/MCB.01485-13

North, T. E., Goessling, W., Peeters, M., Li, P., Ceol, C., Lord, A. M., … Zon, L. I. (2009). Hematopoietic stem cell development is dependent on blood flow. *Cell*, *137*(4), 736–48. doi:10.1016/j.cell.2009.04.023

North, T., Gu, T. L., Stacy, T., Wang, Q., Howard, L., Binder, M., … Speck, N. A. (1999). Cbfa2 is required for the formation of intra-aortic hematopoietic clusters. *Development (Cambridge, England)*, *126*(11), 2563–75.

Nottingham, W. T., Jarratt, A., Burgess, M., Speck, C. L., Cheng, J., Prabhakar, S., … de Bruijn, M. F. T. R. (2007). Runx1-mediated hematopoietic stem-cell emergence is controlled by a Gata/Ets/SCL-regulated enhancer. *Blood*, *110*(13), 4188–97. doi:10.1182/blood-2007-07-100883

Oh, S. P., Seki, T., Goss, K. a, Imamura, T., Yi, Y., Donahoe, P. K., … Li, E. (2000). Activin receptor-like kinase 1 modulates transforming growth factor-beta 1 signaling in the regulation of angiogenesis. *Proceedings of the National Academy of Sciences of the United States of America*, *97*(6), 2626–31.

Okuda, T., van Deursen, J., Hiebert, S. W., Grosveld, G., & Downing, J. R. (1996). AML1, the target of multiple chromosomal translocations in human leukemia, is essential for normal fetal liver hematopoiesis. *Cell*, *84*(2), 321–30.

Oshima, M., Oshima, H., & Taketo, M. M. (1996). TGF-beta receptor type II deficiency results in defects of yolk sac hematopoiesis and vasculogenesis. *Developmental Biology*, *179*(1), 297–302. doi:10.1006/dbio.1996.0259

Ottersbach, K., & Dzierzak, E. (2005). The murine placenta contains hematopoietic stem cells within the vascular labyrinth region. *Developmental Cell*, *8*(3), 377–87. doi:10.1016/j.devcel.2005.02.001

Palacios, R., & Imhof, B. a. (1993). At day 8-8.5 of mouse development the yolk sac, not the embryo proper, has lymphoid precursor potential in vivo and in vitro. *Proceedings of the National Academy of Sciences of the United States of America*, *90*(14), 6581–5.

Palis, J., Robertson, S., Kennedy, M., Wall, C., & Keller, G. (1999). Development of erythroid and myeloid progenitors in the yolk sac and embryo proper of the mouse. *Development (Cambridge, England)*, *126*(22), 5073–84.

Pardali, E., & Ten Dijke, P. (2012). TGFβ signaling and cardiovascular diseases. *International Journal of Biological Sciences*, *8*(2), 195–213. doi:10.7150/ijbs.3805

Pardali, E., Xie, X. Q., Tsapogas, P., Itoh, S., Arvanitidis, K., Heldin, C. H., … Sideras, P. (2000). Smad and AML proteins synergistically confer transforming growth factor beta1 responsiveness to human germ-line IgA genes. *The Journal of Biological Chemistry*, *275*(5), 3552–60. doi:10.1074/jbc.275.5.3552

Pardanaud, L., & Dieterlen-Lièvre, F. (1999). Manipulation of the angiopoietic/hemangiopoietic commitment in the avian embryo. *Development (Cambridge, England)*, *126*(4), 617–27.

Park, C., Afrikanova, I., Chung, Y. S., Zhang, W. J., Arentson, E., Fong Gh, G. H., … Choi, K. (2004). A hierarchical order of factors in the generation of FLK1- and SCL-expressing hematopoietic and endothelial progenitors from embryonic stem cells. *Development (Cambridge, England)*, *131*(11), 2749–62. doi:10.1242/dev.01130

Perlingeiro, R. C. R. (2007). Endoglin is required for hemangioblast and early hematopoietic development. *Development (Cambridge, England)*, *134*(16), 3041–8. doi:10.1242/dev.002907

Potenta, S., Zeisberg, E., & Kalluri, R. (2008). The role of endothelial-to-mesenchymal transition in cancer progression. *British Journal of Cancer*, *99*(9), 1375–9. doi:10.1038/sj.bjc.6604662

Rasmussen, K. D., Simmini, S., Abreu-Goodger, C., Bartonicek, N., Di Giacomo, M., Bilbao-Cortes, D., … O'Carroll, D. (2010). The miR-144/451 locus is required for erythroid homeostasis. *The Journal of Experimental Medicine*, *207*(7), 1351–8. doi:10.1084/jem.20100458

Rhodes, K. E., Gekas, C., Wang, Y., Lux, C. T., Francis, C. S., Chan, D. N., … Mikkola, H. K. a. (2008). The emergence of hematopoietic stem cells is initiated in the placental vasculature in the absence of circulation. *Cell Stem Cell*, *2*(3), 252–63. doi:10.1016/j.stem.2008.01.001

Rieder, F., Kessler, S. P., West, G. a, Bhilocha, S., de la Motte, C., Sadler, T. M., … Fiocchi, C. (2011). Inflammation-induced endothelial-to-mesenchymal transition: a novel mechanism of intestinal fibrosis. *The American Journal of Pathology*, *179*(5), 2660–73. doi:10.1016/j.ajpath.2011.07.042

Robb, L., Lyons, I., Li, R., Hartley, L., Köntgen, F., Harvey, R. P., … Begley, C. G. (1995). Absence of yolk sac hematopoiesis from mice with a targeted disruption of the scl gene. *Proceedings of the National Academy of Sciences of the United States of America*, *92*(15), 7075–9.

Rossant, J., & Cross, J. C. (2001). Placental development: lessons from mouse mutants. *Nature Reviews. Genetics*, *2*(7), 538–48. doi:10.1038/35080570

Sabin, F. R. (1921). STUDIES ON BLOOD: THE VITALLY STAINABLE GRANULES AS A SPECIFIC CRITERION FOR ERYTHRO- BLASTS AND THE DIFFERENTIATION OF ,THE THREE STRAINS OF THE WHITE BLOOD-CELLS AS SEEN IN THE LIVING CHICK'S YOLK-SAC. *The John Hopkins Hospital Bulletin*, (368), 314–321.

Sakamoto, Y., Hara, K., Kanai-Azuma, M., Matsui, T., Miura, Y., Tsunekawa, N., … Kanai, Y. (2007). Redundant roles of Sox17 and Sox18 in early cardiovascular development of mouse embryos. *Biochemical and Biophysical Research Communications*, *360*(3), 539–44. doi:10.1016/j.bbrc.2007.06.093

Samokhvalov, I. M., Samokhvalova, N. I., & Nishikawa, S.-I. (2007). Cell tracing shows the contribution of the yolk sac to adult haematopoiesis. *Nature*, *446*(7139), 1056–61. doi:10.1038/nature05725

Sankar, S., Mahooti-Brooks, N., Bensen, L., McCarthy, T. L., Centrella, M., & Madri, J. A. (1996). Modulation of transforming growth factor beta receptor levels on microvascular endothelial cells during in vitro angiogenesis. *The Journal of Clinical Investigation*, *97*(6), 1436–46. doi:10.1172/JCI118565

Sato, M., Muragaki, Y., Saika, S., & Roberts, A. B. (2003). Targeted disruption of TGF- β 1 / Smad3 signaling protects against renal tubulointerstitial fibrosis induced by unilateral ureteral obstruction, *112*(10). doi:10.1172/JCI19270.thesia

Schmitt, R. M., Bruyns, E., & Snodgrass, H. R. (1991). Hematopoietic development of embryonic stem cells in vitro: cytokine and receptor gene expression. *Genes & Development*, *5*(5), 728–40. doi:10.1101/gad.5.5.728

Serrano, A. G., Gandillet, A., Pearson, S., Lacaud, G., & Kouskoff, V. (2010). Contrasting effects of Sox17- and Sox18-sustained expression at the onset of blood specification. *Blood*, *115*(19), 3895–8. doi:10.1182/blood-2009-10-247395

Shalaby, F., Rossant, J., Yamaguchi, T. P., Gertsenstein, M., Wu, X. F., Breitman, M. L., & Schuh, A. C. (1995). Failure of blood-island formation and vasculogenesis in Flk-1-deficient mice. *Nature*, *376*(6535), 62–6. doi:10.1038/376062a0

Shivdasani, R. A., Mayer, E. L., & Orkin, S. H. (1995). Absence of blood formation in mice lacking the T-cell leukaemia oncoprotein tal-1/SCL. *Nature*, *373*(6513), 432–4. doi:10.1038/373432a0

Shore, E. M., Xu, M., Feldman, G. J., Fenstermacher, D. a, Cho, T.-J., Choi, I. H., … Kaplan, F. S. (2006). A recurrent mutation in the BMP type I receptor ACVR1 causes inherited and sporadic fibrodysplasia ossificans progressiva. *Nature Genetics*, *38*(5), 525–7. doi:10.1038/ng1783

Shull, M. M., Ormsby, I., Kier, A. B., Pawlowski, S., Diebold, R. J., Yin, M., … Calvin, D. (1992). Targeted disruption of the mouse transforming growth factor-beta 1 gene results in multifocal inflammatory disease. *Nature*, *359*(6397), 693–9. doi:10.1038/359693a0

Smith, A. G. (2001). Embryo-derived stem cells: of mice and men. *Annual Review of Cell and Developmental Biology*, *17*, 435–62. doi:10.1146/annurev.cellbio.17.1.435

Spangrude, G. J., Heimfeld, S., & Weissman, I. L. (1988). Purification and characterization of mouse hematopoietic stem cells. *Science (New York, N.Y.)*, *241*(4861), 58–62.

Sroczynska, P., Lancrin, C., Kouskoff, V., & Lacaud, G. (2009a). The differential activities of Runx1 promoters define milestones during embryonic hematopoiesis. *Blood*, *114*(26), 5279–5289. doi:10.1182/blood-2009-05-222307.The

Sroczynska, P., Lancrin, C., Pearson, S., & Lacaud, G. (2009). In Vitro Differentiation of Embryonic Stem Cells as a Model of Early Hematopoietic Development. In C. W. Eric So (Ed.), *Methods in Molecular Biology, Leukemia Methods and Protocols* (Vol. 538, pp. 317–335). Totowa, NJ: Humana Press. doi:10.1007/978-1-59745-418-6

Ståhlberg, A., Rusnakova, V., Forootan, A., Anderova, M., & Kubista, M. (2013). RT-qPCR work-flow for single-cell data analysis. *Methods (San Diego, Calif.)*, *59*(1), 80–8. doi:10.1016/j.ymeth.2012.09.007

Stainier, D. Y., Weinstein, B. M., Detrich, H. W., Zon, L. I., & Fishman, M. C. (1995). Cloche, an early acting zebrafish gene, is required by both the endothelial and hematopoietic lineages. *Development (Cambridge, England)*, *121*(10), 3141–50.

Stevens, L. C. (1970). The development of transplantable teratocarcinomas from intratesticular grafts of pre- and postimplantation mouse embryos. *Developmental Biology*, *21*(3), 364–82.

Swiers, G., Baumann, C., O'Rourke, J., Giannoulatou, E., Taylor, S., Joshi, A., … de Bruijn, M. F. T. R. (2013). Early dynamic fate changes in haemogenic endothelium characterized at the single-cell level. *Nature Communications*, *4*, 2924. doi:10.1038/ncomms3924

Tanaka, Y., Hayashi, M., Kubota, Y., Nagai, H., Sheng, G., Nishikawa, S.-I., & Samokhvalov, I. M. (2012). Early ontogenic origin of the hematopoietic stem cell lineage. *Proceedings of the National Academy of Sciences of the United States of America*, *109*(12), 4515–20. doi:10.1073/pnas.1115828109

Taoudi, S., & Medvinsky, A. (2007). Functional identification of the hematopoietic stem cell niche in the ventral domain of the embryonic dorsal aorta. *Proceedings of the National Academy of Sciences of the United States of America*, *104*(22), 9399–403. doi:10.1073/pnas.0700984104

Tavian, M., Coulombel, L., Luton, D., Clemente, H. S., Dieterlen-Lièvre, F., & Péault, B. (1996). Aorta-associated CD34+ hematopoietic cells in the early human embryo. *Blood*, *87*(1), 67–72.

Thompson, M. A., Ransom, D. G., Pratt, S. J., MacLennan, H., Kieran, M. W., Detrich, H. W., … Zon, L. I. (1998). The cloche and spadetail genes differentially affect hematopoiesis and vasculogenesis. *Developmental Biology*, *197*(2), 248–69. doi:10.1006/dbio.1998.8887

Turpen, J. B., Knudson, C. M., & Hoefen, P. S. (1981). The early ontogeny of hematopoietic cells studied by grafting cytogenetically labeled tissue anlagen: localization of a prospective stem cell compartment. *Developmental Biology*, *85*(1), 99–112. Retrieved from http://www.ncbi.nlm.nih.gov/pubmed/6972885

Van Handel, B., Montel-Hagen, A., Sasidharan, R., Nakano, H., Ferrari, R., Boogerd, C. J., … Mikkola, H. K. a. (2012). Scl represses cardiomyogenesis in prospective hemogenic endothelium and endocardium. *Cell*, *150*(3), 590–605. doi:10.1016/j.cell.2012.06.026

Voyta, J. C., Via, D. P., Butterfield, C. E., & Zetter, B. R. (1984). Identification and isolation of endothelial cells based on their increased uptake of acetylated-low density lipoprotein. *The Journal of Cell Biology*, *99*(6), 2034–40.

Wang, C., Tang, X., Sun, X., Miao, Z., Lv, Y., Yang, Y., … Deng, H. (2012). TGFβ inhibition enhances the generation of hematopoietic progenitors from human ES cell-derived hemogenic endothelial cells using a stepwise strategy. *Cell Research*, *22*(1), 194–207. doi:10.1038/cr.2011.138

Wang, H., Yang, H., Shivalila, C. S., Dawlaty, M. M., Cheng, A. W., Zhang, F., & Jaenisch, R. (2013). One-step generation of mice carrying mutations in multiple genes by CRISPR/Cas-mediated genome engineering. *Cell*, *153*(4), 910–8. doi:10.1016/j.cell.2013.04.025

Wang, Q., Stacy, T., Binder, M., Marin-Padilla, M., Sharpe, A. H., & Speck, N. A. (1996). Disruption of the Cbfa2 gene causes necrosis and hemorrhaging in the central nervous system and blocks definitive hematopoiesis. *Proceedings of the National Academy of Sciences of the United States of America*, *93*(8), 3444–9.

Wang, Q., Stacy, T., Miller, J. D., Lewis, A. F., Gu, T. L., Huang, X., … Speck, N. A. (1996). The CBFbeta subunit is essential for CBFalpha2 (AML1) function in vivo. *Cell*, *87*(4), 697–708. Retrieved from http://www.ncbi.nlm.nih.gov/pubmed/8929538

Wiles, M. V, & Keller, G. (1991). Multiple hematopoietic lineages develop from embryonic stem (ES) cells in culture. *Development (Cambridge, England)*, *111*(2), 259–67. Retrieved from http://www.ncbi.nlm.nih.gov/pubmed/1893864

Wilkinson, A. C., Kawata, V. K. S., Schütte, J., Gao, X., Antoniou, S., Baumann, C., … Göttgens, B. (2014). Single-cell analyses of regulatory network perturbations using enhancer-targeting TALEs suggest novel roles for PU.1 during haematopoietic specification. *Development (Cambridge, England)*, (September), 1–13. doi:10.1242/dev.115709

Yokomizo, T., & Dzierzak, E. (2010). Three-dimensional cartography of hematopoietic clusters in the vasculature of whole mouse embryos. *Development (Cambridge, England)*, *137*(21), 3651–61. doi:10.1242/dev.051094

Yokomizo, T., Hasegawa, K., Ishitobi, H., Osato, M., Ema, M., Ito, Y., … Takahashi, S. (2008). Runx1 is involved in primitive erythropoiesis in the mouse. *Blood*, *111*(8), 4075–80. doi:10.1182/blood-2007-05-091637

Young, P. E., Baumhueter, S., & Lasky, L. A. (1995). The sialomucin CD34 is expressed on hematopoietic cells and blood vessels during murine development. *Blood*, *85*(1), 96–105.

Yu, M., Mazor, T., Huang, H., Huang, H.-T., Kathrein, K. L., Woo, A. J., … Cantor, A. B. (2012). Direct recruitment of polycomb repressive complex 1 to chromatin by core binding transcription factors. *Molecular Cell*, *45*(3), 330–43. doi:10.1016/j.molcel.2011.11.032

Zeisberg, E. M., Potenta, S. E., Sugimoto, H., Zeisberg, M., & Kalluri, R. (2008). Fibroblasts in kidney fibrosis emerge via endothelial-to-mesenchymal transition. *Journal of the American Society of Nephrology : JASN*, *19*(12), 2282–7. doi:10.1681/ASN.2008050513

Zeisberg, E. M., Potenta, S., Xie, L., Zeisberg, M., & Kalluri, R. (2007). Discovery of endothelial to mesenchymal transition as a source for carcinoma-associated fibroblasts. *Cancer Research*, *67*(21), 10123–8. doi:10.1158/0008-5472.CAN-07-3127

Zeisberg, E. M., Tarnavski, O., Zeisberg, M., Dorfman, A. L., McMullen, J. R., Gustafsson, E., … Kalluri, R. (2007). Endothelial-to-mesenchymal transition contributes to cardiac fibrosis. *Nature Medicine*, *13*(8), 952–61. doi:10.1038/nm1613

Zhang, L., Magli, A., Catanese, J., Xu, Z., Kyba, M., & Perlingeiro, R. C. R. (2011). Modulation of TGF-β signaling by endoglin in murine hemangioblast development and primitive hematopoiesis. *Blood*, *118*(1), 88–97. doi:10.1182/blood-2010-12-325019

Zhang, Y., & Derynck, R. (2000). Transcriptional regulation of the transforming growth factor-beta -inducible mouse germ line Ig alpha constant region gene by functional cooperation of Smad, CREB, and AML family members. *The Journal of Biological Chemistry*, *275*(22), 16979–85. doi:10.1074/jbc.M001526200

Zovein, A. C., Hofmann, J. J., Lynch, M., French, W. J., Turlo, K. A., Yang, Y., … Iruela-Arispe, M. L. (2008). Fate tracing reveals the endothelial origin of hematopoietic stem cells. *Cell Stem Cell*, *3*(6), 625–36. doi:10.1016/j.stem.2008.09.018

Appendix

Table 5.8. The list of 96 genes used to see in single cell qPCR expression. The classification indicates the reason to be selected.

Gene name	ENSEMBL Gene ID	Long Gene Name	Classification
PPIA	ENSMUSG00000071866	peptidylprolyl isomerase A	Reference gene
ACTA2	ENSMUSG00000035783	actin, alpha 2, smooth muscle, aorta	EMT related
ACVR1	ENSMUSG00000026836	activin A receptor, type 1	TGFB or BMP pathway
ACVR1B	ENSMUSG00000000532	activin A receptor, type 1B	TGFB or BMP pathway
ACVR2A	ENSMUSG00000052155	activin receptor IIA	TGFB or BMP pathway
ACVR2B	ENSMUSG00000061393	activin receptor IIB	TGFB or BMP pathway
ACVRL1	ENSMUSG00000000530	activin A receptor, type II-like 1	TGFB or BMP pathway
ADCY4	ENSMUSG00000022220	adenylate cyclase 4	common target of Runx1 and Gfi1
ATP2A3	ENSMUSG00000020788	ATPase, Ca++ transporting, ubiquitous	common target of Runx1 and Gfi1
BMP4	ENSMUSG00000021835	bone morphogenetic protein 4	TGFB or BMP pathway
BMPR1A	ENSMUSG00000021796	bone morphogenetic protein receptor, type 1A	TGFB or BMP pathway
BMPR2	ENSMUSG00000067336	bone morphogenic protein receptor, type II (serine/threonine kinase)	TGFB or BMP pathway
CACNA2D1	ENSMUSG00000040118	calcium channel, voltage-dependent, alpha2/delta subunit 1	common target of Runx1 and Gfi1
CDH2	ENSMUSG00000024304	cadherin 2	EMT related
CDH5	ENSMUSG00000031871	cadherin 5	Endothelial gene, common target of Runx1 and Gfi1
CLDN5	ENSMUSG00000041378	claudin 5	Endothelial genes

COL4A2	ENSMUSG00000031503	collagen, type IV, alpha 2	common target of Runx1 and Gfi1
COL4A5	ENSMUSG00000031274	collagen, type IV, alpha 5	common target of Runx1 and Gfi1
CTNNB1	ENSMUSG00000006932	catenin (cadherin associated protein), beta 1	EMT related
DCAF12L1	ENSMUSG00000045284	DDB1 and CUL4 associated factor 12-like 1	common target of Runx1 and Gfi1
DPYSL3	ENSMUSG00000024501	dihydropyrimidinase-like 3	common target of Runx1 and Gfi1
ENG	ENSMUSG00000026814	Endoglin	Endothelial gene, TGFB or BMP pathway
ENPP1	ENSMUSG00000037370	ectonucleotide pyrophosphatase/phosphodiesterase 1	common target of Runx1 and Gfi1
EPO	ENSMUSG00000029711	Erythropoietin	Hematopoietic genes
EPOR	ENSMUSG00000006235	erythropoietin receptor	Hematopoietic genes
EPS8	ENSMUSG00000015766	epidermal growth factor receptor pathway substrate 8	common target of Runx1 and Gfi1
ERG	ENSMUSG00000040732	avian erythroblastosis virus E-26 (v-ets) oncogene related	Endothelial gene, Transcription factors
ESAM	ENSMUSG00000001946	endothelial cell-specific adhesion molecule	Endothelial genes, common target of Runx1 and Gfi1
FAM122B	ENSMUSG00000036022	family with sequence similarity 122, member B	common target of Runx1 and Gfi1
FBN1	ENSMUSG00000027204	fibrillin 1	Endothelial genes, common target of Runx1 and

			Gfi1
FLI1	ENSMUSG00000016087	Friend leukemia integration 1	Transcription factors
FLRT2	ENSMUSG00000047414	fibronectin leucine rich transmembrane protein 2	common target of Runx1 and Gfi1
FMO1	ENSMUSG00000040181	flavin containing monooxygenase 1	common target of Runx1 and Gfi1
GATA1	ENSMUSG00000031162	GATA binding protein 1	Hematopoietic genes, Transcription factors
GATA2	ENSMUSG00000015053	GATA binding protein 2	Hematopoietic genes, Transcription factors
GDPD5	ENSMUSG00000035314	glycerophosphodiester phosphodiesterase domain containing 5	common target of Runx1 and Gfi1
GFI1	ENSMUSG00000029275	growth factor independent 1	Hematopoietic genes, Transcription factors
GFI1B	ENSMUSG00000026815	growth factor independent 1B	Hematopoietic genes, Transcription factors
GPR126	ENSMUSG00000039116	G protein-coupled receptor 126	Endothelial genes, common target of Runx1 and Gfi1
GRIA4	ENSMUSG00000025892	glutamate receptor, ionotropic, AMPA4 (alpha 4)	common target of Runx1 and Gfi1
HBB-B1	ENSMUSG00000073940	hemoglobin, beta adult major chain	Hematopoietic genes
HBB-BH1	ENSMUSG00000052217	hemoglobin Z, beta-like embryonic chain	Hematopoietic genes
ITGA2B	ENSMUSG00000034664	integrin alpha 2b	Hematopoietic genes
ITGAM	ENSMUSG00000030786	integrin alpha M	Hematopoietic genes

ITGB3	ENSMUSG00000020689	integrin beta 3	Endothelial genes
KDR	ENSMUSG00000062960	kinase insert domain protein receptor	Hematopoietic genes
KIT	ENSMUSG00000005672	kit oncogene	Hematopoietic genes
LAD1	ENSMUSG00000041782	Ladinin	common target of Runx1 and Gfi1
LAT	ENSMUSG00000030742	linker for activation of T cells	common target of Runx1 and Gfi1
LGR5	ENSMUSG00000020140	leucine rich repeat containing G protein coupled receptor 5	common target of Runx1 and Gfi1
LMO2	ENSMUSG00000032698	LIM domain only 2	Transcription factors
LYL1	ENSMUSG00000034041	lymphoblastomic leukemia 1	Hematopoietic genes, Transcription factors
MEIS2	ENSMUSG00000027210	Meis homeobox 2	Endothelial genes, Transcription factors, common target of Runx1 and Gfi1
MET	ENSMUSG00000009376	met proto-oncogene	common target of Runx1 and Gfi1
MPO	ENSMUSG00000009350	myeloperoxidase	Hematopoietic genes
MYB	ENSMUSG00000019982	myeloblastosis oncogene	Hematopoietic genes, Transcription factors, common target of Runx1 and Gfi1
MYOM1	ENSMUSG00000024049	myomesin 1	common target of Runx1 and Gfi1

NOTCH1	ENSMUSG00000026923	Notch 1	Endothelial genes, common target of Runx1 and Gfi1
NPR1	ENSMUSG00000027931	natriuretic peptide receptor 1	Endothelial genes, common target of Runx1 and Gfi1
PALLD	ENSMUSG00000058056	palladin, cytoskeletal associated protein	common target of Runx1 and Gfi1
PECAM1	ENSMUSG00000020717	platelet/endothelial cell adhesion molecule 1	Endothelial genes
PCDH12	ENSMUSG00000024440	protocadherin 12	Endothelial genes, common target of Runx1 and Gfi1
PDZD2	ENSMUSG00000022197	PDZ domain containing 2	common target of Runx1 and Gfi1
PLCD1	ENSMUSG00000010660	phospholipase C, delta 1	common target of Runx1 and Gfi1
PPP1R16B	ENSMUSG00000037754	protein phosphatase 1, regulatory (inhibitor) subunit 16B	common target of Runx1 and Gfi1
PTPRB	ENSMUSG00000020154	protein tyrosine phosphatase, receptor type, B	Endothelial genes, common target of Runx1 and Gfi1
PTPRC	ENSMUSG00000026395	protein tyrosine phosphatase, receptor type, C	Hematopoietic genes
PTPRM	ENSMUSG00000033278	protein tyrosine phosphatase, receptor type, M	Endothelial genes, common target of Runx1 and Gfi1

RAMP2	ENSMUSG00000001240	receptor (calcitonin) activity modifying protein 2	Endothelial genes
RUNX1	ENSMUSG00000022952	runt related transcription factor 1	Hematopoietic genes, Transcription factors
SAMD4	ENSMUSG00000021838	sterile alpha motif domain containing 4	common target of Runx1 and Gfi1
SASH1	ENSMUSG00000015305	SAM and SH3 domain containing 1	common target of Runx1 and Gfi1
SERPINE1	ENSMUSG00000037411	serine (or cysteine) peptidase inhibitor, clade E, member 1	EMT related
SFPI1	ENSMUSG00000002111	SFFV proviral integration 1	Hematopoietic genes, Transcription factors
SHE	ENSMUSG00000046280	src homology 2 domain-containing transforming protein E	common target of Runx1 and Gfi1
SLA	ENSMUSG00000022372	src-like adaptor	Hematopoietic genes, common target of Runx1 and Gfi1
SMAD1	ENSMUSG00000031681	SMAD family member 1	TGFB or BMP pathway
SMAD2	ENSMUSG00000024563	SMAD family member 2	TGFB or BMP pathway
SMAD3	ENSMUSG00000032402	SMAD family member 3	TGFB or BMP pathway
SMAD4	ENSMUSG00000024515	SMAD family member 4	TGFB or BMP pathway
SMAD5	ENSMUSG00000021540	SMAD family member 5	TGFB or BMP pathway
SMAD6	ENSMUSG00000036867	SMAD family member 6	TGFB or BMP pathway
SMAD7	ENSMUSG00000025880	SMAD family member 7	TGFB or BMP pathway
SMAD9	ENSMUSG00000027796	SMAD family member 9	TGFB or BMP pathway
SNAI1	ENSMUSG00000042821	snail family zinc finger 1	Transcription factors, EMT related
SNAI2	ENSMUSG00000022676	snail family zinc finger 2	Transcription factors,

			EMT related
SOX7	ENSMUSG00000063060	SRY (sex determining region Y)-box 7	Endothelial genes, Transcription factors
TAL1	ENSMUSG00000028717	T-cell acute lymphocytic leukemia 1	Hematopoietic genes, Transcription factors
TEK	ENSMUSG00000006386	endothelial-specific receptor tyrosine kinase	Endothelial genes
TGFB1	ENSMUSG00000002603	transforming growth factor, beta 1	TGFB or BMP pathway, EMT related
TGFB2	ENSMUSG00000039239	transforming growth factor, beta 2	TGFB or BMP pathway, EMT related
TGFB3	ENSMUSG00000021253	transforming growth factor, beta 3	TGFB or BMP pathway, EMT related
TGFBR1	ENSMUSG00000007613	transforming growth factor, beta receptor I	TGFB or BMP pathway, EMT related
TGFBR2	ENSMUSG00000032440	transforming growth factor, beta receptor II	TGFB or BMP pathway, EMT related
THPO	ENSMUSG00000022847	Thrombopoietin	Hematopoietic genes
UPP1	ENSMUSG00000020407	uridine phosphorylase 1	common target of Runx1 and Gfi1